



2019-06-01

Burner Design for a Pressurized Oxy-Coal Reactor

William Cody Carpenter
Brigham Young University

Follow this and additional works at: <https://scholarsarchive.byu.edu/etd>

BYU ScholarsArchive Citation

Carpenter, William Cody, "Burner Design for a Pressurized Oxy-Coal Reactor" (2019). *Theses and Dissertations*. 7506.
<https://scholarsarchive.byu.edu/etd/7506>

This Thesis is brought to you for free and open access by BYU ScholarsArchive. It has been accepted for inclusion in Theses and Dissertations by an authorized administrator of BYU ScholarsArchive. For more information, please contact scholarsarchive@byu.edu, ellen_amatangelo@byu.edu.

Burner Design for a Pressurized Oxy-Coal Reactor

William Cody Carpenter

A thesis submitted to the faculty of
Brigham Young University
in partial fulfillment of the requirements for the degree of
Master of Science

Dale R. Tree, Chair
Bradley R. Adams
Steven E. Gorrell

Department of Mechanical Engineering

Brigham Young University

Copyright © 2019 William Cody Carpenter

All Rights Reserved

ABSTRACT

Burner Design for a Pressurized Oxy-Coal Reactor

William Cody Carpenter
Department of Mechanical Engineering, BYU
Master of Science

The need for electric power across the globe is ever increasing, as is the need to produce electricity in a sustainable method that does not emit CO₂ into the atmosphere. A proposed technology for efficiently capturing CO₂ while producing electricity is pressurized oxy-combustion (POC). The objective of this work is to design, build, and demonstrate a burner for a 20 atmosphere oxy-coal combustor. Additionally, working engineering drawings for the main pressure vessel and floor plan drawings for the main pressure vessel, exhaust, and fuel feed systems were produced. The POC reactor enables the development of three key POC technologies: a coal dry-feed system, a high pressure burner, and an ash management system. This work focuses on the design of a traditional diffusion flame burner and the design of the main reactor. The burner was designed with the intent to elongate the flame and spread heat flux from the reacting fuel over a longer distance to enable low CO₂ recycle rates. This was done by matching the velocities of the fuel and oxidizer in the burner to minimize shear between incoming jets in order to delay the mixing of the coal and oxygen for as long as possible. A spreadsheet model was used to calculate the jet velocities and sizes of holes needed in the burner, comprehensive combustion modeling was outsourced to Reaction Engineering International (REI) to predict the performance of burner designs. Using the guidance of the modeling results, a burner design was selected and assembled. The burner consists of a center tube where the primary fuel will flow, two concentric secondary tubes making an inner and an outer annulus, and eight tertiary lances. The burner and reactor are ready to be tested once issues involving the control system are resolved. Measurements that will be taken once testing begins include: axial gas and wall temperature, radiative heat flux, outlet gas temperature, and ash composition.

Keywords: burner design, pressurized oxy-coal, combustion, pulverized coal

ACKNOWLEDGEMENTS

I am grateful for the time that I have studied at Brigham Young University and for the rich experiences and vast knowledge I have gained while furthering my education. My successful studies could not have been done without the help and support of my fellow students, faculty, staff, friends and family.

Firstly, I would like to thank my graduate advisor Dr. Tree for his countless hours spent mentoring me and helping me in my academic journey. I would like to thank my fellow graduate students, especially Aaron Skousen and Scott Egbert for their support and friendship over the course of this project. I am also grateful for undergraduate students who have helped in the research process, especially James “Thor” Atchley. My wife Audrey and son Spencer have given me endless support and encouragement to always do my best. They have helped me in more ways than imaginable to achieve my goals, and I truly could not have done any of this without their help. My parents, other family members, and friends have also been encouraging and supportive throughout the entire process of this project.

Lastly, I would like to thank the sources of funding for my education. I am appreciative towards the Department of Energy (DOE) for funding this research project, and the DoD SMART Scholarship for funding my education.

TABLE OF CONTENTS

ABSTRACT	ii
ACKNOWLEDGEMENTS	iii
TABLE OF CONTENTS.....	iv
LIST OF TABLES	vi
LIST OF FIGURES	vii
NOMENCLATURE	x
1 Introduction.....	1
2 Background and Literature Review	4
2.1 Classification of Flame Types	4
2.2 Models and Parameters Impacting Flame Length	7
2.2.1 Laminar Flame Length	7
2.2.2 Turbulent Flame Length.....	10
2.2.3 Buoyancy Effects on Turbulent Flames	11
2.2.4 Swirled Turbulent Flames	12
2.3 Oxy-coal Burner Design	15
2.4 Existing Pressurized Oxy-coal Burners	17
2.5 Summary Related to Pressurized Oxy-coal Combustion.....	18
2.6 Comprehensive Coal Combustion Modeling.....	20
3 Methods.....	21
3.1 Burner Design	21
3.1.1 Performance Requirements and Design Constraints.....	22
3.1.2 Spreadsheet Modeling.....	22

3.1.3	Energy Balance 1-D Modeling.....	26
3.1.4	3-D Comprehensive Modeling.....	27
3.1.5	Manifold Orifice Calculations.....	29
3.2	Design of Reactor Components	30
3.3	Room Layout Design	32
3.4	Burner Test Procedures.....	33
4	Results and Discussion	35
4.1	Description of Entire POC	35
4.2	Burner Design.....	37
4.2.1	Comprehensive Simulation Results	39
4.3	Test Results.....	44
4.3.1	Connections from MFCs to Burner.....	46
4.4	Design of Reactor Components	49
4.4.1	Dome Cap.....	50
4.4.2	Reactor Support Legs	50
4.4.3	Refractory Layout	51
4.4.4	Optical and Access Ports.....	53
4.5	Room Layout Design	54
5	Summary and Conclusions	56
	REFERENCES	58
Appendix A.	CAD Model and Drawing of Burner.....	61
Appendix B.	POC Reactor drawings	65

LIST OF TABLES

Table 2-1. Summary of Atmospheric Oxy-Combustion Reactors.....	17
Table 2-2. Summary of Pressurized Oxy-Combustion Reactor.....	17
Table 3-1: Performance Requirements and Design Constraints.....	23
Table 3-2: Operating Parameters for Three REI Test Cases.....	30
Table 3-3: Components and their Corresponding Masses to be Supported by Central Beam in Reactor Room.	34
Table 4-1: Geometry and Velocity of the Primary, Secondary, and Tertiary Burner Flows.....	39
Table 4-2: Tube Geometry and Select Operating Conditions and Results for Three Different Burner Designs for POC Reactor.....	40
Table 4-3: Distinguishing Parameters from Three REI Test Cases.....	41
Table 4-4: Qualitative Results of Firing Burner Outside of Reactor.....	45
Table B-0-1: Directory of CAD Parts.....	65

LIST OF FIGURES

Figure 2-1: Swirled burner cross-sectional diagram depicting a fuel rich region that is surrounded by a recirculating secondary flow [4].....	6
Figure 2-2: Four different types of swirled flames as designated by the IFRF: (a) Type 0, (b) Type 1, (c) Type 2, and (d) Type 3 [4].	8
Figure 2-3: Schematic diagram of the fuel and air flow of a simple swirled gas flame [15].....	13
Figure 2-4: Schematic of burner studied by Gopan et al [21].....	18
Figure 3-1: Effects of Pressure on Velocity for Given Tube Diameters.....	27
Figure 4-1: Schematic of the POC Reactor (not to scale).....	37
Figure 4-2: Cross-Sectional Schematic of Burner with Dimensions.	38
Figure 4-3: Cross-Sectional Diagram of Burners with Velocities of Different Streams for REI Cases 1, 2, and 3, Respectively.....	41
Figure 4-4: Temperature Profile along the Length of the POC Reactor for each of the Three Burner Design Cases for which CFD was run.....	42
Figure 4-5: CFD Results of Gas Temperature Profile for Three Burner Design Cases.	43
Figure 4-6: Preliminary Burner Testing at 50 KW _{th}	45
Figure 4-7: Piping and Instrumentation Diagram of Tubing and Connections between MFCs and the Manifold and Burner.	48
Figure 4-8: Photograph of Tubing, Swagelok Connections, and Manifold Connecting to the Burner.	49
Figure 4-9: FEA Analysis of Reactor Support Leg.	51

Figure 4-10: Diagram of Refractory Used to Insulate the POC Reactor (Dimensions in in.).....	52
Figure 4-11: Picture of POC Reactor in Reactor Room.	53
Figure 4-12: Layout of Reactor Room Support I-Beams and Calculated Forces for Wall and Square Supports.	55
Figure A1: Drawing of Side View of Cap Burner with Swagelok Fittings	62
Figure A2: Drawing of Isometric View of Cap Burner with Swagelok Fittings and Bill of Materials	63
Figure A3: Drawing of Bottom View of Burner with Tube Dimensions	64
Figure B1: Drawing of POC Reactor Assembly with Cap Burner	68
Figure B2: Drawing of POC Reactor Assembly with Flange Burner.....	69
Figure B3: Drawing of Main Reactor with Refractory Assembly	70
Figure B4: Drawing of 2 Inch Flange Assembly	71
Figure B5: Drawing of Bottom of Reactor with Refractory Assembly	72
Figure B6: Drawing of Cap Burner Assembly	73
Figure B7: Drawing of 6 Inch Blind Flange with Swageloks on Top	74
Figure B8: Drawing of Flange Burner Design Assembly.....	75
Figure B9: Drawing of 8 Inch Blind Flange with Swageloks on Top	76
Figure B10: Drawing of Nozzle.....	77
Figure B11: Drawing of Exit Pipe for Relief Valve	78
Figure B12: Drawing of 12 to 4 Inch Reducer	79
Figure B13: Drawing of Main Reactor Shell.....	80
Figure B14: Drawing of Reactor Support Leg.....	81

Figure B15: Drawing of 2 Inch X-Heavy Steel Pipe	82
Figure B16: Drawing of 30 Inch X-Heavy Pipe with Hole	83
Figure B17: Drawing of 30 Inch Class 300 Blind Flange with Hole for Cap	84
Figure B18: Drawing of 30 Inch Steel Cap Schedule 20.....	85
Figure B19: Drawing of 6 Inch X-Heavy Steel Pipe for Top of Cap	86
Figure B20: Drawing of 6 Inch Class 300 Blind Flange with Holes for Tubes.....	87
Figure B21: Drawing of 8 Inch Class 300 Blind Flange with Hole for 8 Inch Pipe.....	88
Figure B22: Drawing of 8 Inch X-Heavy Steel Pipe	89
Figure B23: Drawing of 30 Inch Class 300 Blind Flange with Hole for 8 Inch Pipe.....	90
Figure B24: Drawing of 8 Inch Class 300 Blind Flange with Holes for Swageloks	91
Figure B25: Drawing of 8 Inch Class 300 Blind Flange with Holes for Swageloks	92
Figure B26: Drawing of 3 Inch X-Heavy Pipe	93
Figure B27: Drawing of 3 Inch Class 300 Blind Flange with Hole for $\frac{3}{4}$ Inch Pipe.....	94
Figure B28: Drawing of 2.5 Inch X-Heavy Steel Pipe	95
Figure B29: Drawing of 12 Inch Class 300 Blind Flange with Hole for 4 Inch Pipe.....	96
Figure B30: Drawing of 4 Inch X-Heavy Steel Pipe	97

NOMENCLATURE

Abbreviations

DOE	Department of Energy
POC	Pressurized Oxy-coal
HHV	Higher Heating Value
CAD	Computer Aided Design
REI	Reaction Engineering International
CFD	Computational Fluid Dynamics
MFC	Mass Flow Controller
FEA	Finite Element Analysis

Symbols

ϕ	Stoichiometric Ratio
\mathcal{D}	Diffusion Coefficient
ϵ	Eddy Viscosity
ρ	Density
μ	Dynamic viscosity
β	Ratio of throat diameter of orifice to diameter of tube

1 INTRODUCTION

In attempts to explore ways of reducing harmful emissions, atmospheric oxy-coal combustion has been demonstrated, but was not as efficient or cost-effective as traditional air combustion [1]. Dramatic increases in the supply of natural gas in the United States have led to an increase in the implementation of natural gas fired plants that are both cheaper and cleaner than burning coal. The Department of Energy (DOE) is now looking for technologies which can improve natural gas CO₂ emissions levels and leverage the vast resources of coal available in the United States. There are three recognized approaches to reduce CO₂ emissions from coal-fired systems: post-combustion, pre-combustion, and oxy-fuel combustion. Studies have shown that of these three options, "...oxy-fuel combustion is the most competitive technology ..." [1]. Since atmospheric oxy-combustion has a proven efficiency penalty, other technologies should be explored. Of the potential technologies available, "boiler pressurization with oxy-combustion has been identified as one of the most promising solutions." [2]. Coal has traditionally been burned at atmospheric pressure with air. Oxy-coal combustion requires coal to be burned with oxygen and recycled flue gas, often at elevated oxygen concentrations. Pressurized oxy-coal combustion requires both elevated oxygen concentrations and elevated pressure. Pressurized combustion provides the advantage of having additional latent heat at the end of the Rankine cycle, when heat is extracted from the flue gases into steam to generate electricity. The additional latent heat is a result of the boiling point of water increasing as pressure increases. This means that steam

will condense from a gas to a liquid at a higher temperature and allow for the water which will be heated to evaporate into steam to generate electricity to be pre-heated to a higher temperature before entering the Rankine cycle. Another benefit of performing combustion at high pressure is less power will need to be spent on pressurizing the carbon dioxide combustion products to liquid form in order to utilize carbon capture and sequestration as a means of reducing the amount of CO₂ emitted into the atmosphere. These advantages counteract the disadvantage in oxy-coal combustion of having to separate the oxygen from the nitrogen found in air, which costs power and decreases plant efficiencies. Overall, the advantages in oxy-coal combustion outweigh the disadvantages inherent with this process, making pressurized oxy-coal combustion an attractive alternative to traditional atmospheric coal combustion.

Brigham Young University has been selected by the DOE to investigate and demonstrate several key technologies related to pressurized oxy-coal combustion partially due to faculty experience with oxy-coal at atmospheric pressure. To do so, a 100 kW_{th} pressurized oxy-coal combustor (POC) was designed, fabricated and is ready to be tested. A new combustor and burner were built that are rated and optimized for the high pressure conditions of these experiments. The design was also made to facilitate wall and gas temperature measurements for the unique conditions of this project. Due to these circumstances, a new combustor was designed and built, rather than modifying an existing combustor. Key technologies of the POC reactor include: a dry coal feed system, a low recycle pulverized-coal burner, and an ash management system.

The objectives of this work include:

- The design and fabrication of a diffusion flame burner for the Pressurized Oxy-coal (POC) Reactor.

- The purpose of this burner is to elongate the flame to distribute heat flux.
 - Test the burner to determine if it can be used under atmospheric conditions with natural gas to warm up the reactor.
- The design and installation of the connections from the mass flow controllers to the burner.
- The design of components of the POC reactor.
- The generation of CAD models and drawings of reactor and components.
- The design of the reactor room layout and support structure, along with the installation of the support structure and the reactor and reactor components in the reactor room.

2 BACKGROUND AND LITERATURE REVIEW

This chapter will provide background information for the classification of flames and how flame length and shape relate to the geometry of a burner. The chapter begins with the historical classification for pulverized coal flame types established for atmospheric combustion. Methods from the literature for calculating flame length for laminar, turbulent and buoyancy driven flames will then be presented. These flame types are described for atmospheric flames as a foundation for understanding flames at elevated pressure.

2.1 Classification of Flame Types

A flame is a thin reaction zone separating reactants (fuel and oxygen) and products. A flame requires fuel, oxygen, and ignition energy (a high enough temperature to ignite the mixture). A flame typically resides where a mixture of fuel and oxygen are near stoichiometric and energy diffuses or is mixed into the fuel and air producing the ignition source. Stoichiometric is when there is an ideal ratio of oxidizer to fuel in order to burn all of the fuel with no excess oxidizer. A flame can propagate upstream in a fuel air mixture to the point where the two are mixed and therefore it is dangerous to have them mix before entering a space where a flame can safely reside. A burner is therefore a device which introduces fuel and oxidizer in such a way that the flame resides in a desired location. Fuel can mix slowly with oxidant by diffusion or more rapidly by making the fuel or oxidizer into a jet that shears with the other reactant.

A basic burner is shown in cross section in Figure 2-1 with components identified that will be useful for describing most burners. Fuel is introduced through a tube call the primary tube. The primary tube can have oxidizer in it but only at small amounts relative to stoichiometric or otherwise the flame could propagate up the primary tube. The primary mixture produces a gaseous jet when leaving the tube exit where it can be exposed to hot walls and mix with oxidizer and product gases.

Oxidizer is introduced through the secondary tube. In this case the secondary tube is an annulus surrounding the primary tube. The oxidizer can be swirled as shown in the figure or it can be unswirled and proceed as an annular jet adjacent to the primary jet. Swirl produces tangential motion which moves out radially when the oxidizer leaves the confinement of the tube. A quarl is an expanding conical enclosure that confines the swirled gases and expands them within the confined geometry. The outward or radial motion of the flame produces an increased stagnation pressure at the quarl boundary and a negative pressure at the axial centerline. The pressures induced a flow as shown in Figure 2-1 called an internal recirculation zone. Swirl is a well-known technique for increasing the mixing of fuel, oxidizer and products in a desired location within a small volume and thus shortening the length of a flame. Swirl can be quantified by calculating the ratio of the axial flux of angular momentum to the axial flux of axial momentum [3].

The International Flame Research Foundation, IFRF, has classified four different types of flames that utilize jets and swirl to create flames of different shapes. (M. Hupa [5]). Figure 2-2 below shows each of the four flame types. Flame type 0 refers to a flame created by a turbulent center jet of fuel injected into a relatively low velocity jet of oxidizer surrounded by hot products. The center jet shears with the outer jet creating an external recirculation zone. The

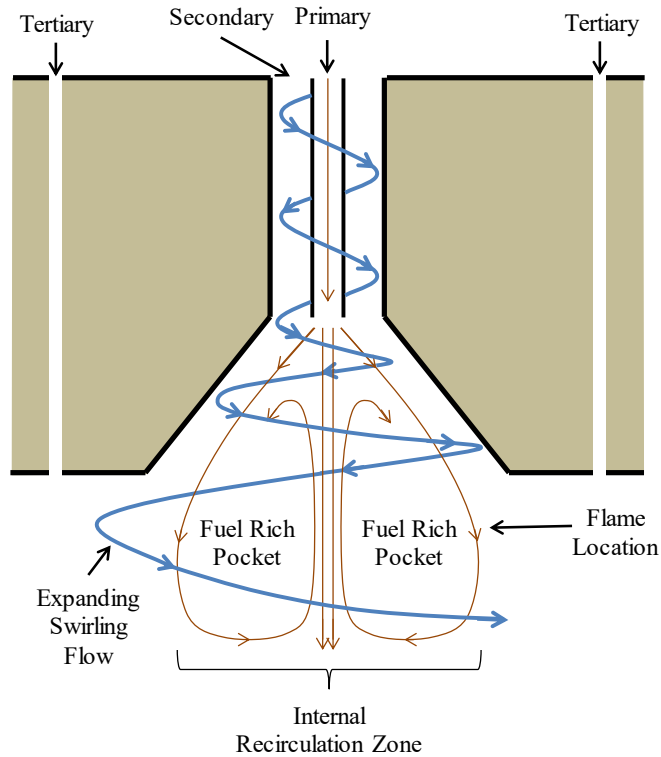


Figure 2-1: Swirled burner cross-sectional diagram depicting a fuel rich region that is surrounded by a recirculating secondary flow [4].

external recirculation produces a slow mixing of oxidizer and products from the outside of the jet toward the center jet producing a long flame. It will be seen later that the length of this flame is dominated by the diameter of the center jet, taking longer for the oxidizer to penetrate through the jet the larger the fuel jet diameter.

Flame type 1 is created by swirling the outer oxidizer jet which then move radially outward upon exiting the burner. This outward motion of the oxidizer creates a low pressure or vacuum pressure in the center of the jet causing product gases to flow upward toward the burner in the center of the jet. The internal recirculation zone flows in the opposite direction to the fuel at the centerline but in the case of Type 1 flames, the fuel momentum is higher than the recirculated

gas and the fuel penetrates through the recirculation zone producing a flame beyond this recirculating region.

Flame type 2 refers to a flame where the swirl is increased such that the fuel jet momentum is not strong enough to penetrate the recirculation zone and stagnates. This shortens and widens the flame. The rich fuel mixture is trapped within the recirculation zone and reacts at the boundary creating a conical flame on the boundary of the recirculation zone.

Flame type 3 is the same as flame type 1 but has an additional internal recirculation zone downstream of the initial recirculation zone. This flame type has two closed recirculation zones, and has high confinement. It is unusual to have a Type 3 flame.

2.2 Models and Parameters Impacting Flame Length

The burner described above can be used with laminar flow of gaseous fuel only in the center tube to highly turbulent annular flow and two phase solid/gaseous mixtures in the center tube and turbulent swirled oxidizer in the annulus. The flame length for these geometries and fuel oxidizer locations is determined by the axial distance downstream from the burner exit where the fuel and oxidizer have reached a stoichiometric mixture. Equations describing this mixing are given here for laminar flows, turbulent flows and swirled turbulent two phase flows. It is important to have a long flame length to better distribute the heat flux from the combustion and avoid hot spots in the reactor.

2.2.1 Laminar Flame Length

Laminar diffusion flames have been extensively studied and modeled for several decades since they have the easiest geometry and flow to understand. Models of even the simplest of

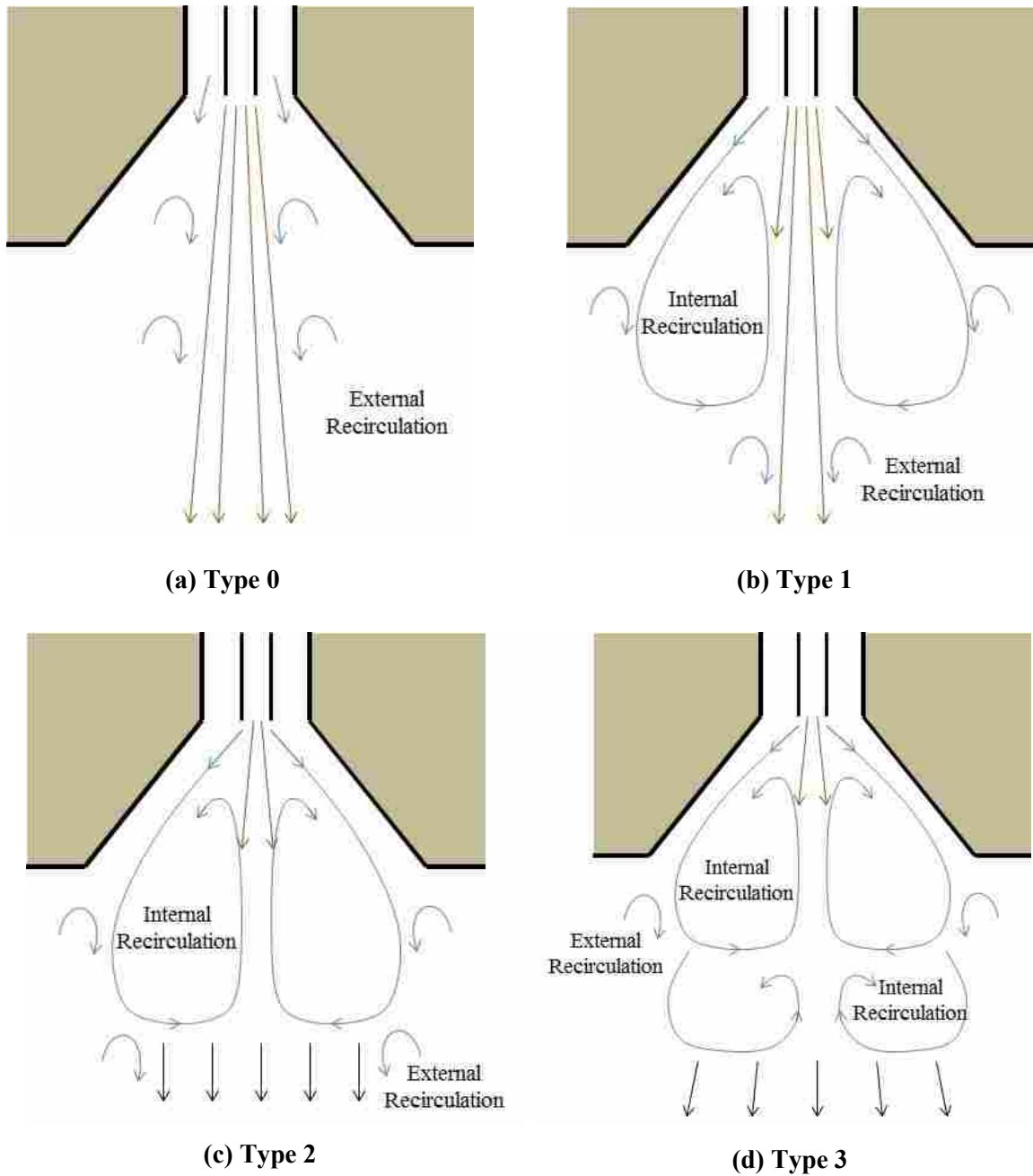


Figure 2-2: Four different types of swirled flames as designated by the IFRF: (a) Type 0, (b) Type 1, (c) Type 2, and (d) Type 3 [4].

these flames, however, are extremely complicated because equations for mass, energy, momentum, and chemical reactions must all be solved simultaneously.

Turns [6] built upon the work done by Burke and Schumann [7] and Roper [8,9] to create models for laminar flame length in a reacting circular jet. In this model, the mass, energy, species, and momentum equations were all solved for by using the mixture fraction as a scalar quantity in the mass transport equation. These equations are then solved for at the centerline (where $r = 0$) at the axial location where the mixture is stoichiometric, which allows the user to determine the flame length. This is shown below as Equation (2-1) where: Q_F represents the volumetric flow rate of the gaseous fuel, \mathcal{D} is the diffusion coefficient, and $Y_{F,stoic}$ is the stoichiometric mass fraction of fuel. The derivation of this equation assumes that the axial velocity of the oxidizer and gas streams were equal to each other so that the only mixing that occurred was due to molecular diffusion and that buoyancy effects are negligible. The result of this analysis shows the flame length for a gaseous laminar flame is only a function of the volumetric flow rate of the fuel.

$$L_f \approx \frac{3}{8\pi} \frac{1}{\mathcal{D}} \frac{Q_F}{Y_{F,stoic}} \quad (2-1)$$

Although buoyancy is neglected, the results align with data obtained experimentally. Buoyancy causes the fluid to accelerate which increases the volumetric flow rate Q_F and increases flame length but the increased velocity accelerates mixing between the fuel and oxidizer increasing viscous shearing and mixing. Thus, the two effects are offsetting. As a result, the parameters that determine the flame length of a laminar diffusion flame are the volumetric flow rate of the gaseous fuel, the diffusion coefficient, and the mass fraction of fuel under stoichiometric conditions.

2.2.2 Turbulent Flame Length

While laminar diffusion flames are much simpler to understand and model, turbulent diffusion flames are much more practical since they are more widely used in industry. Turbulence has a significant effect on fluid flow and mixing. Turbulence will cause shearing to occur between the fuel and the oxidizer and can create eddies which also accelerate the rate at which the two fluids mix with each other. Turns [10] shows that the turbulent eddy viscosity (ϵ) can be used to replace the kinematic viscosity and the simplified derivation of flame length given in Equation (2-1) becomes Equation (2-2), but now the eddy viscosity is a function of the jet velocity and the flame length is no longer a function of only the volume flow rate. Turns shows that one of the simplest models for eddy viscosity generated using mixing length models is given by Equation (2-3) where V_e is the exit velocity of the jet and R is the primary jet radius at the exit. When the eddy viscosity is substituted into Equation (2-2), the result matches empirical measurements that show the flame length is no longer a function of the volume flow rate but is dependent only on the radius or diameter of the primary jet. Thus when a jet changes from laminar to turbulent, the flame length no longer increases with increasing volume flow rate but remains a constant length. The reason the flame length remains nearly constant is that as the competing effects of increased velocity and increased mixing are offset for turbulent jets. Increased velocity causes the fuel to penetrate further in a fixed amount of time which would increase flame length but the time required to mix oxidizer into the fuel is reduced which offset the increased length.

$$L_f \approx \frac{3}{8\pi} \frac{1}{\epsilon} \frac{Q_F}{Y_{F,stoic}} \quad (2-2)$$

$$\epsilon = 0.285V_e R \quad (2-3)$$

Turns [10] shows the empirical results by Wohl et al. [11] that match this conclusion. At low volume flow rates, the flow is laminar and flame length increases with increasing flow rate but after transitioning to turbulent jets, the flame lengths become a function of primary jet diameter and remain constant with increasing volume flow rate.

2.2.3 Buoyancy Effects on Turbulent Flames

Delichatsios [12] further investigated the research performed by Becker and Liang [13] to determine buoyancy effects by examining a wide variety of turbulent vertical flames. The result of this research found that the flame length of turbulent diffusion flames was correlated to the flame Froude number of the flow. A means of calculating flame Froude number for jet flames was then developed taking into consideration the effects of stoichiometry in combustion. Turns [10] reports the results of Delichatsios in Equations (2-4) through (2-6). where relations between the Froude number, Fr_f , dimensionless flame length, L^* , and flame length, L_f are given. In these equations d_j represents the diameter of the exit nozzle (or tube in the case of this work), The subscript (∞) represents ambient air conditions, V_e is the fuel nozzle exit velocity, f_s is stoichiometric mixture fraction, ρ_e is the fuel density, and ΔT_f is the characteristic temperature rise from combustion.

From this model, it can be seen that the four primary factors that affect the length of turbulent jet diffusion flames are: 1) initial jet momentum flux and buoyant forces acting on the

flame (Fr_f), 2) stoichiometry (f_s), 3) ratio of the density of fuel exiting the nozzle and the ambient gas (ρ_e/ρ_∞), and 4) exit jet diameter (d_j). When the flame Froude number is much

$$Fr_f = \frac{V_e f_s^{3/2}}{\left(\frac{\rho_e}{\rho_\infty}\right)^{1/4} \left(\frac{\Delta T_f}{T_\infty} g d_j\right)^{1/2}} \quad (2-4)$$

$$L^* = \frac{13.5 Fr_f^{2/5}}{(1 + 0.07 Fr_f^2)^{1/5}} \quad (2-5)$$

$$L_f = \frac{L^* d_j \sqrt{\rho_e/\rho_\infty}}{f_s} \quad (2-6)$$

larger than 1, meaning the fuel jet has a strong initial momentum, the effects of momentum overcome the effects of buoyancy and the flame length is no longer a function of the flame Froude number, Fr_f . Under these conditions, the flame length is only a function of the burner jet diameter, and the fuel stoichiometric mixture fraction. This means that for a specified fuel type, the flame length is only a function of the burner diameter when there is a strong initial momentum in the fuel jet.

2.2.4 Swirled Turbulent Flames

Chen and Driscoll [14] developed a model for the length of swirl stabilized turbulent flames. Using the same fundamental idea that the flame length is fixed by the length required to mix a stoichiometric amount of oxidizer into the fuel, they argued that the swirled oxidizer

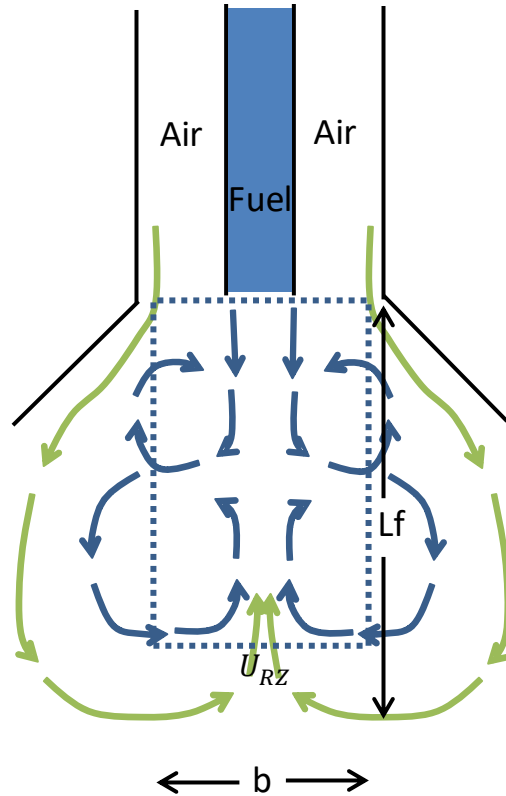


Figure 2-3: Schematic diagram of the fuel and air flow of a simple swirled gas flame [15].

surrounding a fuel jet could mix with the jet in two ways: 1) through diffusion at the interface between the fuel and the oxidizer jets, just as is done with non-swirled laminar and turbulent flames and 2) by oxidizer flowing into the fuel caused by the radial component of axial velocity (U_{RZ}) created by the internal recirculation zone. An imaginary cylinder shown in Figure 2-3 represents the boundary where oxidizer is crossing into the fuel rich region.

Chen and Driscoll [14] set the ratio of the mixture of stoichiometric air to fuel equal to a constant C_s . as seen in Equation (2-7), where the numerator is the volumetric flow rate of the fuel exiting the fuel nozzle and the denominator is the volumetric flow rate of the oxidizer mixing with the fuel stream. There are two components of oxidizer velocity shown in Equation (2-8) flowing into the fuel rich zone. The first term is flow due to recirculation created by U_{RZ} and the

second is flow created by shearing between the different velocities of the fuel U_F and the secondary oxidizer U_A . In Equation (2-7), d_F represents the diameter of the primary fuel nozzle, L , the length of the cylindrical boundary where oxidizer is entrained, which is the flame length, and a diameter of b , which is the widest diameter at which the calculated average axial velocity is zero. This makes the area πbL , as seen in the denominator of the Equation (2-7).

$$C_s = \frac{\frac{\pi d_F^2}{4} U_F}{\pi b L U_C} \quad (2-7)$$

$$U_C = \pi b L U_{RZ} + \pi L |U_F - U_A| d_F C_{const} \quad (2-8)$$

When Equation (2-8) is combined with Equation (2-7) and then re-arranged, Equation (2-9) is formed which predicts a flame length, L . In Equation (2-9), the subscript A represents properties referring to the air stream and subscript F represents properties referring to the fuel stream, U refers to velocity, d refers to diameter, \dot{m} refers to mass flow, and c_1 and c_2 are empirically derived proportionality constants.

$$\frac{L}{d_A} = \frac{c_1 (\dot{m}_F / \dot{m}_A)}{\left(\frac{U_{RZ} b}{U_A d_A} + \frac{|U_A - U_F| d_F}{U_A d_A} c_2 \right)} \quad (2-9)$$

Note that the flame length can be reduced by increasing the recirculation mixing velocity U_{RZ} . The characteristic recirculation zone velocity, U_{RZ} , as defined by Equation (2-10) was measured empirically by Chen and Driscoll [14] and a correlation was developed from their data by Ashworth [15] as shown in Equation (2-11).

The correlation for the flame length given by Equation (2-9) for a turbulent swirled diffusion flame suggests that the flame length scales with the diameter of the fuel tube and can be reduced by increasing the swirl or by increasing the difference in velocity between the primary fuel and the secondary oxidizer.

$$U_{RZ} = \int_0^b -U_z 2\pi r dr / \pi b^2 \quad (2-10)$$

$$U_{RZ} = \frac{0.23 * S^4 * V_{sec}}{0.004 + S^4} \quad (2-11)$$

2.3 Oxy-coal Burner Design

Burners for oxy-coal combustion are uncommon and burners for pressurized oxy-coal combustion have yet to be demonstrated. This section will review existing oxy-coal burners in context of flame types and flame lengths as described in the previous sections.

In particular, some examples of oxy-coal burners in the range of 20-300 kW_{th} were studied and compared to get a baseline for the design of a pressurized oxy-coal burner. A list of burners, heat rates and design features is shown in Table 2-1. Three design features are classified in the table: the geometric location of the fuel and oxidizer (annular vs. separated tube delivery), the amount of swirl, the presence of a quarl (quarl or no quarl).

In each of the burners, the fuel is conveyed to and through the burner using a carrier gas of CO₂ as a surrogate for recycled flue gas. In some instances, small amounts of oxygen were added to this primary carrier gas to simulate the oxygen present in air which is normally used in coal burners. The concentration of oxygen in the carrier gas was held to 30% or less of the total

carrier gas or 10% or less of the stoichiometric amount needed to completely oxidize the coal. For air-fired burners, pulverized coal is conveyed with approximately an equal mass of air and coal.

All five of the burners used fuel introduced in a primary tube with oxygen introduced in annular tubes surrounding the primary tube but the Huazhong burner also had tertiary tubes separated from the primary tube to introduce some of the oxidizer. Tubes that are separated from the center of the burner where fuel is introduced can be called lances although this term is also reserved for a tube which protrudes from the burner. Either way, these tubes are spatially separated from the primary and secondary oxygen in order to delay oxygen mixing into the fuel stream until later.

All five of the burners used swirl to some degree to stabilize the flame with swirl ranging from 0.47 to 1.75. In addition to swirl, the burners from Darmstadt and Aachen used a bluff body to stabilize the flame. A bluff body is a disc or some other object placed perpendicular to the flows such that the flow produces a recirculation zone as it moves around the object. All but one of the burners utilized a quarl to confine the flame.

One of the main goals of the burners studied was to produce a stable and attached flame but also an elongated flame so that the heat flux profile stretched axially and the heat could be more evenly distributed from the burner downstream throughout the combustion vessel. Although swirl is not desirable for producing a long flame, all five burners which were studied introduced swirl indicating that it is at least a parameter that was desired to change flame shape if not necessary to stabilize the flame. For those similar reasons, four of the five burners studied also had a quarl, to facilitate a recirculation zone and enhance mixing. The burner that did not have a quarl had the ability to add one later during testing. Each of the five studied burners

Table 2-1. Summary of Atmospheric Oxy-Combustion Reactors.

Burner Location	Burner Size (kW) _{th}	Burner Types	Swirl	Quarl	Reference
Brigham Young University (USA)	150	Tri-axial with annuli	0.6-1.5	Yes	[15], [16]
Technological Educational Institute Chalkis (Greece)	100	Annuli with central gas stream	0.6-0.9	No	[17]
State Key Laboratory of Coal Combustion (Huazhong Univ. of Science and Technology, China)	300	Annuli for Primary and Secondary streams, with oxygen jet lances	0-1.75	Yes	[18]
TU Darmstadt (Germany)	20	Annuli w/ bluff body	0.47	Yes	[19]
RWTH Aachen University (Germany)	60	Annuli w/ bluff body	0.95	Yes	[20]

utilized at least one annulus, many of them had a few layers of annuli for separate delivery of the oxygen, coal, and carrier gas.

2.4 Existing Pressurized Oxy-coal Burners

Details could only be found for one pressurized oxy-coal burner design by Gopan et al. [21] which is summarized in Table 2-2 and a cross-section of the schematic is shown in Figure 2-4. The figure shows the layout of the burner with pure O₂ in the center tube, coal and CO₂ (which acts as a carrier gas for the coal) in the narrow inner annulus, and more O₂ as well as additional CO₂ in the outer annulus. The primary objective of Gopan et al. [21] was to prolong the mixing of the fuel and oxidizer for as long as possible in order to elongate the flame. This

Table 2-2. Summary of Pressurized Oxy-Combustion Reactor.

Burner Location	Burner Size (MW) _{th}	Burner Types	Swirl	Quarl	Reference
Wash. U in St. L.	385	Tri-axial with Annuli	0	No	[21]

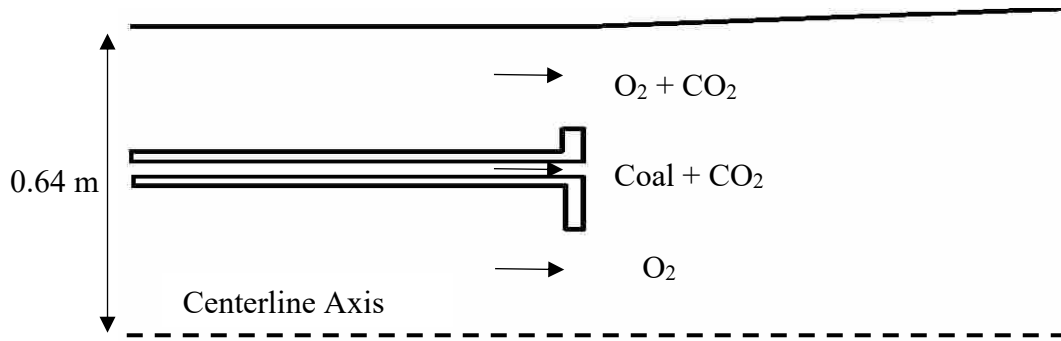


Figure 2-4: Schematic of burner studied by Gopan et al [21].

was done by matching the velocities of the fuel and oxidizer streams in order to prevent shear between the different jets of gases. The design of their burner also included a gradually increasing diameter to the outer wall to account for the gases expanding as they heated up in the reactor to further prevent shear between the gaseous jets.

It should be noted that this burner was never actually built, and relied solely on CFD models with no experimental data to support the calculated results. This burner was also designed for a very large scale (385 MW) compared to the laboratory scale burners (20 – 300 kW) summarized in Table 2-2.

2.5 Summary Related to Pressurized Oxy-coal Combustion

It is important to consider the implications of existing designs and correlations on the design of an oxy-coal burner. If laminar, the flame length for an oxy-coal burner would be expected to scale with volumetric flow rate. The volumetric flow rate decreases proportionally with pressure and therefore the oxy-coal flame would be 20 times shorter at 20 atm. compared to 1 atm. This is the challenge of the oxy-coal burner because such a short flame length would release high amounts of energy in a short distance from the burner creating very high

temperatures and potentially melting the burner and nearby components. The challenge for the pressurized oxy-coal burner is to prolong this flame length over a reasonable length.

An important parameter to consider for the burner is the primary flow Reynolds number as shown in Equation (2-12). An increase in the Reynolds number could produce a turbulent jet for which the flame length becomes a function of primary tube diameter. The density, velocity and viscosity in the Reynolds number have been related to pressure, temperature and tube diameter and result in an expression for how the Reynolds number will change with a change in pressure and tube diameter. The result shows that Reynolds number will increase proportional to pressure and will increase yet again if the tube diameter is increased. It is therefore likely that a turbulent primary jet will be produced and the flame length will be dominated by the tube diameter as long as that diameter produces turbulent flow.

If turbulent, increasing the diameter of the jet will produce the longest flame which argues for increasing the diameter. However, a third consideration must be made. For a down-fired reactor, the flame Froude number must be high enough that momentum dominates the forces on the primary flow. If buoyancy dominates, the flow will stagnate and reverse direction back towards the burner. According to Turns [10], a flame Froude number of 4 is required for a flow to be dominated by momentum. This would require that the primary tube diameter be smaller than 2 mm which would begin to plug the tube with pulverized coal.

$$Re = \frac{\rho V D}{\mu} \approx \frac{P}{RT} \frac{1}{D^2} D = \frac{P}{RT^{1/2} D} \quad (2-12)$$

Decreasing the diameter of the primary tube will add velocity to the primary mixture such that a decrease in diameter will produce an increase in velocity squared.

2.6 Comprehensive Coal Combustion Modeling

While the flame types and correlations discussed can provide insights into the variables that impact flame length and shape, the simplifications and assumptions made to produce these correlations are insufficient for the complex mechanisms occurring in pulverized coal combustion. All of the above results apply to gaseous flames but coal begins as a solid and requires heating and devolatilization before gaseous fuel is produced. Char and ash remain after devolatilization and prolong the reaction zone and heat release. A complete model of coal combustion requires energy, mass, momentum, and reaction equations and is far beyond the scope of this work. However, given the importance of predictions in selecting a design, Reaction Engineering Incorporated (REI) was hired to produce simulations of three burner designs; one at low primary flow velocities and one at high primary flow velocities in order to produce result that could be interpolated to produce a final design which was also simulated. All designs had coal and CO₂ in the center, primary tube, CO₂ and O₂ in the inner secondary annulus, CO₂ and O₂ in the tertiary lances, and were run at a pressure of 20 atm.

3 METHODS

The calculations and methods used to design the diffusion flame burner, POC reactor, and layout of the room that houses the POC reactor are presented in this section. Schematics, equations, and design parameters are included as part of this design documentation.

3.1 Burner Design

The burner design process began by defining performance requirements and design constraints. A simple spreadsheet model was used to calculate flow rates, areas, and velocities in order to size components. A one-dimensional energy model was run to estimate the required dilution ratio of CO₂ to keep the outlet gas temperature in the correct range. Finally, a three dimensional comprehensive combustion model was used to predict gas and wall temperature distributions, outlet temperature, and flow patterns. The comprehensive 3-D combustion model was then used to determine the final design of the burner based on the results of the simulations. The objective of the burner design was to create a Type 0 flame, as shown in Figure 2-2 and described in Section 2.1. A Type 0 flame will result in a longer flame since the recirculation zones in the other flame types will enhance mixing and cause shorter flames.

3.1.1 Performance Requirements and Design Constraints

The design requirements for the POC reactor are listed in Table 3-1. The desired thermal output of the reactor was set at 100 kW and the coal selected was a Utah bituminous coal from the Skyline mine because it would feed more easily than lower rank higher moisture coals. The steel shell temperature must remain below 505.4 K (450 °F) in order to safely contain the required pressure of 20 atm. The inner refractory material was selected to be Ultragreen SR based on past experience which is rated up to 2144.3 K (3400 °F). In order to keep the ash component of the coal molten and the slag flowing, the gas temperature at the reactor exit needed to be 1588.7 K (2400 °F). The coal is to be fed with a CO₂ carrier gas. It was unknown how much gas will be required but a 1:1 coal to CO₂ ratio is typically reasonable as a minimum while higher flow rates of CO₂ might be necessary to keep temperatures low enough for refractory and shell. Additionally, the reactor had to accommodate a flame sensor which require a line-of-sight no more than 254 mm (10 inches) below the burner through a cylindrical access port with a diameter of 12.7 mm (1/2 inch). Another important requirement was that any component that needed adjustments or fabrication in-house had to be less than 152.4 mm (6 inches) in diameter due to pressure vessel safety regulations.

In addition to these quantitative requirements, it was desirable to use as little CO₂ as possible in order to reduce the amount of recycled flue gas required. It was also important to distribute the energy released from the coal over as wide a distance as possible in order to avoid hot spots and facilitate an even heat flux to surrounding walls.

3.1.2 Spreadsheet Modeling

The driving factors for designing the burner were the mass flow rates of the various streams that were to flow into the POC reactor. The calculation for these burner flow rates began

Table 3-1: Performance Requirements and Design Constraints

Requirement or Constraint	English Units	S.I.
Thermal Output	341200 Btu/hr	100 kW
Fuel – Skyline Coal	N/A	N/A
Pressure – 20 atm.	294 psi	2020 kPa
Max. Shell Temperature	450 °F	505 K
Refractory Max Temperature	3400 °F	2144 K
Min. Exit Gas Temperature	2400 °F	1589 K

by first determining the flow rate of coal. The target power output of the POC reactor is 100 kW_{th}. Using Skyline Utah Bituminous Coal which has a Higher Heating Value (HHV) of 29,322 kJ/kg, the calculated flow rate of coal was 0.00341 kg/s. The target stoichiometric ratio (ϕ) was 1.11 as running lean would allow for the coal to more fully mix to allow more complete combustion while considering imperfect mixing. The stoichiometric ratio is the ratio of the mass of the fuel divided by the mass of the oxidizer divided by the stoichiometric mass ratio of fuel to oxidizer, as shown in Equation (3-1). Based on the coal mass flow rate, and ϕ , the resulting O₂ flow rate was 0.00834 kg/s. It was assumed that a 1-to-1 mass flow ratio of CO₂ to coal was needed to carry the coal into the reactor since the reactor operates on a dry-feed system. In addition to the CO₂ needed to carry the coal into the reactor, additional CO₂ was needed to act as a diluent to decrease the temperature inside the combustion chamber and also provide more mass with which to increase the momentum of the oxygen streams in order to propel those jets farther down the reactor.

$$\frac{(m_{fuel}/m_{ox})}{(m_{fuel}/m_{ox})_{stoich}} \quad (3-1)$$

A spreadsheet model was created in order to quickly relate flow rate, velocity and diameter of components in the burner. Equations (3-2) through (3-7) were used in the

spreadsheet model for these calculations. It was expected that the burner would have separate primary, secondary and tertiary flows with one or more tubes for each of these flows. The burner geometry including the diameter and number of tubes was drawn in a CAD model to ensure the sizes could be reasonably manufactured and fit within the given requirements. The burner inputs, along with the spreadsheet results were sent to Reaction Engineering International (REI) for comprehensive combustion simulations.

It was assumed that all of the flows would be passing through tubing of circular geometry with an average velocity profiles such that the flow rate and velocity were represented by Equation (3-2); where ρ is the density, U is the velocity, and A is the area. The tubes may contain a mixture of either an ideal gas or an ideal gas and pulverized coal.

$$\dot{m} = \rho UA \quad (3-2)$$

For an ideal gas mixture, the density can be replaced by the density of the mixture as given by Equation (3-3) where P and T are pressure and temperature respectively and R_{mix} , the gas constant for the mixture is found from Equation (3-4) with R_u being the universal gas constant.

$$\rho_{mix} = \frac{P}{R_{mix} * T} \quad (3-3)$$

$$R_{mix} = \frac{R_u}{MW_{mix}} \quad (3-4)$$

The molecular weight of the mixture can be found by Equation (3-5) with y_i being the molar fraction for a given species in the mixture.

$$MW_{mix} = \sum y_i MW_i \quad (3-5)$$

When the mixture consists of an ideal gas and a solid such as CO₂ and pulverized coal, the density of the mixture becomes Equation (3-6).

$$\rho_{mix} = \frac{m_{gas} + m_{coal}}{V_{total}} = \frac{m_{gas}(1 + K)}{m_{gas}/\rho_{gas} + m_{coal}/\rho_{coal}} \quad (3-6)$$

Where: K is the coal to gas mass ratio.

The area for an annulus is related to the inner and outer diameters by Equation (3-7).

$$A = \frac{\pi}{4} (D_{outer}^2 - D_{inner}^2) \quad (3-7)$$

In order to produce a burner that would operate at both atmospheric pressure during heat up and 20 atm. during normal operation, it was necessary to feed the oxidizer through different diameter tubes. While the density increases drastically, the mass flow rate remains constant between heat up and full pressure operation. Therefore, it was decided to utilize an outer annulus for the secondary air during heat up with a larger area and then switch the oxidizer to a smaller annulus during high pressure operation. Another significant challenge was to get a significant velocity in the primary and secondary flows without making the tube so small that fuel particles could not pass through. Once the ideal tube diameters were calculated, commercially available tubes were identified with sizes that matched as closely as possible to the calculated diameters. It was impossible to find tubing that was exactly the diameter that was calculated, but available

sizes that matched the calculated sizes fairly well were found and used in the construction of the burner.

Figure 3-1 demonstrates the drastic affect that pressure has on the velocity of a flow for a given tube diameter. In this figure, the mass flow rate, mixture gas constant, and temperature are all held constant for the given diameters, but the pressures are different for the two different lines. It can be seen that while holding all other properties constant, pressure is inversely proportional to the velocity of a mixture for a given diameter.

3.1.3 Energy Balance 1-D Modeling

A one dimensional energy balance program, Steamgen Expert, was run by Dr. Bradley Adams and his students to identify flow rates that could be used to meet the design criteria for reactor exit temperature to predict the performance of the burner design in the reactor. The results were then compared to the process models of the energy balance on the reactor performed by other researchers at BYU led by Dr. Adams. This process was iterated three times to make adjustments in order to optimize the design. The first iteration was to examine what the flame would look like with a moderate velocity (5 m/s) in the primary flow, a slow velocity around 1 m/s in the secondary annulus, and a relatively fast velocity of 10 m/s in the tertiary flow. The second iteration was to see what the performance would be with slow velocities in all of the flows (~0.5 m/s). The third and final iteration was with moderate velocities of 5 m/s in the primary, secondary, and tertiary flows.

The main goal for this burner design was to elongate the flame. This was done by designing the burner to match the velocities in each of the gas jets to minimize shear between

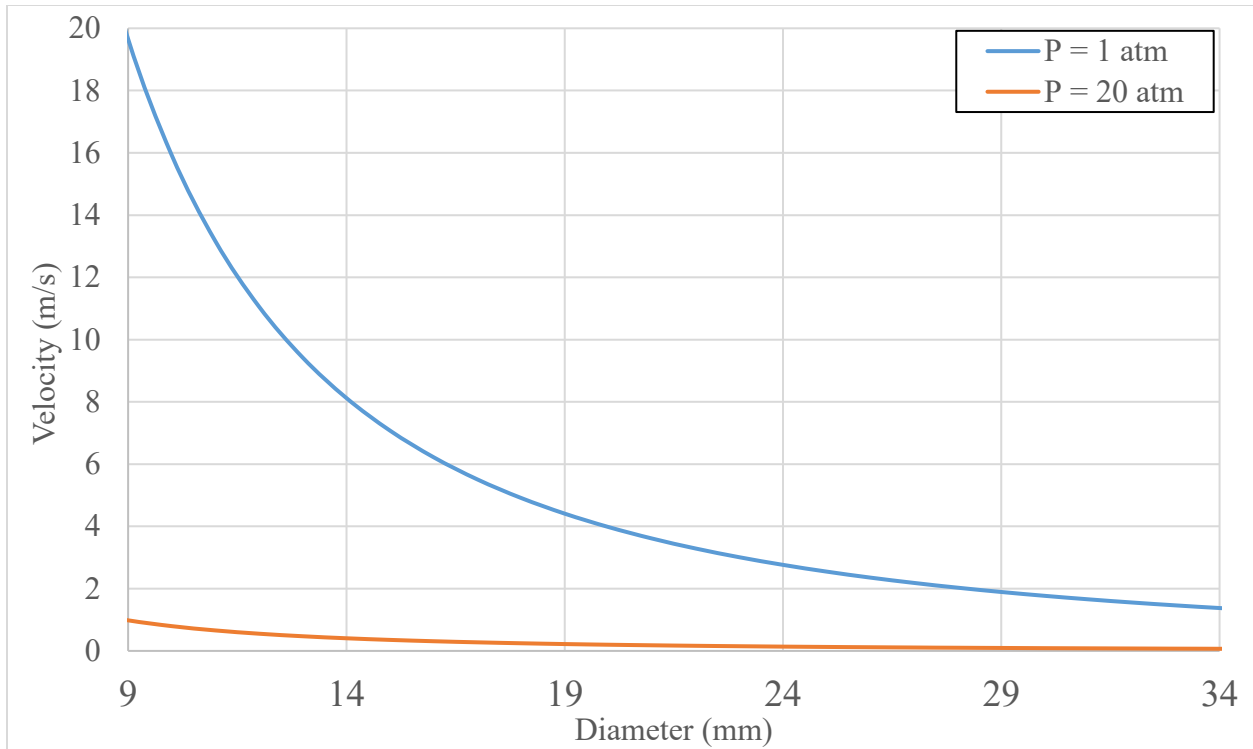


Figure 3-1: Effects of Pressure on Velocity for Given Tube Diameters.

incoming jets in order to delay the mixing of the coal and oxygen for as long as possible. The objective was to prevent, or at the very least minimize, any formation of a recirculation zone, as characterized by Type 0 flames, which would drastically speed up the rate at which the fuel and oxidizer was mixed thus making the flame shorter. The inlet gases are considered ideal gases, and velocity is inversely proportional to density and pressure for a given flow rate.

3.1.4 3-D Comprehensive Modeling

Three iterations of reactor operating parameters were sent to Reaction Engineering International (REI) for simulation. Table 3-2 shows the operating conditions for each of the three test cases that were performed by REI. All three cases have the flow rate of coal necessary to generate 100 kW_{th} of heat, the first case used a slightly different proximate analysis for Skyline specifications of coal with a slightly different heating value than was used for the other two

cases, which is why the coal mass flow rate of Case 1 is slightly different from Cases 2 and 3. Each of the three cases has a 1-to-1 mass flow ratio of CO₂ to coal to carry the coal into the reactor. The first case was set up to use as little CO₂ as possible and push the limit of having enough diluent gas. The secondary annulus had 20% of the total oxygen for that case, and had no CO₂. There were four tertiary lances in this case, and they had the remaining oxygen and CO₂. The idea for having 20% of the oxygen in the secondary annulus was to provide a sufficient amount of oxidizer so that the flame would remain attached, but have the majority of the oxygen separated from the fuel in order to delay mixing and reaction with the coal.

The second case went to the other extreme with the overall CO₂ to coal ratio, with CO₂ having eight times the mass flow rate as coal in the reactor. This would provide more than enough CO₂ to act as a diluent. The reasoning behind this method was to undershoot the amount of CO₂ needed in the first case, and overshoot in the second case in order to determine the sensitivity of the performance of the burner to the amount of CO₂ present in the reactor. The third case was then designed to be in the middle of these two scenarios with the results of the first two cases being used to determine whether or not to go more towards the high or low end of CO₂ used in the reactor. Case 2 again had 20% of the total amount of oxygen and no CO₂ in the secondary annulus with the remaining oxygen and CO₂ in the tertiary lances. This case also consisted of eight lances, rather than four from the previous case in order to distribute the oxygen more evenly around the perimeter of the burner.

For the third and final test case, it was decided to use only 10.4% of the total oxygen in the secondary annulus in order to have an even higher percentage of the oxygen further removed from the flame, this was to help delay the mixing of the fuel and oxidizer even more and it was estimated that 10.4% of the oxygen in the secondary annulus was sufficient to maintain an

attached and stable flame. Since less oxygen was present in the secondary annulus, CO₂ was added to the secondary flow in order to provide enough mass flow rate to have a sufficient velocity to carry the oxidizer downstream and maintain the same velocity as the fuel in the primary jet. For this case a coal to CO₂ ratio of 4.21 was used, as this would lower the amount of diluent gas from the previous case, but still provide enough to keep the temperatures in an acceptable range. Again, eight tertiary lances were used in this design to more evenly spread out the oxygen around the perimeter of the burner.

3.1.5 Manifold Orifice Calculations

In addition to designing the tube sizes and layout for the burner, a manifold also had to be designed and built upstream of the burner in order to get the mixture of oxygen and carbon dioxide from a single tube to eight separate tubes for the tertiary lances. A major concern with the manifold was getting even flow rates in each of the lines leaving the manifold. In order to achieve this, a large pressure drop was needed across a restrictive orifice at each of the manifold output lines going into the tertiary lances. Ideally, the flow would be choked across each orifice to allow the flow to be regulated by the upstream pressure only. However, the supply tank pressure (3,103 KPa) was not large enough for the given back pressure of 2,026.5 KPa to produce choked flow. As a result, Equations (3-8) through (3-10), below, from Çengel and Cimbala [22], were used to calculate the anticipated flow from for each tertiary tube. In Equation (3-7), the area, A_o represents the orifice size. The discharge coefficient, C_d , was calculated in Equation (3-9),

Table 3-2: Operating Parameters for Three REI Test Cases.

		Case 1	Case 2	Case 3
Primary Stream	$\dot{m}_{\text{coal.primary}}$	0.00379 kg/s	0.00341 kg/s	0.00341 kg/s
	$\dot{m}_{\text{CO}_2.\text{primary}}$	0.00379 kg/s	0.00341 kg/s	0.00341 kg/s
Secondary Stream	$\dot{m}_{\text{O}_2.\text{secondary}}$	0.0016 kg/s	0.001668 kg/s	0.000874 kg/s
	$\dot{m}_{\text{CO}_2.\text{secondary}}$	0 kg/s	0 kg/s	0.003497 kg/s
	% O ₂ in Secondary	20	20	10.4
Tertiary Stream	$\dot{m}_{\text{O}_2.\text{tertiary}}$	0.0064 kg/s	0.006672 kg/s	0.007466 kg/s
	$\dot{m}_{\text{CO}_2.\text{tertiary}}$	0.00303 kg/s	0.02387 kg/s	0.007466 kg/s
	Number of Lances	4	8	8
	Overall CO ₂ to Coal Ratio	1.8:1	8:1	4.21:1

$$\dot{V} = A_o * C_d \sqrt{\frac{2(P_1 - P_2)}{\rho(1 - \beta^4)}} \quad (3-8)$$

$$C_d = 0.5959 + .0312\beta^{2.1} - 0.184\beta^8 + \frac{91.71\beta^{2.5}}{Re^{0.75}} \quad (3-9)$$

where β is calculated in Equation below with d being the throat diameter of the orifice and D the diameter of the tube.

$$\beta = \frac{d}{D} \quad (3-10)$$

3.2 Design of Reactor Components

The engineering drawings of the POC reactor were created throughout the burner design phase. Pre-determined factors for the design of the reactor included the carbon steel shell that

would be air-cooled and be 1.829 m (6 feet) in length and have an outer diameter of 762 mm (30 inches). Iterations of the design of the number, sizing, and orientation of access ports along the reactor main section were completed as part of this work. The objective was to have as many ports as close to each other as possible in the axial direction, while still allowing enough clearance between parts to adjust bolts and install parts on the reactor. The appropriate size and number of flanges, threaded studs, washers, and bolts was determined for the various components that made up the reactor. The size and location of piping connected to the reactor in order to accommodate a pressure relief was also determined through iterations of CAD modeling. An exit nozzle was designed to allow the reactor to connect with the exhaust system for the flue gases. The length of this nozzle had to be carefully designed in conjunction of the design of the room layout in order to place the components in advantageous positions close enough to I-beams for support, without interfering with the necessary support structure to hold the reactor and its accompanying components. The shape and dimensions of the castable refractory in the bottom section of the reactor to accommodate the pressure relief valve and the exit nozzle were also designed through iterations of CAD modeling to ensure slag would flow past the openings and allow for the exhaust products to flow through the exit to the components of the exhaust system.

Support legs to mount the reactor onto I-beams were also designed as part of this project. CAD designs were created for three different widths of support legs. The CAD models were used to determine clearances and ensure that the necessary nuts and bolts could fit between the webs of the legs onto the reactor, and still have enough room to use the necessary tools to install the nuts and bolts to connect the reactor to the support I-beams. Finite element analysis (FEA) of each of these three different designs were used to ensure the support legs were strong enough,

with a sizable safety factor. The first design was 152.4 mm (6 inches) wide, the second was 203.2 mm (8 inches) wide, and the final design was 304.8 mm (12 inches) wide.

Upon completion of the design, the drawings were sent to Structural Steel and Plate Fabrication, an engineering firm, to fabricate the pressure vessel components and get them stamped by licensed engineers. All components with a diameter greater than 152.4 mm (6 inches) had to be fabricated by a professional engineering firm and get an engineering stamp of approval before being put in operation. Components less than 0.1524 m (6 inches) in diameter were manufactured and adjusted on campus as part of this project along with the adjustment of some Swagelok fittings. The casting and placement of refractory, along with thermocouples and other sensors also took place at BYU by student researchers.

The reactor assembly is complete and ready to be used to test the burner, feed, and exhaust systems. Measurements expected to be read from the reactor include: reactor fuel and oxidizer flow rates, wall temperature profile, reactor shell temperature profile, radiative heat flux, gas temperature profile, visual flame position, and exit gas temperature. The skin temperatures will be monitored in order to meet the design restrictions, and diluent flow rates will be adjusted in order to maintain acceptable burner and reactor shell temperatures. The reactor will also be inspected to see the amount of wall deposition inside of the reactor to ensure proper slagging of the ash.

3.3 Room Layout Design

In order to make the best use of the room that houses the POC reactor, the layout of the components of the POC reactor along with the support structure had to be carefully designed. Once the best location and orientation for the reactor to be situated in the room was established, the subsequent components of the system were imported into a CAD model of the room to

determine the other component spacing and orientation. The CAD model of the room and all reactor components were to scale. Care was taken to ensure that there was sufficient space between components and walls to maneuver in the room, and make necessary adjustments to equipment which often requires the use of tools and ladders. Some of the major components that had to be considered when designing the layout and support system of the room included: the POC reactor, the exit nozzle with spray, the heat exchanger, the cyclone, valves/ductwork to pressurize the system and exhaust the flue gas, the mezzanine, and the stairway to reach the second floor mezzanine. The reactor was by far the heaviest component that needed to be held by the support structure. Table 3-3 shows the components of the reactor and their respective masses. The orientation and spacing of the I-beams was designed to distribute the weight of the reactor as evenly as possible between several wall connections, and support columns that were installed where walls could not be used, such as in the center of the room, and along the north wall, where the wall is not load-bearing.

3.4 Burner Test Procedures

Testing of the burner was performed outside of the reactor in an open room in order to troubleshoot problems that may have been encountered. Flexible PVC hoses were used with Swagelok components to connect the burner to the mass flow controllers. The burner was laid down horizontally for this testing. The stoichiometric ratio was calculated for methane-air with stoichiometric values of fuel and air for certain flow rates corresponding to thermal energy for methane. Testing was first performed by only turning on the methane and letting the air from the room mix with the fuel to provide the oxidizer. Air from the mass flow controllers was then turned on to see how that affected the flame. The last type of testing performed on the burner

Table 3-3: Components and their Corresponding Masses to be Supported by Central Beam in Reactor Room.

Component	Total Mass of Components (in kg)	Mass Supported by Central Beam (in kg)
Reactor	5469.39	1367.35
I beams	361.12	90.28
Grating	867.75	216.94
Side Rails	58.96	33.56
Square Tube	191.84	191.84
	Total Mass Supported by Center Column:	1900 (kg)

was an attempt to introduce swirl to the air in the secondary annulus and again see how that affected the flame.

The atmospheric burner tests were performed to determine if the burner, which was designed and optimized to operate at high pressure burning coal, could also be used to heat up the reactor at low pressure using natural gas. This testing was also to see if any adjustments to the flow would be needed, such as adding swirl to the outer secondary annulus through which air flows. Due to unforeseen and uncontrollable circumstances with building utilities, construction of the building and the POC reactor, along with delays in the control system of the reactor, burner testing in the reactor was unable to be performed.

4 RESULTS AND DISCUSSION

Results including the design of the burner, reactor, and room layout for the Pressurized Oxy-coal (POC) reactor, combustion simulation results obtained from Reaction Engineering International (REI), and preliminary measurements from the burner are included in this chapter. Engineering drawings, schematics, equations, and design parameters are included as part of this design documentation.

4.1 Description of Entire POC

The POC reactor shown in Figure 4-1 is a down fired 100 KW_{th} reactor that consists of four refractory-lined sections: 1) the top section, 2) the burner which sits inside the top section, 3) the main combustion chamber section, and 4) the bottom exhaust section.

The top section is comprised of a dome shaped cap that is 762 mm (30") in diameter at the base with a 203 mm (8 inch) pipe welded on top. A 203 mm (8 inch) slip-on-flange is welded onto the pipe. A 203 mm (8 inch) pipe attached to the top of the cap. Inside the cap is a 101.6 mm (4 inch) refractory ring with an inner diameter of 210 mm (8.25 inch) and an outer diameter that matches the inner wall of the dome. This hole in the refractory is designed to allow a 203 mm (8 inch) burner to be installed inside the refractory. This top section houses the burner and sits on top of the main section as labelled in Figure 4-1.

The burner is made up of a refractory cylinder connected to a 203.2mm (9 inch) flange with concentric tubes that transport the primary, secondary, and tertiary flows into the reactor so they can mix and react with one another. Details of the burner geometry can be seen in Section 4.2. The burner begins on top of the top section of the reactor, and ends at the top of the main section of the reactor as can be seen in Figure 4-1.

The main section of the reactor is where the combustion will occur and various measurements will be taken. This section has a 0.762 m (30") outer diameter steel shell with several layers of refractory inside of it, with an inner diameter of 0.203 m (8 inch), which is where the combustion happens and the gases and particles flow. This section is 1.83 m (6 feet) long and has five sets evenly distributed along the axis of the reactor with four ports rotated evenly around the reactor in each set. Each set is spaced 0.305 m (1 foot) from the other set along the axis of the reactor. These ports have an inner diameter of 0.0492 m (1.939") and are used to provide optical access into the reactor, along with access for thermocouples and other measurement devices. The outline of the main section of the reactor, with the attached optical and access ports is shown in Figure 4-1.

Below the main section of the reactor is the bottom or exhaust section also shown in Figure 4-1. This section was designed for slag collection, and provides an exit nozzle for the flue gases to leave the reactor and enter the exhaust system. The bottom section also includes a pressure relief valve as a safety precaution to prevent the pressure in the POC reactor from building up too high and becoming unsafe. The castable refractory in this section is a shaped like a converging-diverging nozzle. The refractory was designed that way to act as a slag tap, and the exit nozzle intersects with the throat of this nozzle-shaped refractory.

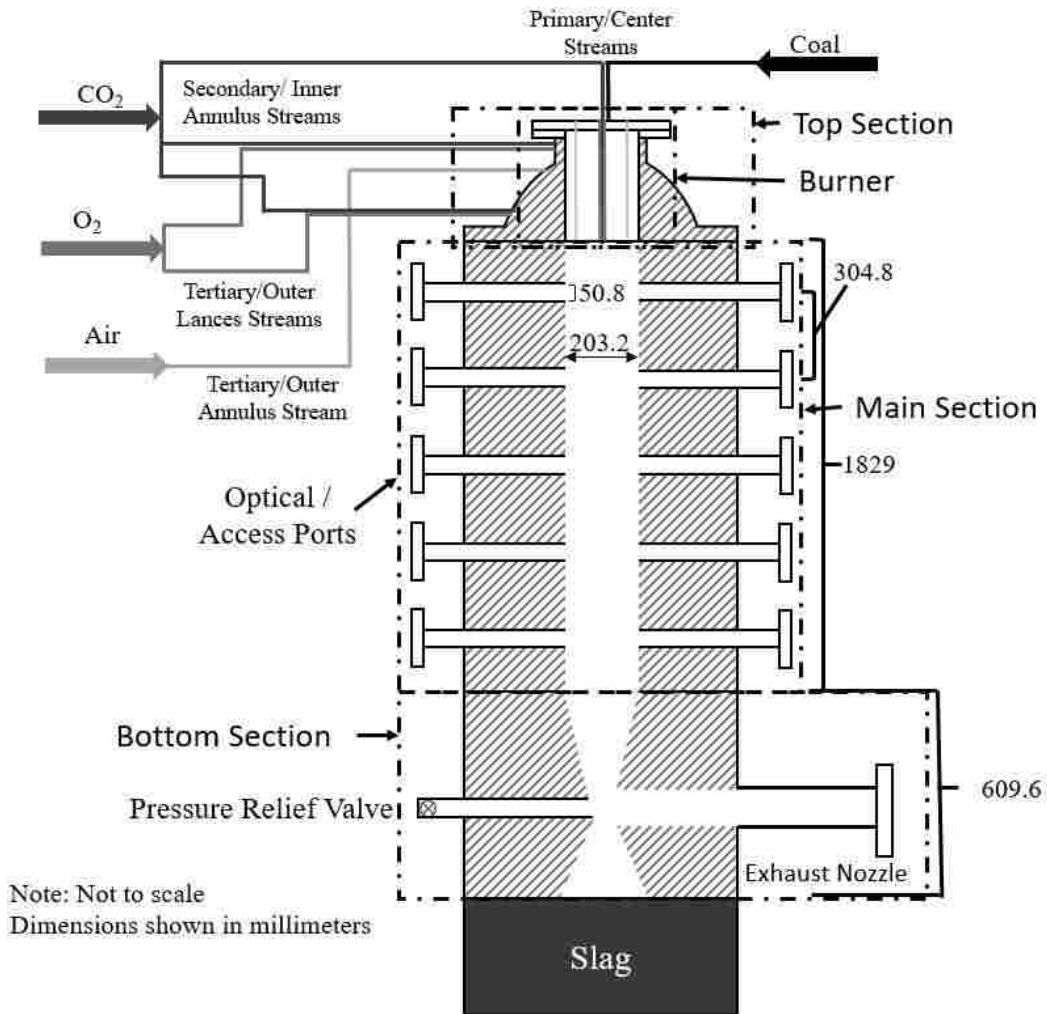


Figure 4-1: Schematic of the POC Reactor (not to scale).

4.2 Burner Design

A cross section of the final burner design resulting from the spreadsheet analysis and comprehensive combustion analysis is shown in Figure 4-2. The burner consists of a center tube, two center annuli, and eight tertiary tubes. Dimension for the tubes are shown in the figure and in Table 4-1. The burner was designed to warm up the POC from atmospheric pressure using natural gas, then switch over to high pressure

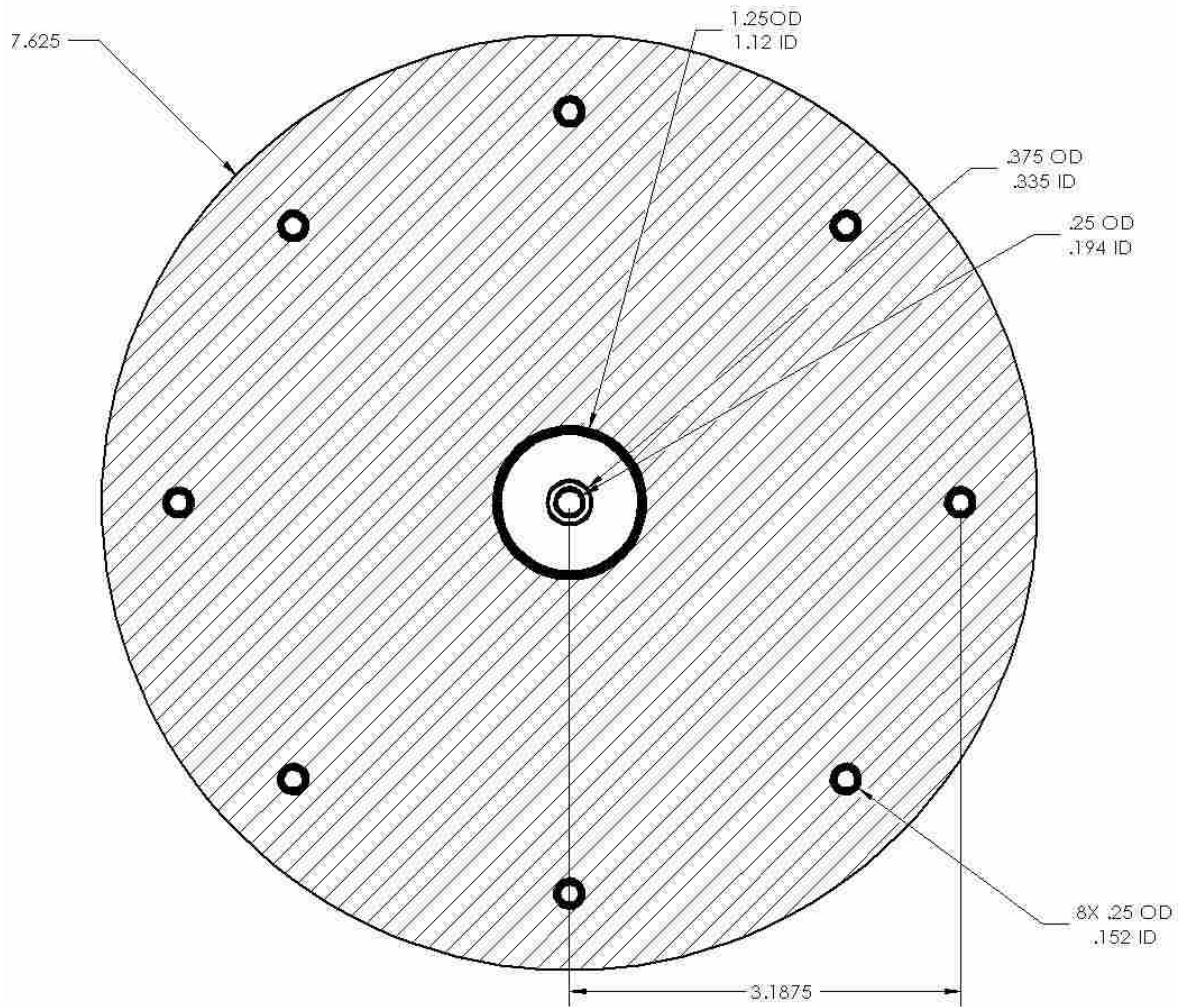


Figure 4-2: Cross-Sectional Schematic of Burner with Dimensions.

natural gas to pressurize the POC and, finally, switch to high-pressure oxy-coal combustion for testing.

The burner is made up of a central tube for the primary stream which has dry-fed coal with CO₂ used as the carrier gas. The inner secondary stream is an annulus for CO₂ and O₂. The outer annulus is intended to be used only during atmospheric heat-up and therefore the velocity shown in Table 4-1 is zero for coal fired conditions. There are eight tertiary tubes designed for the flow of CO₂ and O₂ that are separated from the primary and secondary flows. The results

from the comprehensive code analysis that led to this geometry is shown Section 4.2.1. The resulting design from the mass flow controllers to the burner inlet is a series of tubes, connections, and a manifold plenum to correctly distribute the desired amount of each gas to the correct locations.

Through use of Steamgen Expert software Dr. Adams determined the final CO₂ to coal mass-flow ratio to provide a sufficient amount of CO₂ to dilute the heat, and provide additional momentum was 4.21-1. Burner geometry in the primary, secondary, and tertiary flows was calculated using the equation for mass flow rate, following the methods described in Section 3.1.2, with a design velocity (u) of 5 m/s. Detailed engineering drawings of the burner can be found in Appendix A.

Table 4-1: Geometry and Velocity of the Primary, Secondary, and Tertiary Burner Flows.

	Primary	Inner Secondary	Outer Secondary	Tertiary
Inner Diameter (mm/in.)	4.928/0.194	8.509/0.335	9.525/0.375	3.861/0.152
Outer Diameter (mm/in.)	6.35/0.25	9.525/0.375	28.45/1.12	6.35/0.25
Cross-Sectional Area (mm ² /in. ²)	19.07/0.0296	25.20/0.039	564.4/.8748	93.66/0.145
Velocity (m/s)	4.68	4.68	0.0	4.92

4.2.1 Comprehensive Simulation Results

Reaction Engineering International (REI) was contracted to run comprehensive combustion simulations to predict the performance of the reactor for the three different burner geometries and flows outlined in the methods Section 3.1.4. Results from the REI analysis included: 3-D temperature contours, refractory and shell temperature profiles, and exit gas temperature and gas composition. The tube diameters are repeated from the methods section with

results showing velocities for each tube, exit gas temperature and exit gas O₂ and CO concentrations, as seen in Table 4-2. The tube velocities closely match those calculated with the

Table 4-2: Tube Geometry and Select Operating Conditions and Results for Three Different Burner Designs for POC Reactor.

	Case #1	Case #2	Case #3
Number of Tertiary Tubes	4	8	8
Inner Diameter of Tertiary Tubes (mm)	3.1496	16.5608	3.8608
Inner Diameter of Central Tube (mm)	5.0292	15.3924	4.9276
Inner Diameter of Annulus (mm)	9.0932	19.05	6.35
Outer Diameter of Annulus (mm)	12.5984	22.9108	8.509
Central Tube Velocity (m/s)	5.33	0.51	5.00
Annulus Velocity (m/s)	1.03	0.50	5.21
Tertiary Flow Velocity (m/s)	10.5	0.54	5.29
Exit Plane Gas Temperature (K)	2150	1659	1951
Exit Plane CO Concentration (vol%, wet)	0.49	0.01	0.11
Exit Plane O ₂ Concentration (vol%, wet)	4.27	3.00	4.32

spreadsheet model and show that Cases 1 and 2 have varying velocities in the different tubes while Case 3 has matching velocities in the primary, secondary and tertiary tubes. This should lead to lower mixing rates between the fuel and oxidizer for Case 3. All three of the exit temperatures are above the minimum exhaust gas temperature of 1589 K.

Figure 4-3 is a visual representation of the burner configurations and flow velocities for the three cases simulated by REI, as summarized in Table 4-2. It should also be remembered that the three cases had different overall CO₂ to coal ratios and a different percentage of total O₂ in

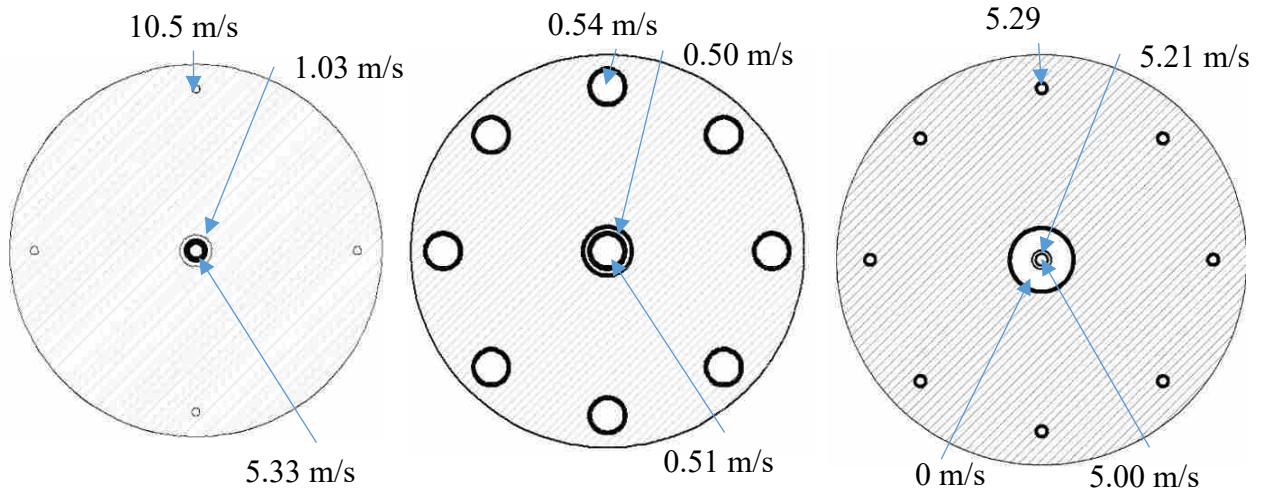


Figure 4-3: Cross-Sectional Diagram of Burners with Velocities of Different Streams for REI Cases 1, 2, and 3, Respectively.

Table 4-3: Distinguishing Parameters from Three REI Test Cases.

	Case #1	Case #2	Case #3
CO₂ to Coal Ratio	1.8:1	8:1	4.21:1
% of Total O₂ in Secondary	20	20	10.4

the inner secondary annulus for the three different cases. The values for the CO₂ to coal ratio and percentage of O₂ in the inner secondary annulus for the three different cases is shown in Table 4-3.

Figure 4-4 shows the average gas temperature profile for each burner design along the length of the reactor from the burner exit to the reactor exit plane. It can be seen that Case #3 has a profile that is between Case #1 and Case 2. This is primarily because the dilution of CO₂ is highest for Case #2 (8:1 CO₂ to coal) and lowest for Case #1 (1.8:1). Case #1 had shell temperatures in excess of the 505 K limit. Case #2 utilizes more CO₂ than is desirable. The temperature profiles also show that Cases #2 and #3 delay the rapid temperature rise a distance

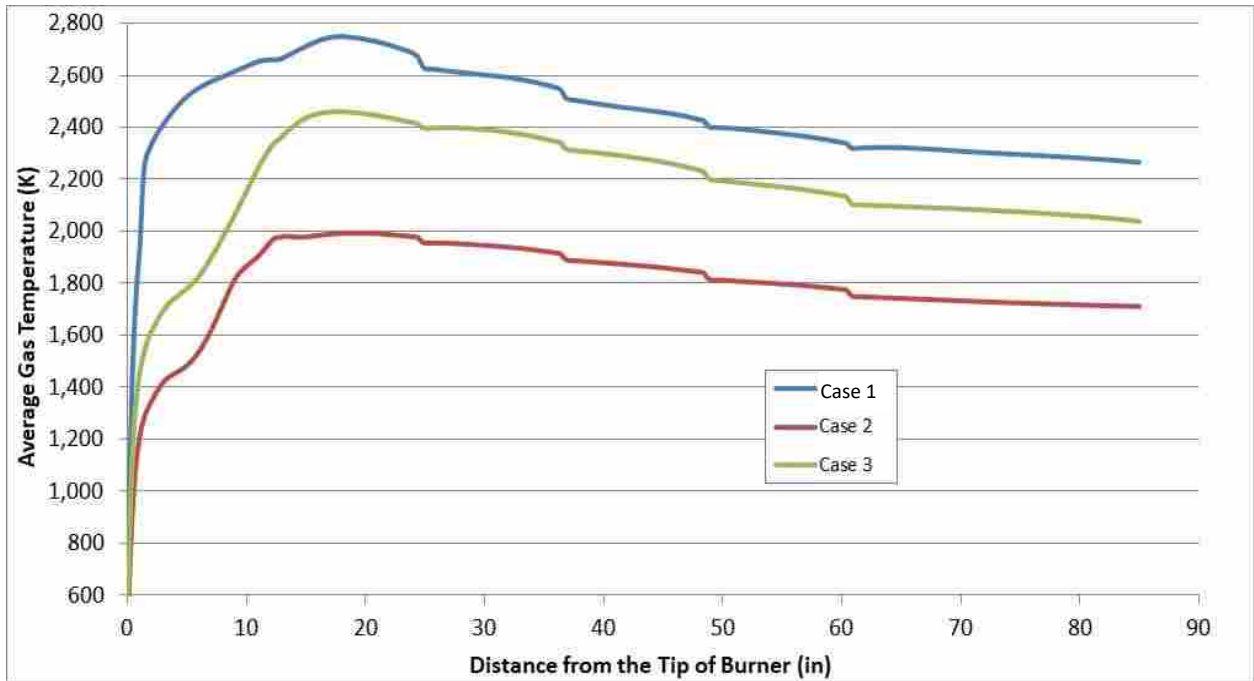


Figure 4-4: Temperature Profile along the Length of the POC Reactor for each of the Three Burner Design Cases for which CFD was run.

of 7 – 8 inches below the burner which is beneficial to distributing the heat flux and for keeping the burner cool. The temperature profiles are not smooth due to the effects of the access ports along the axis of the reactor that were modeled in the comprehensive 3-D combustion simulations. There was increased heat lost through these ports, which causes the little blimps in the average temperature profiles along the axis of the reactor.

Figure 4-5 shows a 2-D slice of temperature contours along the center axis of the reactor. Note that in all three the color contour scale is different and therefore care should be taken to compare temperatures by the color indicated. Case #1 shows narrow cold jets produced by the high velocities in the center and tertiary tubes. These jets lead to recirculation zones above the first observation port. High temperatures exist near the burner at the top of the reactor. For Case #2, the velocities of each jet are matched and the flow of CO₂ is high causing much lower temperatures overall but the flow rate is so low that it appears a reaction zone forms near the

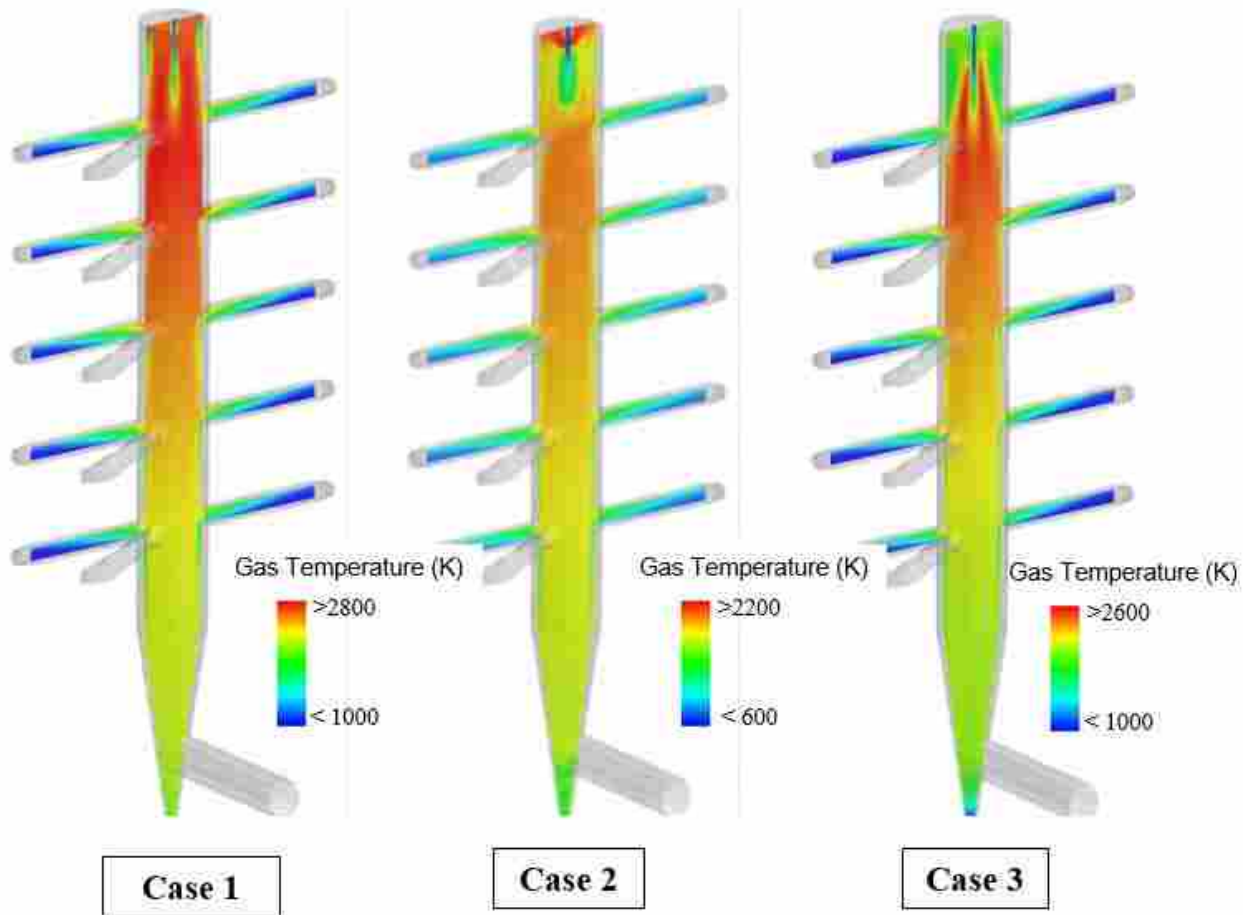


Figure 4-5: CFD Results of Gas Temperature Profile for Three Burner Design Cases.

burner. Although the larger diameters for the jets and the lower velocities have delayed reactions, it would be beneficial to achieve the delay without such high flow rates of CO_2 . Case #3 exhibits a good mixture of the first two cases, with a peak temperature between these first two cases, and an elongation of the gases that have an elevated temperature. The hottest gases in Case #3 are towards the center of the combustion chamber which will help keep the refractory temperatures below their maximum allowable value. The region near the burner is also seen to be cooler producing a more durable design.

A summary of the CFD models from REI for the three burner test cases shows that in comparison with Case 1 and Case 2, Case 3 resulted in:

- Intermediate exit gas temperature of 1951 K, O₂ concentration of 4.32% (vol, wet), and CO concentration of 0.11% (vol, wet)
- Delayed heat release with peak incident heat fluxes between the first and second set of observation windows
- A weaker recirculation pattern spreading the mixing over a larger volume
- Delayed combustion due to delayed mixing with O₂
- Intermediate heat loss through refractory (41.05% of coal firing rate based on HHV)
- Predicted steel outer shell temperature for the main reactor and the observation window in the range of 366~ 519 K (199 ~ 475 °F)
- Predicted maximum interior refractory surface temperature of 2439 K

4.3 Test Results

Table 4-4 shows the qualitative results from testing the burner outside of the reactor. For these data there is no air flow and the burner is oriented horizontally. This was a preliminary test under atmospheric conditions where the purpose was not to determine how the flame will look at higher pressures, but rather to see if the burner would work to heat up the reactor using natural gas at atmospheric pressure. The intent for this test was to start burning the natural gas at a low flow rate, corresponding to a low energy output around 30 kW_{th} and go as high as possible until either the flow rate was enough to provide 100 kW_{th} of energy, or the flame blew out or became too unsteady. The flames from 30 – 50 kW_{th} were buoyancy driven and almost immediately after leaving the burner shifted from horizontal to vertical as can be seen in Figure 4-6 which shows the flame at approximately 50 kW_{th}. The qualitative results for burner at various flow rates are summarized in Table 4-4. As the set point for the methane natural gas MFC increased above 50

Table 4-4: Qualitative Results of Firing Burner Outside of Reactor.

kW_{th}	Comments
30	The flame hardly went out horizontally, it went almost straight up vertically. The flame was dominated by buoyancy rather than momentum, and was a lazy flame.
40	Flame went higher a little, and came out a little bit more horizontally.
50	Flame went even higher, no significant differences.



Figure 4-6: Preliminary Burner Testing at 50 KW_{th} .

kW_{th} the flow of natural gas did not increase. The blow off limit of the flame was therefore not found due to issues with mass flow control.

When stoichiometric air was added to the secondary flow in the burner, it caused the flame to instantly blow out. The mass flow controller was not able to produce air flows low enough to keep the burner from blowing out.

When swirl was added to the air, rather than having the jet flow only in the axial direction, the flame got shorter, and was attached. With an air mass flow of three times the natural gas flow, the flame was blue and attached. This is well below stoichiometric but the swirl produces a recirculation zone that entrains surrounding air in the room to enable the fuel to burn out. For this testing, the use of the tertiary lances to also transport oxygen through the burner was unavailable but when mounted in the reactor, the tertiary air will be needed to supply the remainder of the stoichiometric air. It was determined that this burner would not be suitable for heating up the reactor under atmospheric conditions with natural gas without the addition of swirl to the secondary air flow.

4.3.1 Connections from MFCs to Burner

Seven mass flow controllers (MFCs) will be used to control the flow rates of the different gases in the primary, secondary, and tertiary flows, in addition to the MFCs utilized for the CO₂ carrying the coal in the coal feed system. An air MFC and a low pressure natural gas MFC will be needed to start the warm-up process of the reactor under atmospheric conditions. The low pressure natural gas will be delivered to the central primary stream and the secondary stream in the inner annulus. The air will be split between the outer annulus and the tertiary lances. As the reactor is pressurized, two O₂ and two CO₂ MFCs along with a high pressure natural gas MFC will be used. The oxygen and carbon dioxide MFCs will be paired up with each other, with one set being mixed and delivered to the secondary stream in the inner annulus of the burner, and the other set being mixed and delivered to the tertiary lances of the burner. During high pressure

operation while firing coal, the O₂ and CO₂ mixtures will still flow in the secondary and tertiary streams, and the primary stream will consist of the dry-fed coal and CO₂ mixture.

The size and location of the output connections of the MFCs along with the input connections of the burner were already established, so a design had to be created to combine the correct flows together, and get these mixed flows delivered to the right inputs of the burner. Due to the different tube sizes of the MFC outputs and the burner inputs, along with the need to combine different flows for the low pressure natural gas warm-up, high pressure natural gas warm-up and pressurization, and high pressure coal firing of the reactor, several connections had to be made between the MFCs and the burner to allow for the varying tube sizes as well as splitting some flows and combining others. A piping and instrumentation diagram (P&ID) was created to aid in the design of this system, and ensure that the correct sized parts were ordered for this assembly. This P&ID is shown in Figure 4-7, and shows the MFCs, tubing, Swagelok connections, and valves from the MFCs to the burner inputs. All connections in Figure 4-7 that are labelled with a number followed by the letter “a”, with the exception of “8a,” represent Swagelok fittings. Connection “8a” is an electrically actuated 3-way ball valve to switch back and forth between low pressure natural gas during low pressure warm-up, and CO₂ and O₂ for both other operating conditions. This ball valve functions in such a way as to prevent the oxygen and the natural gas from ever being able to be in the inner annulus at the same time for safety reasons.

Following the methods described in Section 3.1.5, the orifice sizing for the manifold leading into the burner was calculated. The resulting throat diameter to achieve the desired pressure drop across the orifice was 1.952 mm, or 0.07685 in. Figure 4-8 shows a picture of the manifold and some tubing and Swagelok connections to the burner.

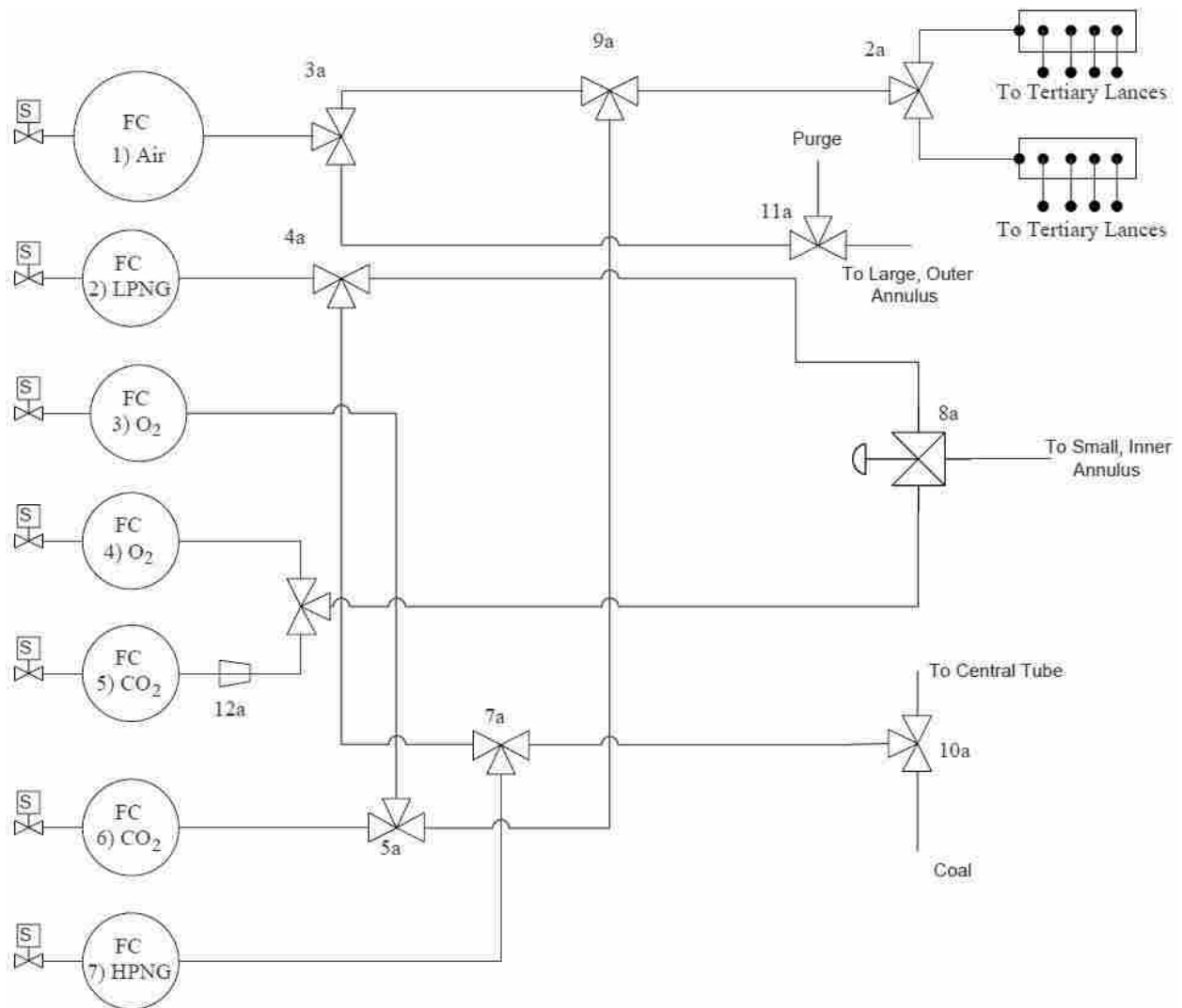


Figure 4-7: Piping and Instrumentation Diagram of Tubing and Connections between MFCs and the Manifold and Burner.

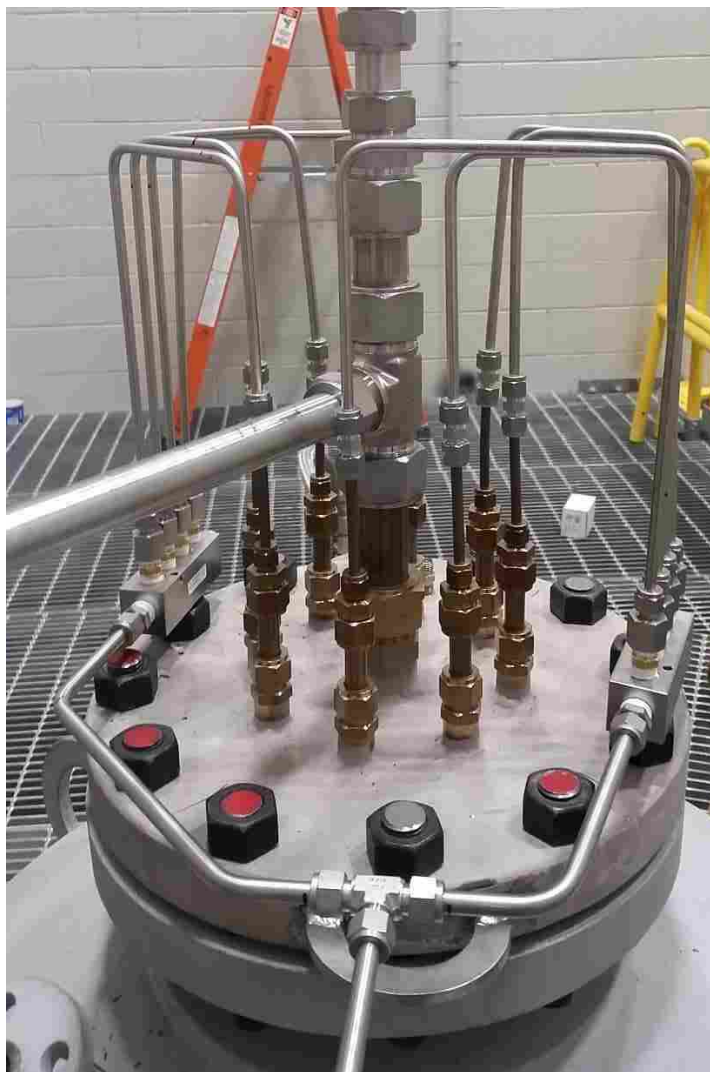


Figure 4-8: Photograph of Tubing, Swagelok Connections, and Manifold Connecting to the Burner.

4.4 Design of Reactor Components

The scope of this project included generating computer Aided Design (CAD) models and engineering drawings for the POC reactor from the burner through the exit nozzle in addition to the design, construction, and operation of a diffusion flame burner for the POC reactor.

4.4.1 Dome Cap

The reactor was designed with a dome cap on top with a 203.2 mm (8 inch) slip-on-flange to allow for the attachment of the burner to the reactor. The dome cap provided space to place refractory which protected the steel shell of the reactor from the radiative heat transfer due to the high gas temperatures inside the reactor. The dome also has two 12.7 mm (1/2 in.) pipes welded onto it that are rotated 90° from each other to provide optical access for a UV scanner to be used as a flame scanner. These flame detector ports were positioned at an angle such that they provided a line of sight that would intersect with the center axis of the reactor a distance of 8-10 inches below the top of the reactor. Three lifting rings were designed and welded onto the cap for cranes in the building to attach to in order to allow for lifting and movement of the cap.

4.4.2 Reactor Support Legs

Support legs were designed and welded onto the reactor to allow the reactor to hang from structural I-beams. These support legs are made with 12.7 mm (1/2 in.) carbon steel and are 8 inches wide. There are two support legs welded onto the main section of the reactor steel shell 180° from each other. Each leg has four holes drilled into them to allow for bolts and nuts to connect the support legs to the structural I-beams. These support legs were overdesigned in order to withstand any unforeseeable excess force on the reactor. A finite element analysis of the design was performed to confirm the legs would be more than sufficient to support the entire weight of the reactor components including the main section of the reactor, top section of the reactor, bottom section of reactor, burner, all refractory in these aforementioned sections, and any other weight these legs may have to support. As seen in Figure 4-9, the maximum stress anticipated to be felt in the support legs is $37.3 \times 10^6 \text{ N/m}^2$, while the yield strength of the carbon steel is approximately $710 \times 10^6 \text{ N/m}^2$, this leaves a factor of safety of approximately 20.

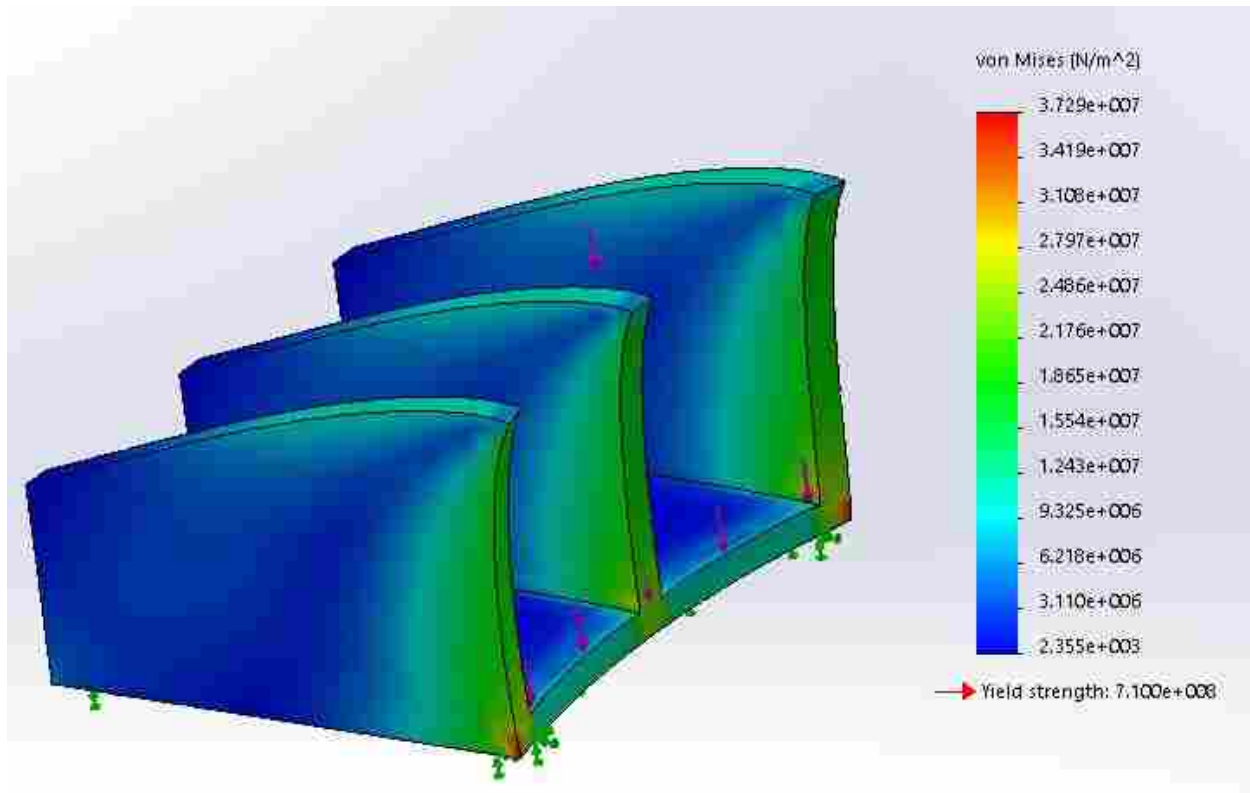


Figure 4-9: FEA Analysis of Reactor Support Leg.

4.4.3 Refractory Layout

Four different layers of refractory, comprised of three different types of refractory were used to insulate the steel shell of the reactor from the core of the reactor where the combustion reactions occur. The outer-most layer of refractory attached to the inside wall of the reactor shell was a 50.8 mm (2 inch) thick layer of Insboard 2600. The next layer was a 25.4 mm (1 inch) layer of Insboard 2600. The third layer was comprised of Greentherm 28 LI Bricks that were 63.5 mm (2.5 inches) thick. The final layer of refractory was a castable UltraGreen SR cement-like layer that was poured into the center of the refractory with a circular Sonotube cement form in the center so as to maintain an open 228.6 mm (8 inch) diameter in the middle of the reactor as the combustion chamber. Refractory cement was used to attach each of the layers of refractory to each other, and to the shell of the reactor.

A schematic of the layout of the refractory is shown in Figure 4-10. Each piece of the Insboard and Greentherm brick had to be cut on a table saw. In order to get the correct angles on the saw, a scaled picture of each layer of refractory was printed and then cut out in order to set the table saw blade at the correct angle so as to ensure the pieces of refractory would properly fit onto each other.

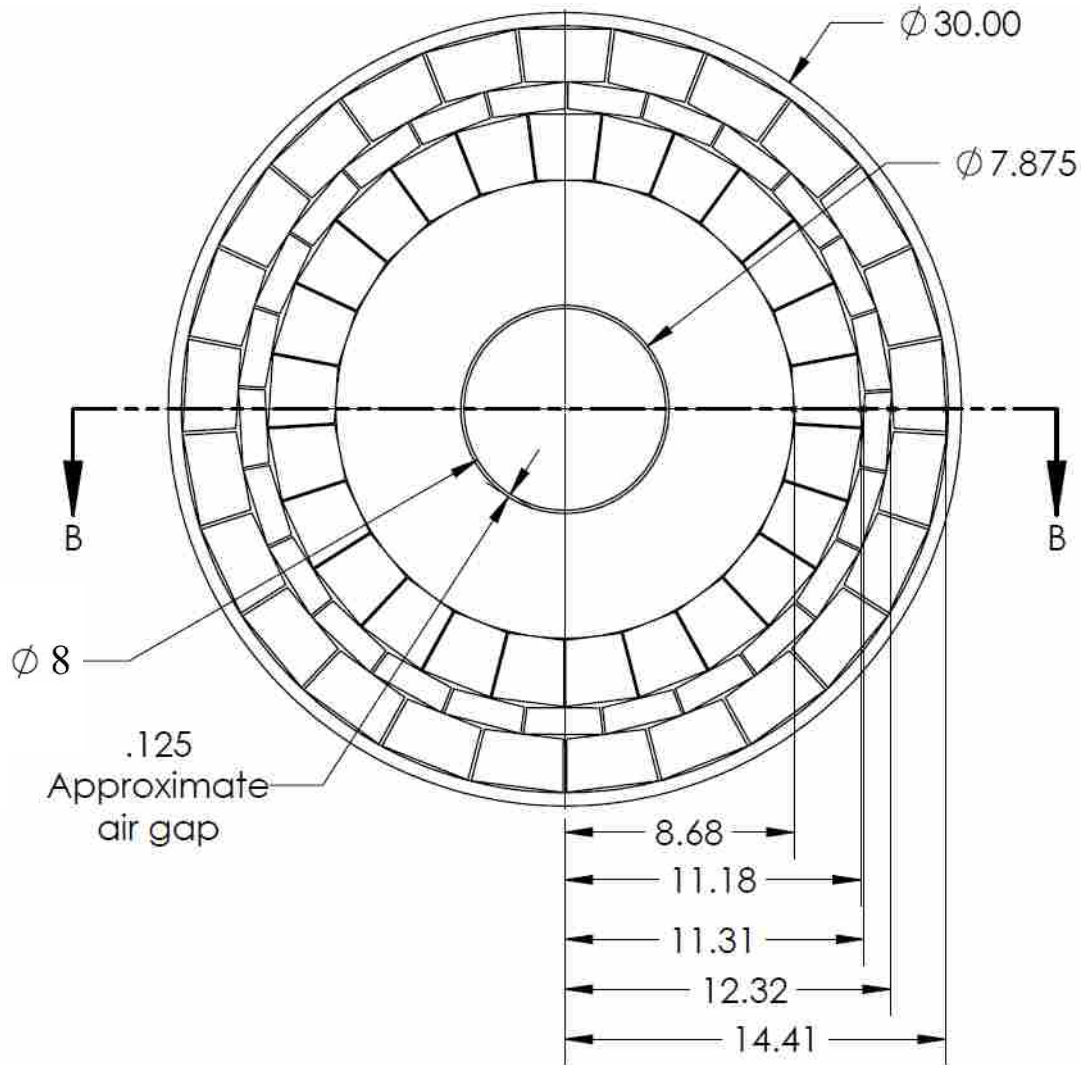


Figure 4-10: Diagram of Refractory Used to Insulate the POC Reactor (Dimensions in in.).

4.4.4 Optical and Access Ports

Twenty optical and access ports were built onto the reactor, 4 rows of 5 ports each row rotated 90° from the other rows. One pair of these rows, directly across from each other, were cored out in order to provide a line-of-sight for laser and other optical measurements. Other ports were used for thermocouple readings and other measurements. These ports are comprised of a 50.8 mm (2 in.) pipe that are approximately 146 mm (5.75) inches long with a slip-on flange welded to them. A picture of the reactor and supporting equipment can be seen in Figure 4-11.

Detailed engineering drawings of the POC reactor can be found in Appendix B.

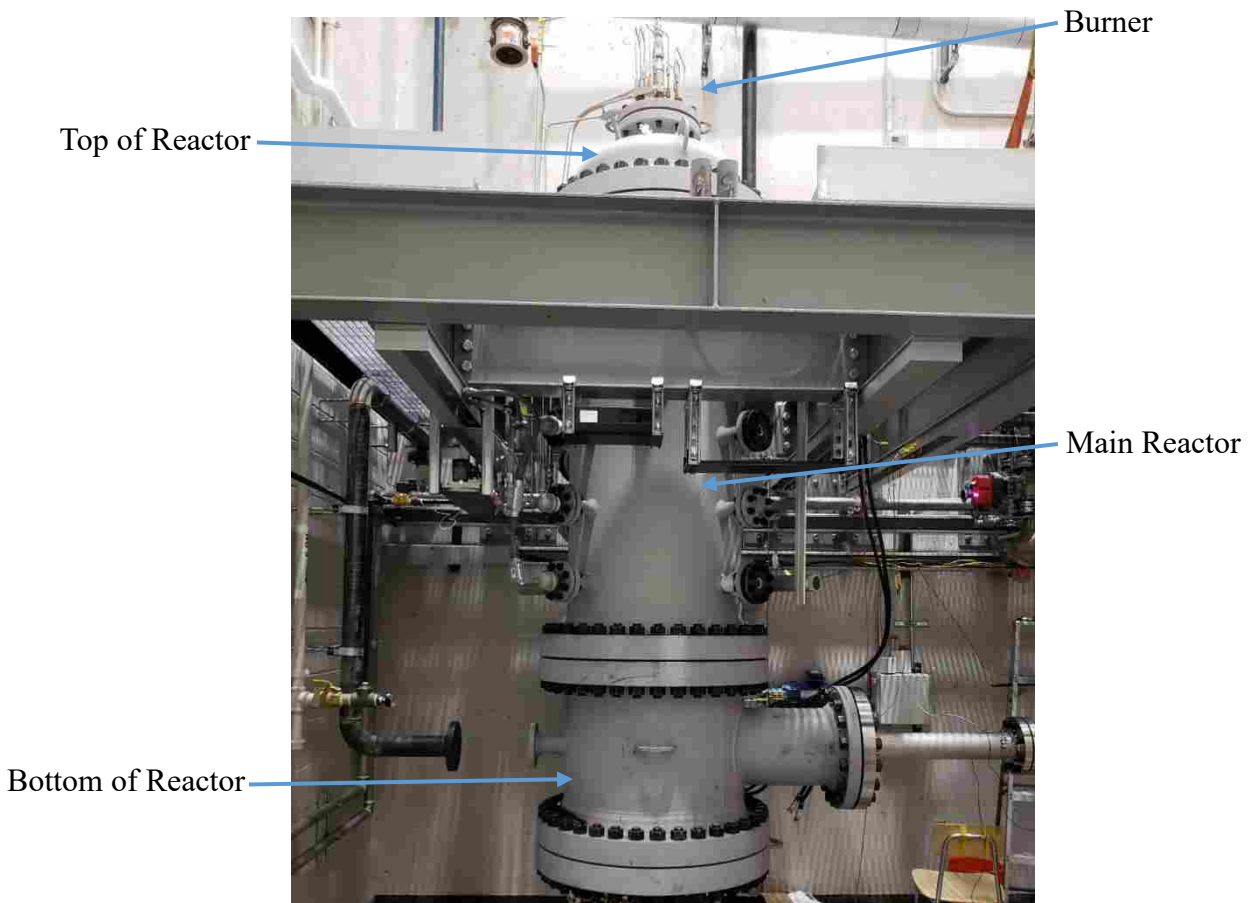


Figure 4-11: Picture of POC Reactor in Reactor Room.

4.5 Room Layout Design

After the component positions were determined, the support system was designed so that it would be sufficiently strong to safely hold these heavy pieces of equipment. The weight of these components, along with their position were used to determine how much total weight each wall connection and a square beam placed in the center of the room would have to support. These values were used to help create the layout of the support I-beams and calculate the forces for the wall connections in Figure 4-12. These results were then sent to a professional engineering firm to finalize the design of the support structure to ensure it was designed sufficiently to conform to seismic building codes.

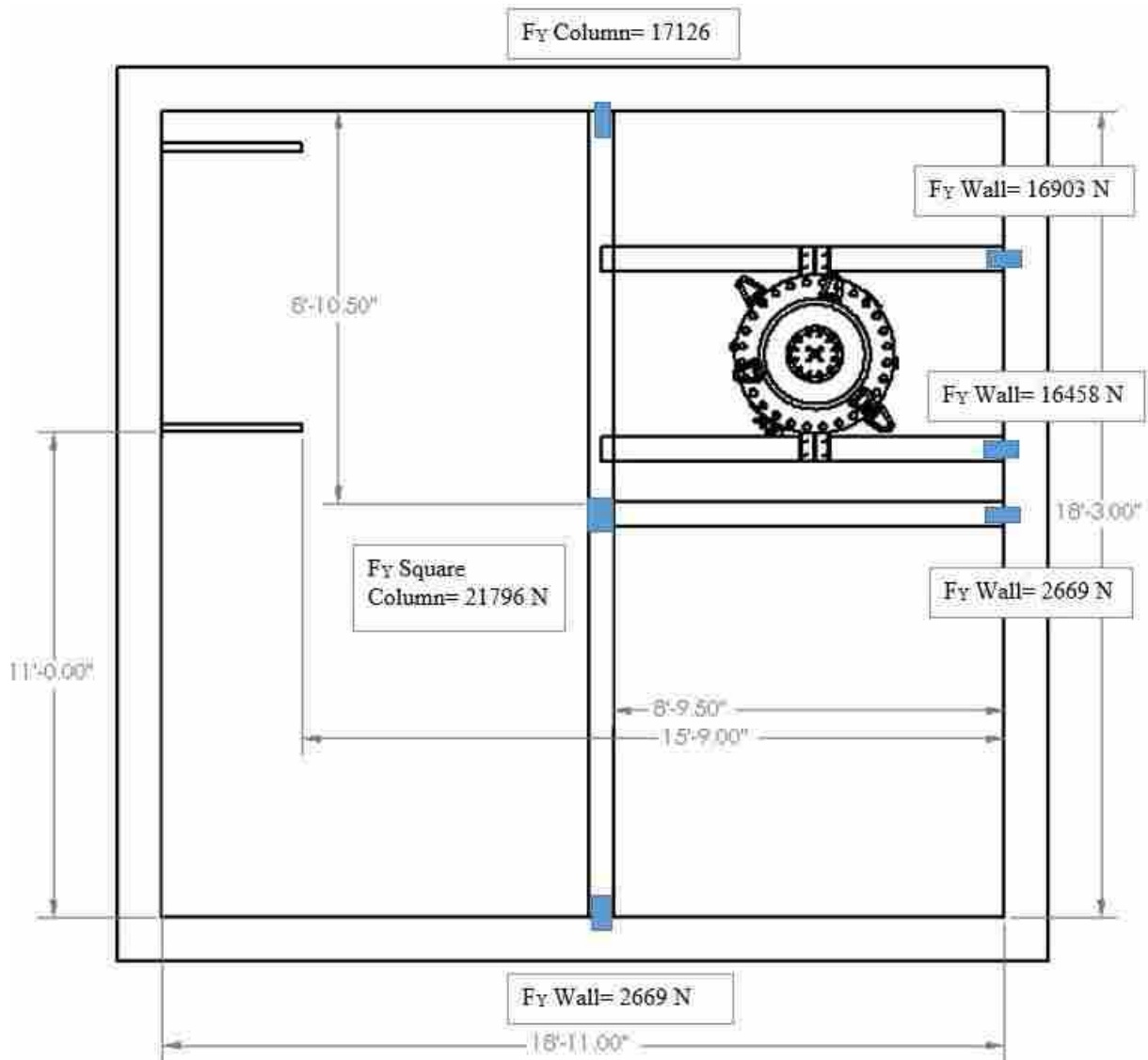


Figure 4-12: Layout of Reactor Room Support I-Beams and Calculated Forces for Wall and Square Supports.

5 SUMMARY AND CONCLUSIONS

A Pressurized Oxy-Coal Combustor (POC) has been designed, fabricated, and assembled for the purpose of developing a pressurized dry coal feed system, a high pressure coal burner and an oxy-coal ash collection system. The first version of a high pressure burner has been design, fabricated and installed for this reactor. Both the reactor and the burner components are described in detail in this document. The following is a summary of accomplishments completed to date for the design of the burner and reactor.

- The POC main reactor has been designed, fabricated, and assembled.
- The structure to support the POC reactor, and all components needed to run the reactor, was designed, modified by a professional engineering firm, assembled, and now houses the POC reactor and components.
- Three different burner designs were modeled using comprehensive combustion simulations.
- The final design of the burner utilizes matching velocities in the primary and secondary streams to reduce shearing between the streams in order to elongate the flame.
- The diffusion flame burner for the POC reactor was designed and assembled, and is now ready for testing.

- The burner was tested outside of the reactor under atmospheric conditions to determine the functionality for atmospheric warm-up. After testing, it was determined that swirl was needed to stabilize and attach the flame for warm-up at atmospheric pressure.
- The mass flow controllers and connections from the mass flow controllers to the manifold and then to the burner are assembled and connected to the burner but have not yet been tested due to delays in the control system of the reactor.
- The burner and reactor are installed and ready to be used in order to test the burner, coal feeder, and ash management system installed in the POC reactor system.
- Tests planned with the POC reactor include: radiative heat flux measurements, thermocouple data, laser and optical measurements, ash composition analysis, and more.

While this reactor was designed and built for the development of a dry feed system, high pressure burner, and ash management system, it is anticipated that this reactor will be used for many fundamental studies on the combustion of coal and other solid fuel at pressures up to 20 atm. The design allows both optical and probe access at numerous locations. The fuel, oxygen and CO₂ flow rates are small enough to be provide affordable repeatable experiments with detailed measurements. The work done and documented here will be utilized and referenced by the future faculty and graduate students that utilize this facility.

REFERENCES

- [1] L. Chen, S. Yong, and A. Ghoniem, "Oxy-fuel combustion of pulverized coal: Characterization, fundamentals, stabilization and CFD modeling." *Progress in Energy and Combustion Science*, vol. 38(2), pp. 156-214. doi:10.1016/j.pecs.2011.09.003, 2012.
- [2] H. Hagi, M. Nemer, Y. Le Moullec, and C. Bouallou, "Towards second generation oxy-pulverized coal power plants: Energy penalty reduction potential of pressurized oxy-combustion systems." *Energy Procedia*, vol. 63, pp. 431-439, 2014.
- [3] A. Gupta, D. Lilley, and N. Syred, "Swirl Flows", Abacus Press, Kent. 1984.
- [4] S. Owen, *Burnout, NO, and Flame Characterization from an Oxygen-Enriched Biomass Flame*, Provo: Brigham Young University, 2015.
- [5] M. Hupa, "International Flame Research Foundation," 24 January 2006. [Online]. Available: www.ffrc.fi/Liekkipaiva_2006/Liekkipaiva2006_IFRF_Today_HUPA.pdf. [Accessed 11 March 2015].
- [6] S. R. Turns, "Laminar Diffusion Flames," in *An Introduction to Combustion Concepts and Applications*, New York, McGraw Hill Education, 2014, pp. 311-365.
- [7] S. P. Burke and T. E. W. Schumann, "Diffusion Flames," *Industrial and Engineering Chemistry*, vol. 20, no. 10, pp. 998-1004, 1928.
- [8] F. G. Roper, "The Prediction of Laminar Jet Diffusion Flame Sizes: Part I. Theoretical Model," *Combustion and Flame*, vol. 29, pp. 219-226, 1977.
- [9] F. G. Roper, "The Prediction of Laminar Jet Diffusion Flame Sizes: Part II. Experimental Verification," *Combustion and Flame*, vol. 29, pp. 227-234, 1977.
- [10] S. R. Turns, "Turbulent Nonpremixed Flames," in *An Introduction to Combustion Concepts and Applications*, New York, McGraw Hill Education, 2014, pp. 486-520.

- [11] K. Wohl, C. Gazley and N. Kapp, "Diffusion Flames," in Third Symposium on Combustion and Flame and Explosion Phenomena, Baltimore, 1949.
- [12] M. A. Delichatsios, "Transition from Momentum to Buoyancy-Controlled Turbulent Jet Diffusion Flames and Flame Height Relationships," *Combustion and Flame*, vol. 92, pp. 349-364, 1993.
- [13] H. A. Becker and D. Liang, "Visible Length of Vertical Free Turbulent Diffusion Flames," *Combustion and Flame*, vol. 32, pp. 115-137, 1978.
- [14] R.-H. Chen and J. F. Driscoll, "The Role of the Recirculation Vortex in Improving Fuel-Air Mixing within Swirling Flames," in Twenty-Second Symposium (International) on Combustion/The Combustion Institute, 1988.
- [15] D. Ashworth, D. R. Tree, and J. Tobiasson, "A Correlation for Flame Length of Oxygen-Assisted, Swirled, Coal, and Biomass Flames," The 41st International Technical Conference on Clean Coal & Fuel Systems, Clearwater Florida, 2016.
- [16] J. Thornock, D. Tovar, D. R. Tree, Y. Xue, and R. Tsiava, "Radiative intensity, NO emissions, and burnout for oxygen enriched biomass combustion," *Proceedings of the Combustion Institute*, vol. 35, pp. 2777-2784, 2015.
- [17] N. Orfanoudakis, A. Hatzia Apostolou, E. Mastorakos, E. Sardi, K. Krallis, N. Vlachakis, and S. Mavromatis, "Design, evaluation measurements and CFD modeling of a small swirl stabilised laboratory burner," *Computational Methods in Sciences and Engineering 2003*: pp. 474-478, 2003.
- [18] J. Liu, Z. Liu, S. Chen, S. O. Santos, and C. Zheng, "A numerical investigation on flame stability of oxy-coal combustion: Effects of blockage ratio, swirl number, recycle ratio and partial pressure ratio of oxygen," *International Journal of Greenhouse Gas Control*, vol. 57, pp. 63-72, 2017.
- [19] L. G. Becker, H. Kosaka, B. Böhm, S. Doost, R. Knappstein, M. Habermehl, M., and A. Dreizler, "Experimental investigation of flame stabilization inside the swirl of an oxyfuel swirl burner," *Fuel*, vol. 201, pp. 124-135, 2017.
- [20] D. Zabrodiec, J. Hees, A. Massmeyer, F. vom Lehn, M. Habermehl, O. Hatzfeld, and R. Kneer, "Experimental investigation of pulverized coal flames in CO₂/O₂ - and N₂/O₂ -atmospheres: Comparison of solid particle radiative characteristics," *Fuel*, vol. 201, pp. 136-147, 2017.
- [21] A. Gopan, Z. Yang, A. Adeosun, B. M. Kumfer, and R. L. Axelbaum, "Burner and boiler design concepts for a low recycle, staged-pressurized oxy-combustion power plant," The Clearwater Clean Energy Conference (42nd International Technical Conference on Clean Energy), 2017.

- [22] Çengel, Yunus A., and John M. Cimbala. 2010. Fluid mechanics : fundamentals and applications (McGraw-Hill Higher Education: Boston).

APPENDIX A. CAD MODEL AND DRAWING OF BURNER

The engineering drawings and schematic of the layout for the burner used in the POC Reactor are contained in this appendix.

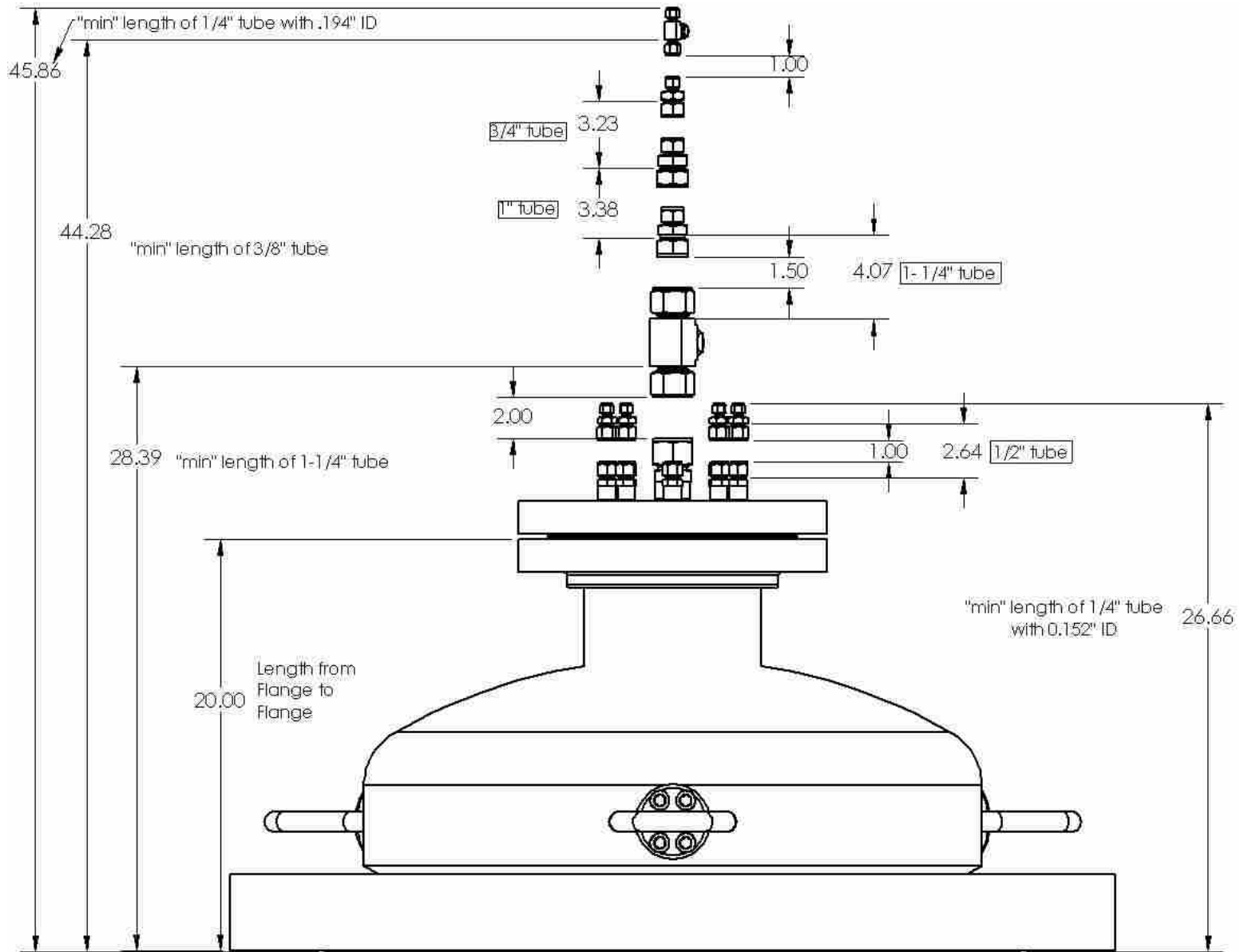


Figure A1: Drawing of Side View of Cap Burner with Swagelok Fittings

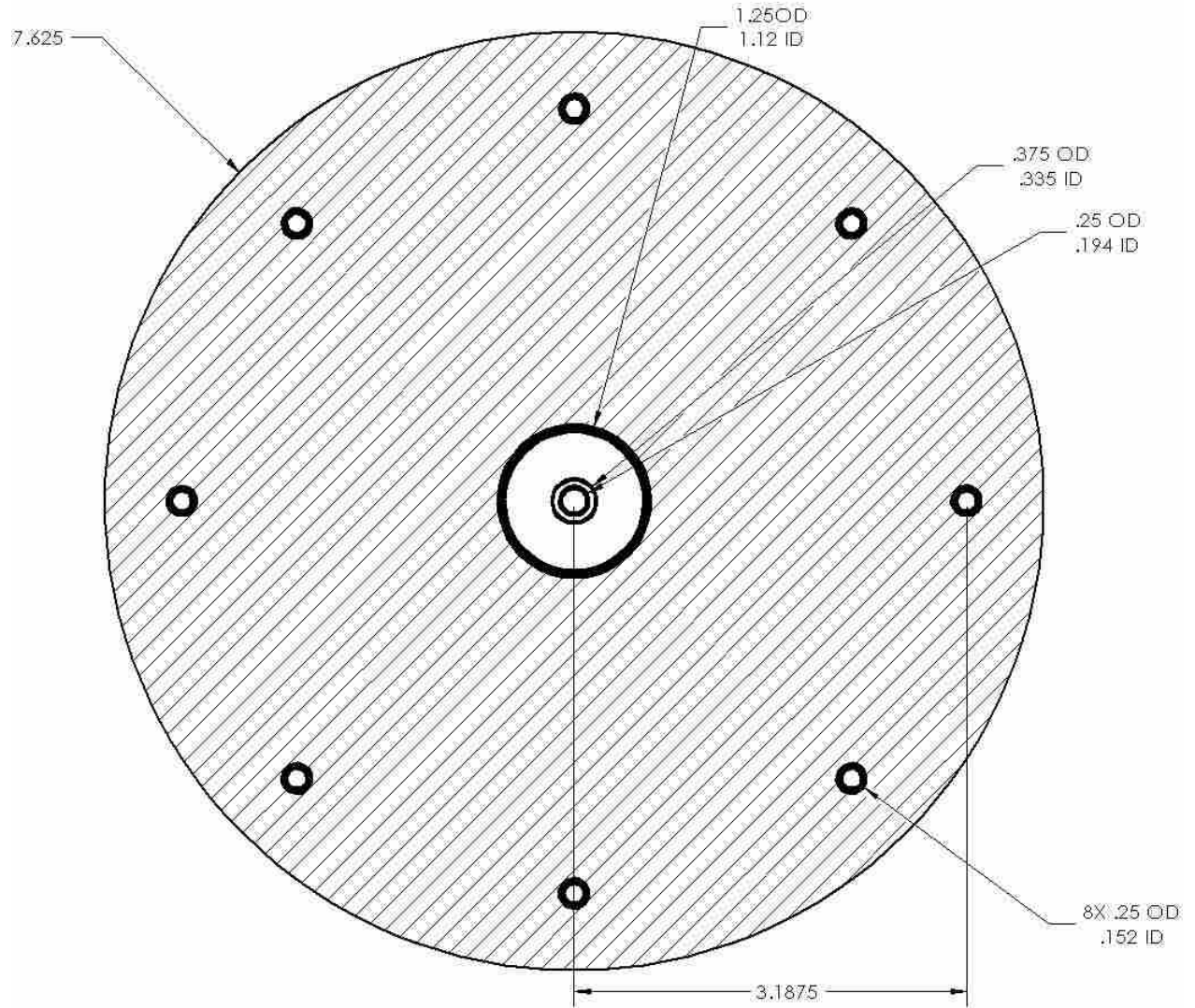
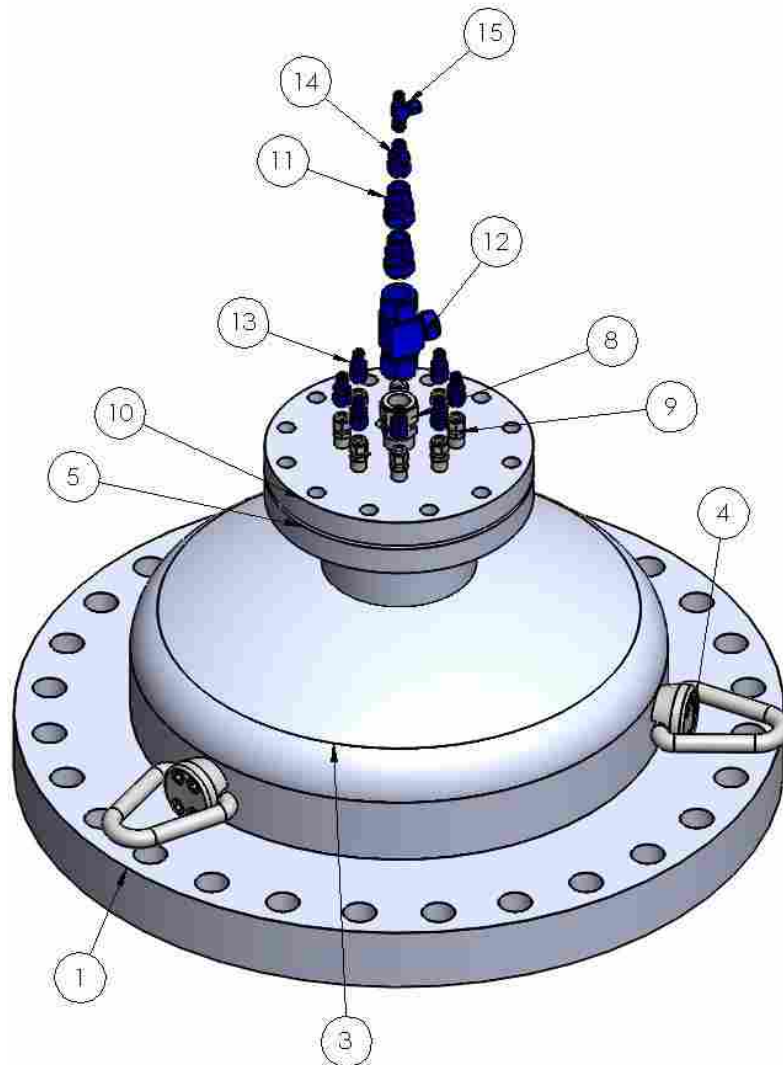


Figure A2: Drawing of Isometric View of Cap Burner with Swagelok Fittings and Bill of Materials



ITEM NO.	PART NUMBER	DESCRIPTION	QTY.
1	30 in class 300 Blind Flange with hole for cap		1
2	Refractory for inside of Cap		1
3	30 in steel cap schedule 20		1
4	Lifting Ring		3
5	8 in class 300 Slip on Flange		1
6	8 in flexatalic gasket		1
7	22		1
8	SS-2000-1-20W-SwagelokCompany	1 1/4 in. Tube Male Pipe Weld Swagelok	1
9	SS-810-1-8W-SwagelokCompany	1/2 in. Tube Male Pipe Weld Swagelok	8
10	24		1
11	SS-1610-6-12-SwagelokCompany-03-07-2018		2
12	SS-2000-3-20-16-SwagelokCompany-03-05-2018		1
13	SS-810-6-4-SwagelokCompany-03-07-2018		8
14	SS-1210-6-6-SwagelokCompany-03-20-2018		1
15	SS-600-3-4-6-SwagelokCompany		1

Figure A3: Drawing of Bottom View of Burner with Tube Dimensions

APPENDIX B. POC REACTOR DRAWINGS

The directory of CAD parts and the engineering drawings used to fabricate the POC Reactor are contained in this appendix.

Table B-0-1: Directory of CAD Parts.

Part Name	Drawing No.	Folder Path	File Name
Reactor Assembly with Cap Burner	1	J:\groups\doe-poc\Reactor Design\Reactor\CAD Models\8 In flanges and pipes	Reactor assembly with new cap burner design
Reactor Assembly with flange Burner	2	J:\groups\doe-poc\Reactor Design\Reactor\CAD Models\8 In flanges and pipes	Reactor assembly with 8 in pipe Burner Design
Main Reactor With Refractory	3	J:\groups\doe-poc\Reactor Design\Reactor\CAD Models	Main Reactor with Refractory
2 in. Flange Assembly	4	J:\groups\doe-poc\Reactor Design\Reactor\CAD Models	2 in flange assembly
Bottom of Reactor with Refractory	5	J:\groups\doe-poc\Reactor Design\Reactor\CAD Models	Bottom of Reactor with Refractory
Cap Burner Assembly	6	J:\groups\doe-poc\Reactor Design\Reactor\CAD Models\8 In flanges and pipes	Cap Burner Design Assembly
6 in. Blind Flange with Swageloks on top	7	J:\groups\doe-poc\Reactor Design\Reactor\CAD Models\8 In flanges and pipes	6 in class 300 Blind Flange
Flange Burner Design	8	J:\groups\doe-poc\Reactor Design\Reactor\CAD	Burner Design with 8 in Pipe on Top

		Models\8 In flanges and pipes	
8" Blind Flange with Swageloks on Top	9	J:\groups\doe-poc\Reactor Design\Reactor\CAD Models\8 In flanges and pipes	8 in class 300 Blind Flange with holes for Swageloks
Nozzle	10	J:\groups\doe-poc\Reactor Design\Reactor\CAD Models	Nozzle
Exit Pipe for Relief Valve	11	J:\groups\doe-poc\Reactor Design\Reactor\CAD Models	Exit pipe for Relief Valve
12-4" Reducer	12	J:\groups\doe-poc\Reactor Design\Reactor\CAD Models\8 In flanges and pipes	12-4 in Reducer
Main Reactor Shell	13	J:\groups\doe-poc\Reactor Design\Reactor\CAD Models	Main Reactor Steel Shell
Reactor Support Leg	14	J:\groups\doe-poc\Reactor Design\Reactor\CAD Models\Leg Support for Reactor	8 in wide Support Leg
2" X-Heavy Steel Pipe	15	J:\groups\doe-poc\Reactor Design\Reactor\CAD Models	2 in steel pipe x-heavy
30" X-Heavy Steel Pipe with Hole	16	J:\groups\doe-poc\Reactor Design\Reactor\CAD Models	Bottom section of Reactor 30 in steel pipe x-heavy
30" 300# Blind Flange with Hole for Cap	17	J:\groups\doe-poc\Reactor Design\Reactor\CAD Models\8 In flanges and pipes	30 in class 300 Blind Flange with hole for cap
30" Steel Cap Schedule 20	18	J:\groups\doe-poc\Reactor Design\Reactor\CAD Models\8 In flanges and pipes	30 in steel cap schedule 20
6" X-Heavy Steel Pipe	19	J:\groups\doe-poc\Reactor Design\Reactor\CAD Models\8 In flanges and pipes	6 in steel pipe x-heavy for top of cap
Blind Flange with Holes	20	J:\groups\doe-poc\Reactor Design\Reactor\CAD Models\8 In flanges and pipes	6 in class 300 Blind Flange

8" Blind Flange with hole for 6" Pipe	21	J:\groups\doe-poc\Reactor Design\Reactor\CAD Models\8 In flanges and pipes	8 in class 300 Blind Flange with hole for 6 in pipe
8" Steel Pipe X-Heavy	22	J:\groups\doe-poc\Reactor Design\Reactor\CAD Models\8 In flanges and pipes	8 in steel pipe x-heavy
30" #300 Blind Flange with hole for 8" Pipe	23	J:\groups\doe-poc\Reactor Design\Reactor\CAD Models\8 In flanges and pipes	30 in class 300 Blind Flange with hole for 8in pipe and UV detector
8" 300# Blind Flange with Holes for Swageloks	24	J:\groups\doe-poc\Reactor Design\Reactor\CAD Models\8 In flanges and pipes	8 in class 300 Blind Flange with holes for Swageloks
12" Sch 80 Steel Pipe	25	J:\groups\doe-poc\Reactor Design\Reactor\CAD Models\8 In flanges and pipes	12 spray pipe
3" Pipe X-Heavy	26	J:\groups\doe-poc\Reactor Design\Reactor\CAD Models	3 in steel pipe x-heavy
3" 300# Blind Flange with Hole for 3/4" Pipe	27	J:\groups\doe-poc\Reactor Design\Reactor\CAD Models\8 In flanges and pipes	3 in class 300 Blind Flange with 1 in hole
2.5" X-Heavy Steel Pipe	28	J:\groups\doe-poc\Reactor Design\Reactor\CAD Models	2.5 in steel pipe x-heavy
12" 300# Blind Flange with Hole for 4" Pipe	29	J:\groups\doe-poc\Reactor Design\Reactor\CAD Models\8 In flanges and pipes	12 in class 300 Blind Flange with hole for 4 in pipe
4" X-Heavy Steel Pipe	30	J:\groups\doe-poc\Reactor Design\Reactor\CAD Models\8 In flanges and pipes	4 in steel pipe x-heavy

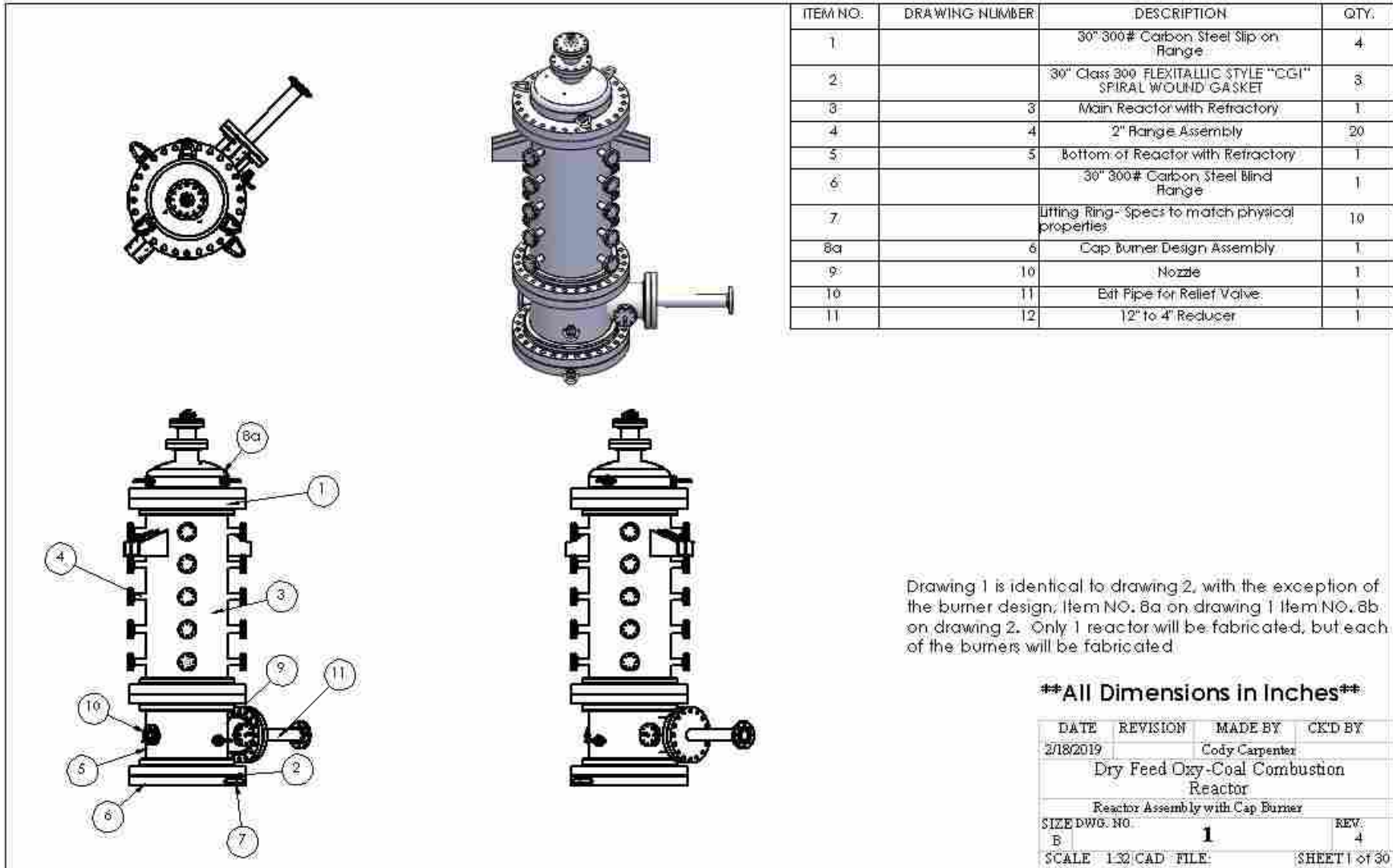


Figure B1: Drawing of POC Reactor Assembly with Cap Burner

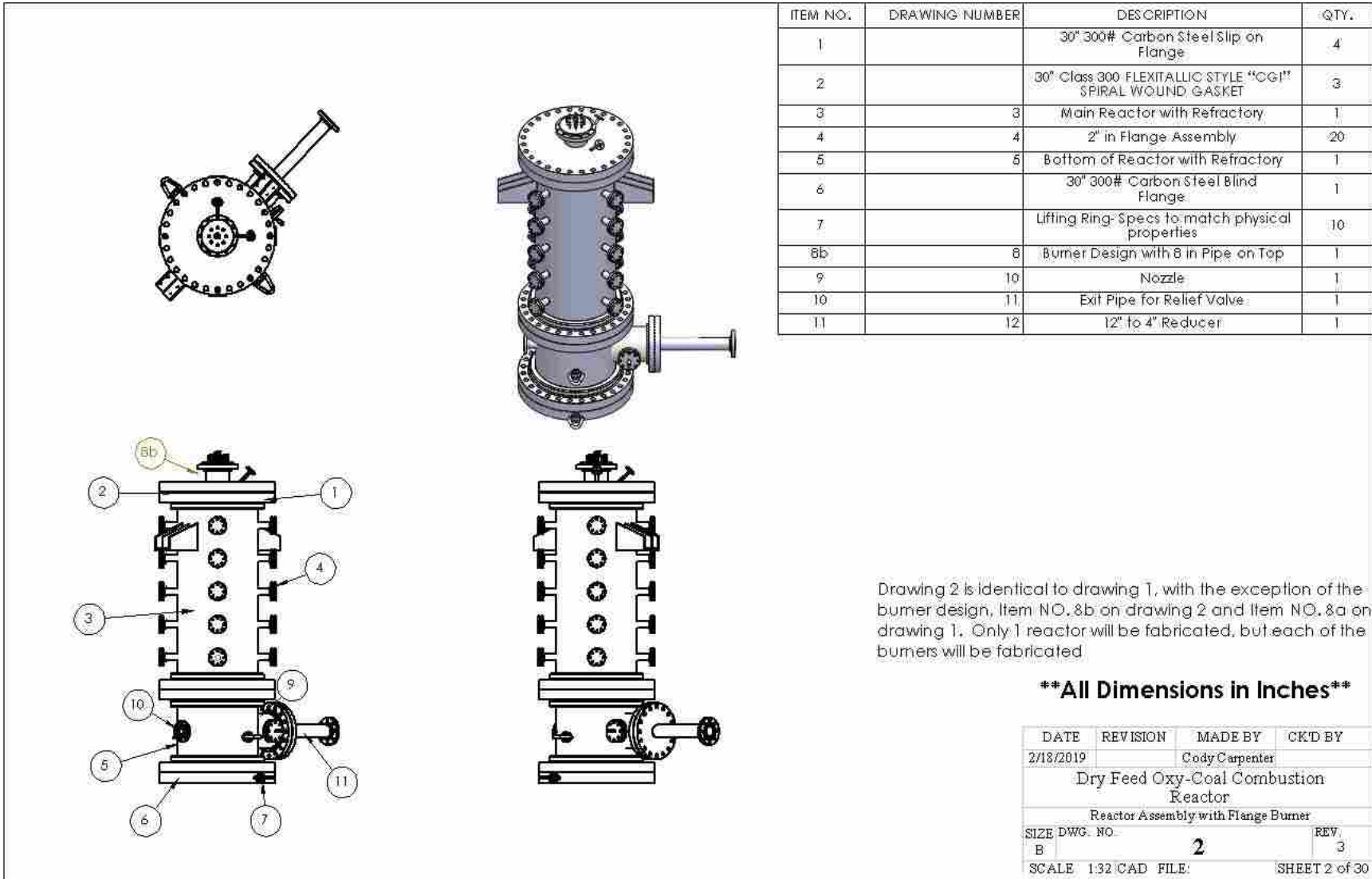


Figure B2: Drawing of POC Reactor Assembly with Flange Burner

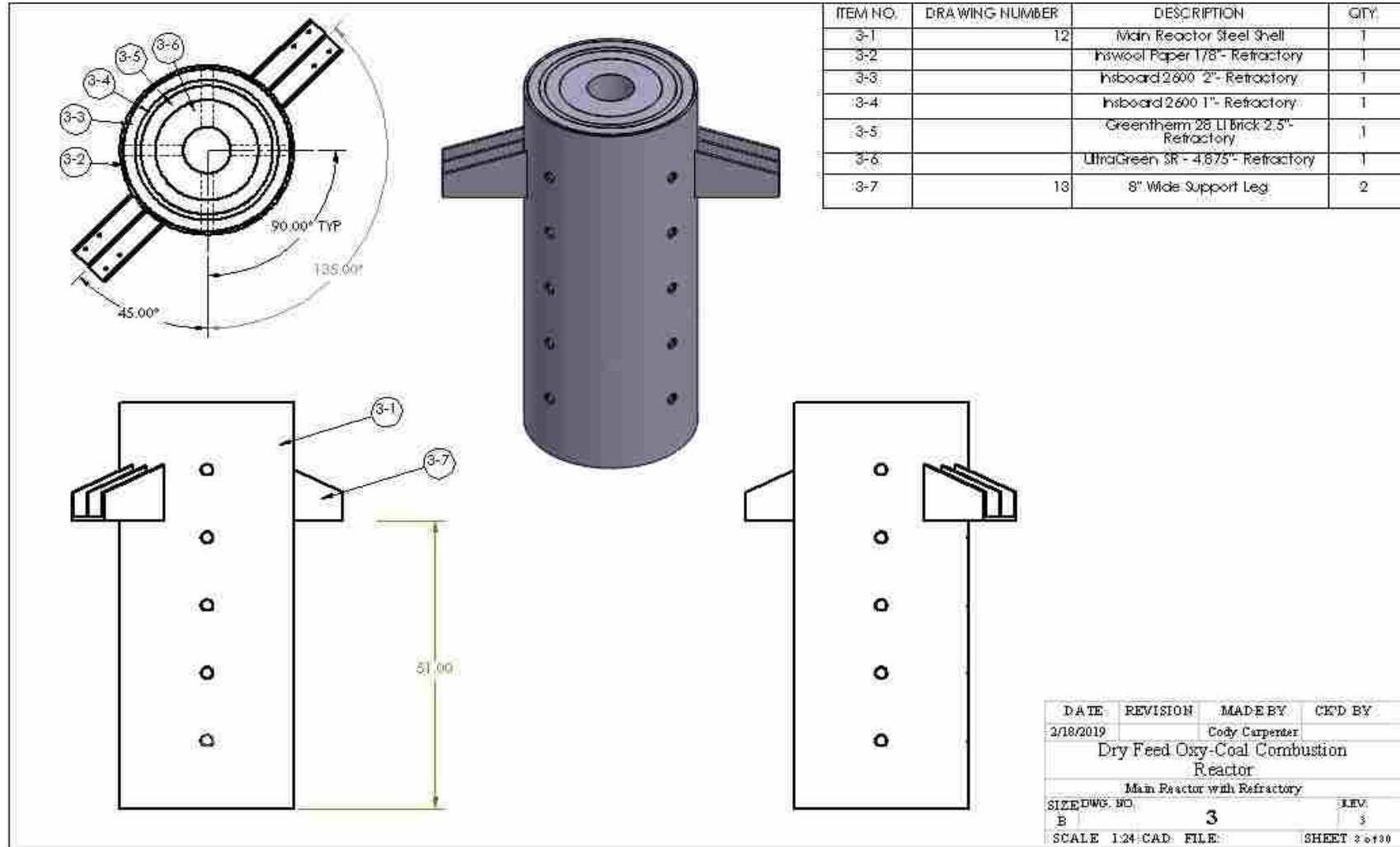
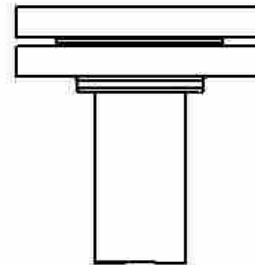
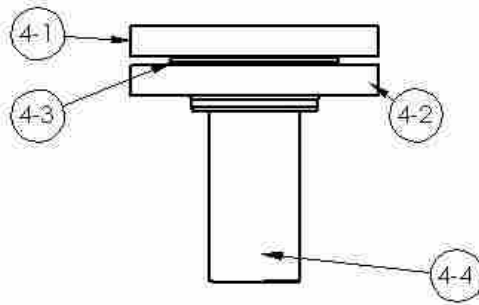
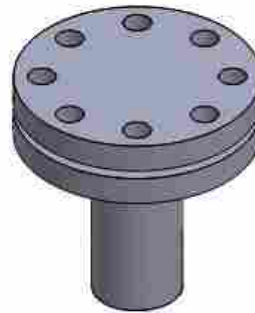
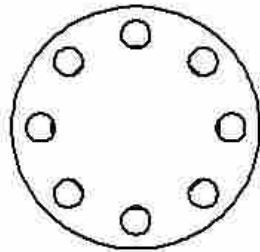


Figure B3: Drawing of Main Reactor with Refractory Assembly

ITEM NO.	PART NUMBER	DESCRIPTION	QTY.
4-1		2" 300# Carbon Steel Blind Flange	1
4-2		2" 300# Carbon Steel Slip on Flange	1
4-3		2" Class 300 FLEXITALLIC STYLE "CGI" SPIRAL WOUND GASKET	1
4-4	15	2" Steel Pipe X-Heavy	1



DATE	REVISION	MADE BY	CHK BY
09-27-2017		C. J. C. Carpenter	
Dry Feed Oxy-Coal Combustion Reactor			
2 in. Flange Assembly			
SIZE	DWG. NO.		REV
A		4	5
SCALE 1:24 CAD FILE			SHEET 4 of 30

Figure B4: Drawing of 2 Inch Flange Assembly

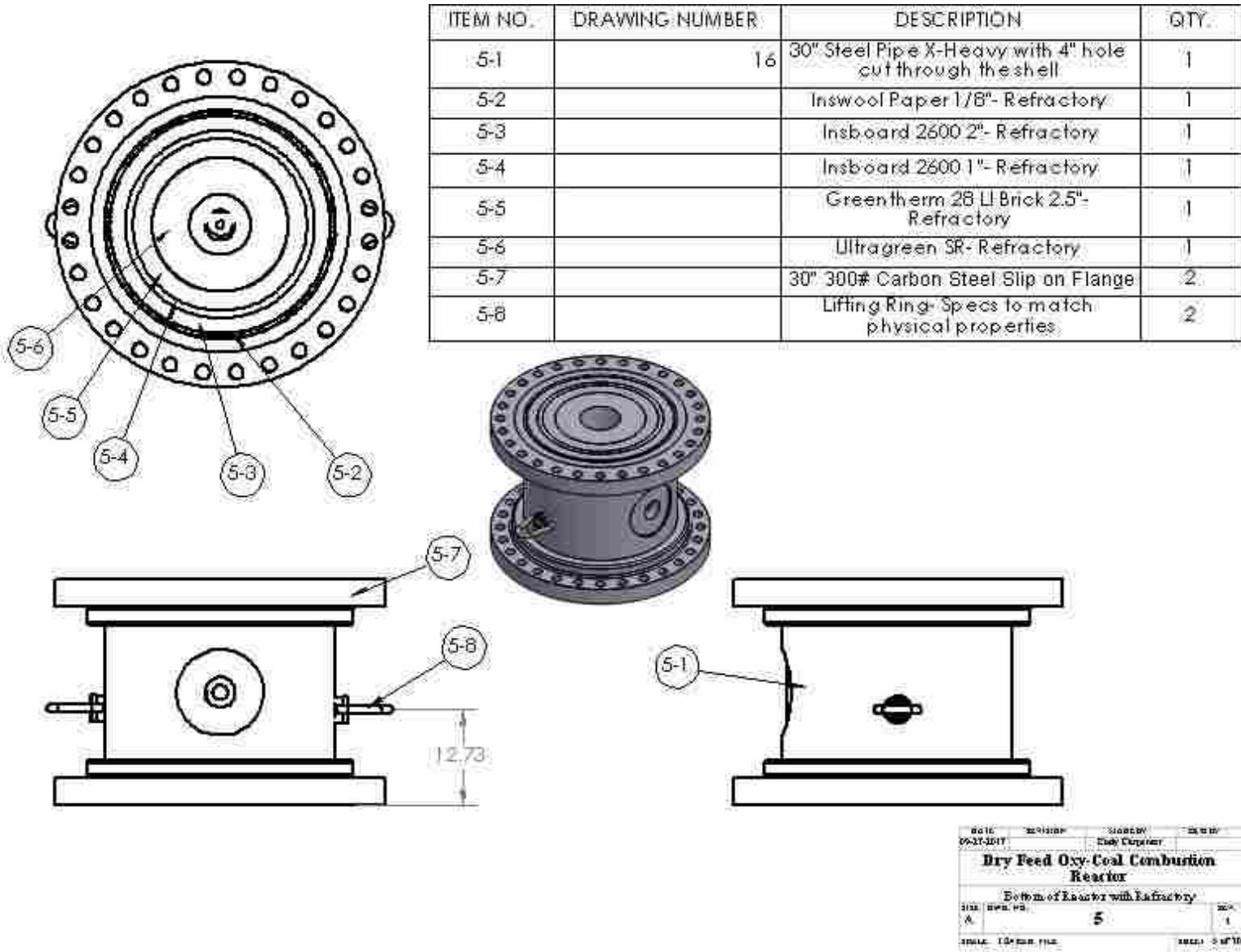
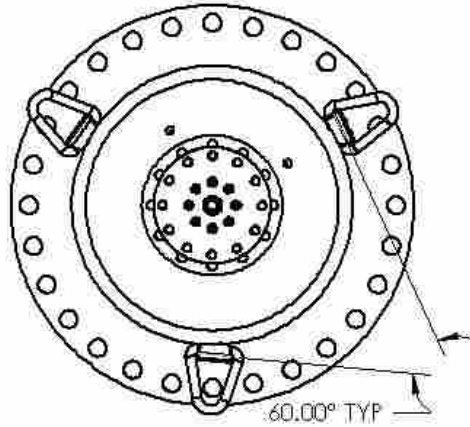
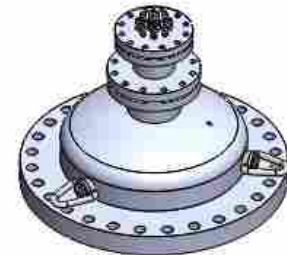
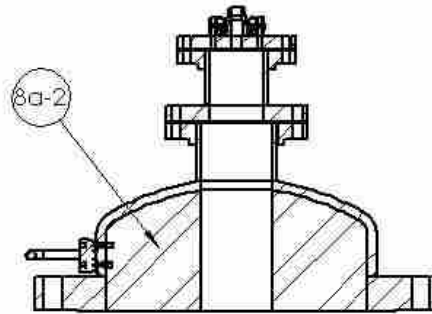
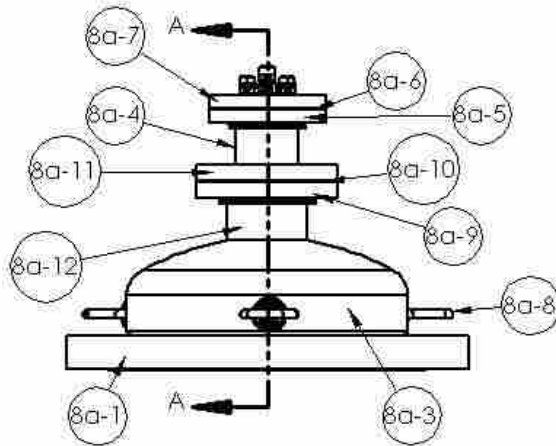


Figure B5: Drawing of Bottom of Reactor with Refractory Assembly



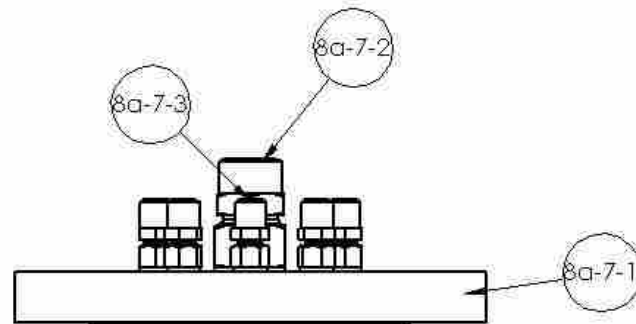
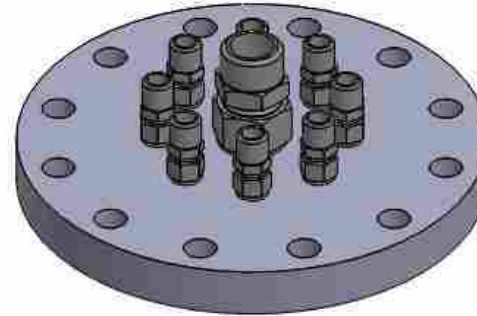
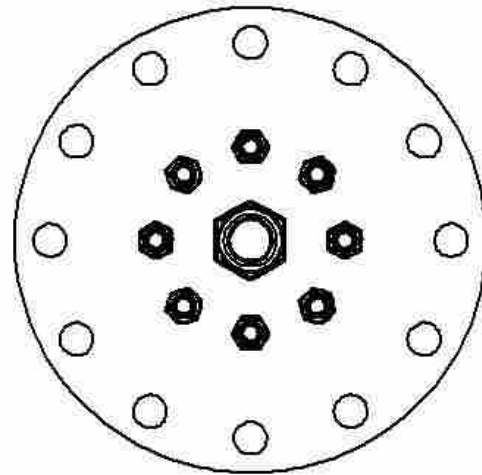
ITEM NO.	PART NUMBER	DESCRIPTION	QTY.
8a-1	17	30" 300# Blind Flange with Hole for Cap	1
8a-2		Refractory for Inside of Cap	1
8a-3	18	30" Steel Cap Schedule 20 with Hole in Top	1
8a-4	19	6" Steel Pipe X-Heavy for Top of Cap	1
8a-5		6" 300# Carbon Steel Slip on Flange	1
8a-6		6" Class 300 FLEXITALLIC STYLE "CGI" SPIRAL WOUND GASKET	2
8a-7	7	6" Blind Flange with Swageloks Sub-Assembly	1
8a-8		Lifting Ring- Specs to match physical properties	3
8a-9		8" 300# Carbon Steel Slip on Flange	1
8a-10		8" Class 300 FLEXITALLIC STYLE "CGI" SPIRAL WOUND GASKET	1
8a-11	21	8" 300# Blind Flange with Hole for 6" Pipe	1
8a-12	22	8" Steel Pipe X-Heavy	1



DATE	2/8/2019	MADE BY	Colby C. Saperstein	CREATED BY	
Dry Feed Oxy-Coal Combustion Reactor					
Cap Burner Assembly					
SIZE	DWG NO	6	REV	5	
A					
SCALE	1:1	CAD FILE		SHEET	4 of 30

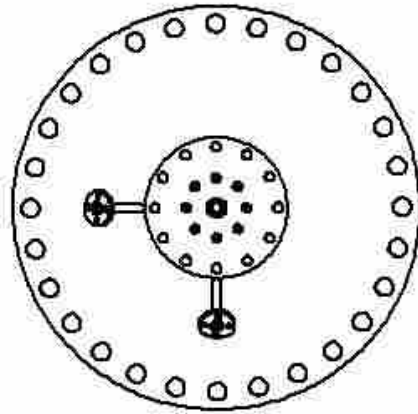
Figure B6: Drawing of Cap Burner Assembly

ITEM NO.	DRAWING NUMBER	DESCRIPTION	QTY.
8a-7-1	20	6" 300# Blind Flange with Holes for Tubes	1
8a-7-2		1 1/4 in. Tube Male Pipe Weld Swagelok- SS-2000-1-20W	1
8a-7-3		1/2 in. Tube Male Pipe Weld Swagelok- SS-810-1-8W	8

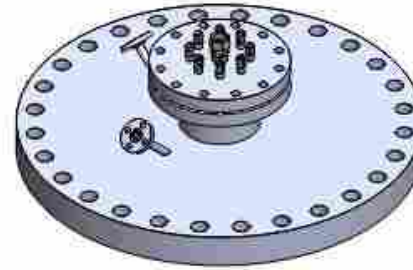
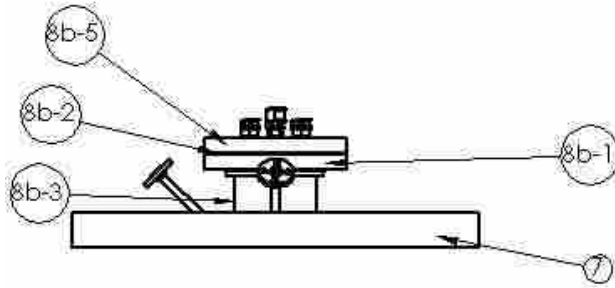


DATE	MADE BY	CRD BY
2/18/2019	Cody Carpenter	
Dry Feed Oxy-Coal Combustion Reactor		
6 in Blind Flange with Swageloks on top		
SIZE	DWG. NO.	REV.
A	7	1
SCALE 1:1	CAD FILE:	SHEET 7 of 36

Figure B7: Drawing of 6 Inch Blind Flange with Swageloks on Top



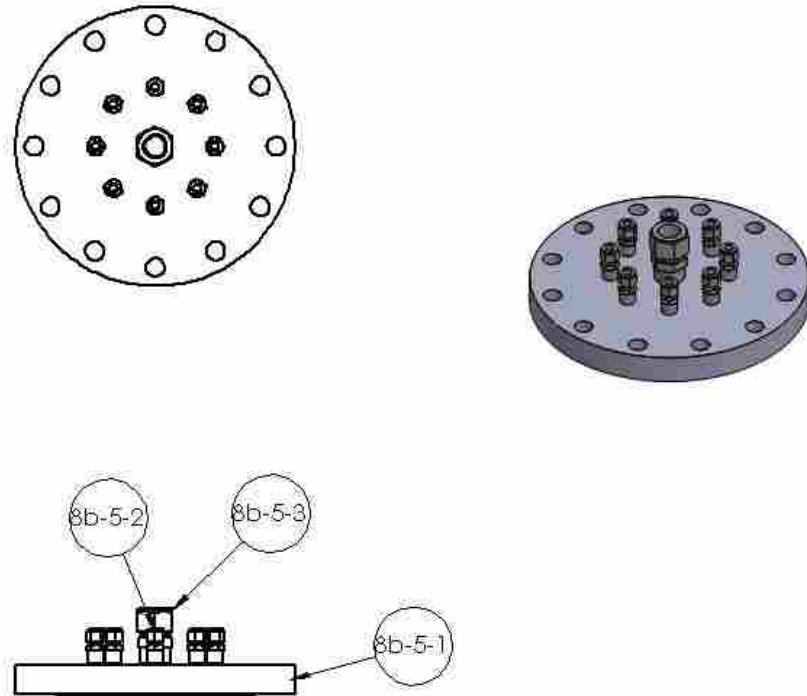
ITEM NO.	PART NUMBER	DESCRIPTION	QTY.
8b-1		8" 300# Carbon Steel Slip on Flange	1
8b-2		8" Class 300 FLEXITALLIC STYLE "CGI" SPIRAL WOUND GASKET	1
8b-3	22	8" Steel Pipe X-Heavy	1
8b-5	9	8" 300# Blind Flange with Holes for Swageloks Sub-Assembly	1
7	23		1
8		1-2 in class 300 Slip on Flange	2
9		UV Port for Flange Burner Design through Flange-2	2



DATE	2/12/2019	MADE BY	Colby Capron	DESIGN BY	
Dry Feed Oxy-Coal Combustion Reactor					
Flange Burner Design					
SIZE	OVERALL	8	REV	2	
SCALE: 1:1 (AS SHOWN)					
SHEET 2 OF 30					

Figure B8: Drawing of Flange Burner Design Assembly

ITEM NO.	DRAWING NUMBER	DESCRIPTION	QTY.
8b-5-1	8 In class 300 Blind Flange with holes for Swageloks	8" 300# Blind Flange with Holes for Swageloks	1
8b-5-2		1/2 in. Tube Male Pipe Weld Swagelok- SS-810-1-8W	8
8b-5-3		1 1/4 in. Tube Male Pipe Weld Swagelok- SS-2000-1-20W	1



DATE	2/28/2019	MADE BY	Colby Carpenter	CR'D BY	
Dry Feed Oxy-Coal Combustion Reactor					
8" Blind Flange with Swageloks on Top					
SIZE	OWS NO.	9	REV	1	
A					
SCALE 1:8 CAD FILE:				SHEET 9 of 36	

Figure B9: Drawing of 8 Inch Blind Flange with Swageloks on Top

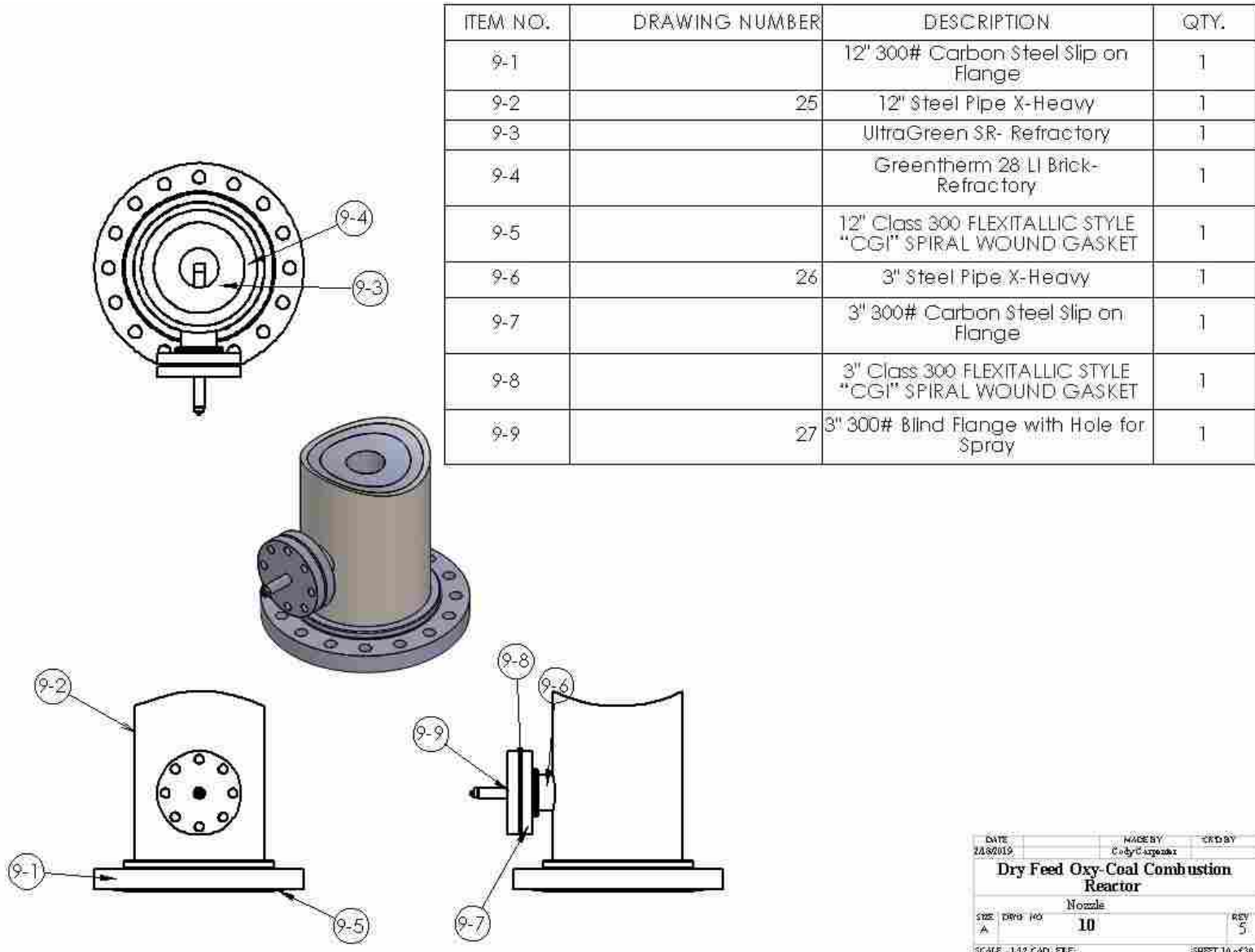
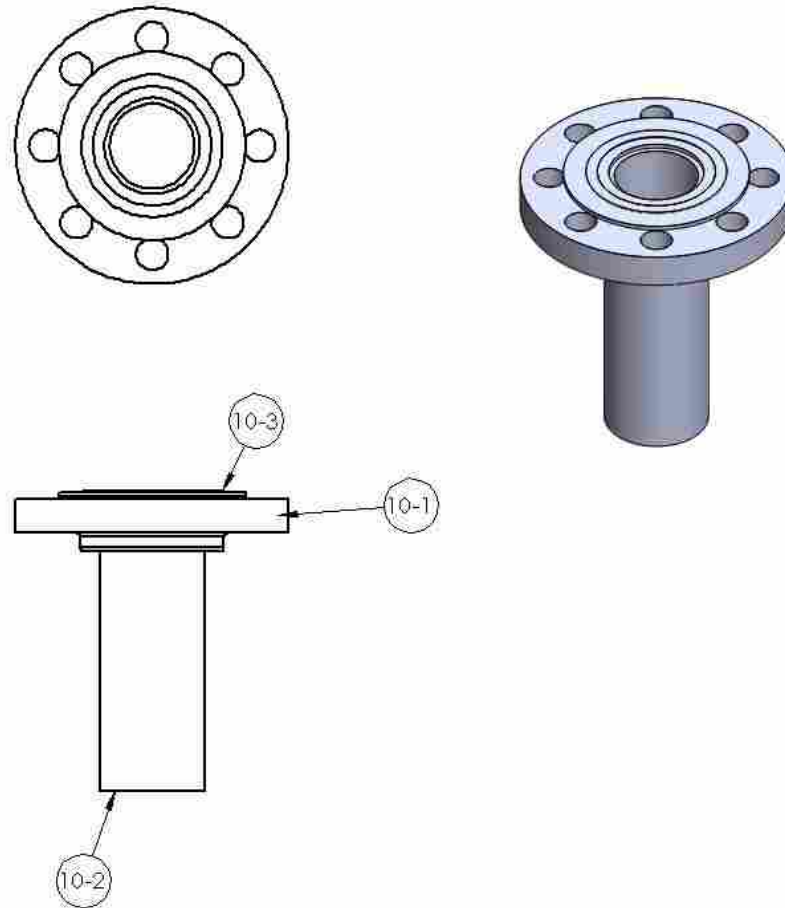


Figure B10: Drawing of Nozzle

DATE	2/8/2019	MADE BY	Cody C. Argonza	CRD BY	
Dry Feed Oxy-Coal Combustion Reactor					
Nozzle					
SIZE	DRWG NO	10	REV	5	
SCALE: 1:12 CAD FILE				SHEET 10 of 30	

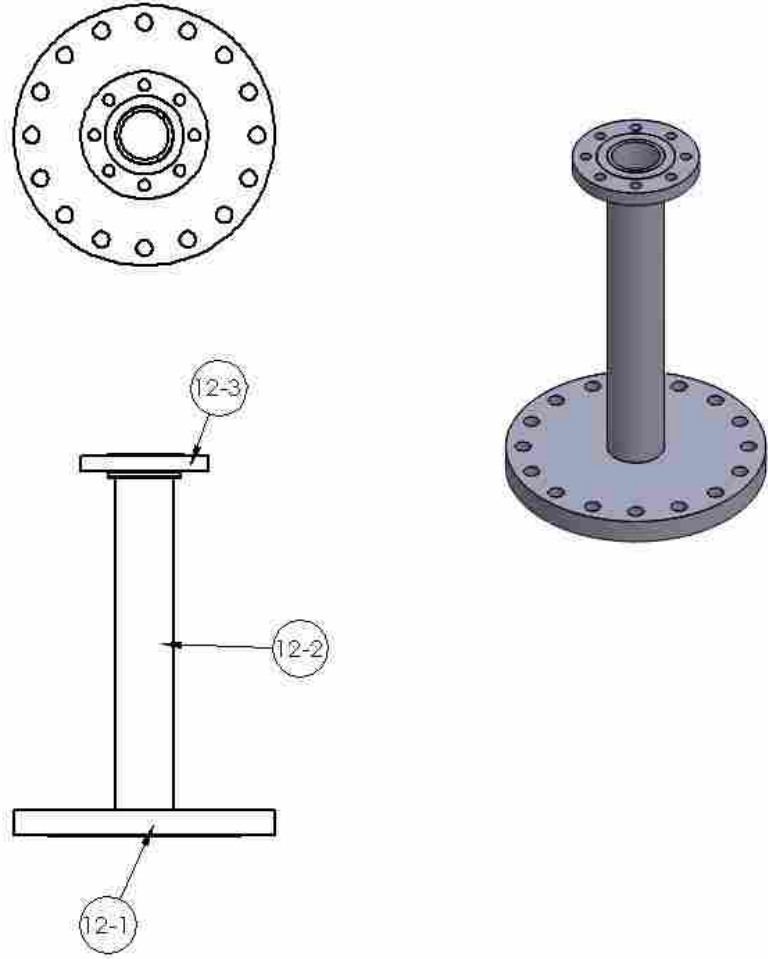
ITEM NO.	DRAWING NUMBER	DESCRIPTION	QTY.
10-1		2.5" 300# Carbon Steel Slip on Flange	1
10-2	28	2.5" Steel Pipe X-Heavy	1
10-3		2.5" Class 300 FLEXITALLIC STYLE "CGI" SPIRAL WOUND GASKET	1



DATE	MADE BY	CR/DRAW
2/18/2019	Cody Carpenter	
Dry Feed Oxy-Coal Combustion Reactor		
Exit Pipe for Relief Valve		
SIZE	DRWG NO.	REV
A	11	3
SCALE 1:4	CAD FILE	SHEET 11 of 30

Figure B11: Drawing of Exit Pipe for Relief Valve

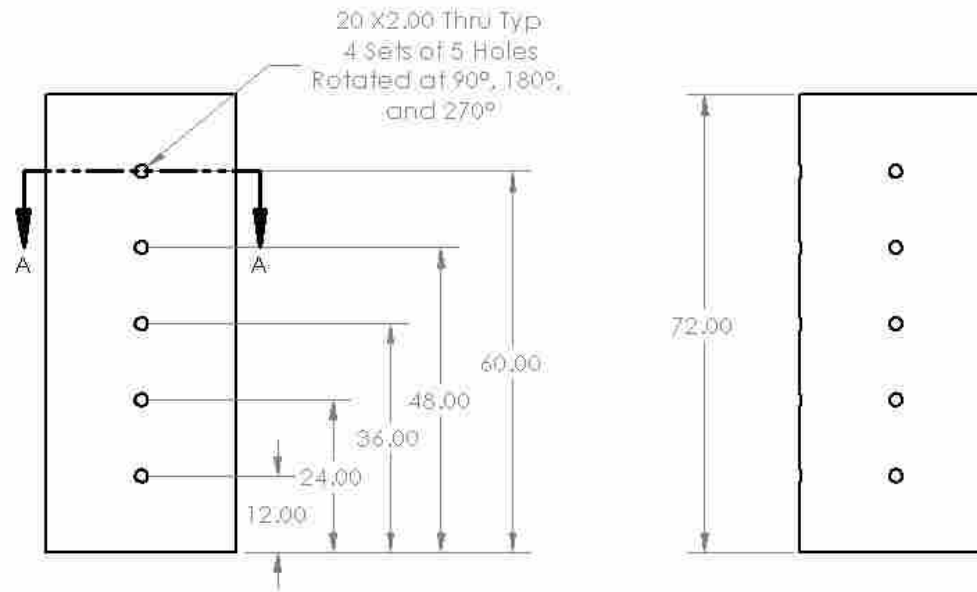
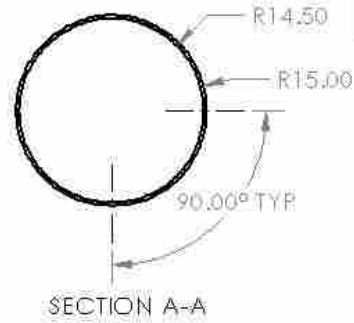
ITEM NO.	DRAWING NUMBER	DESCRIPTION	QTY:
12-1	29	12" 300# Blind Flange with Hole for 4" Pipe	1
12-2	30	4" Steel Pipe X-Heavy	1
12-3		4" 300# 309 Steel Slip on Flange	1



DATE	DESIGNED BY	CHECKED BY
2/19/2019	Cody Carpenter	
Dry Feed Oxy-Coal Combustion Reactor		
12-4" Reducer		
SHEET	DWG. NO.	REV.
A	12	
SCALE	1:12 CAD FILE	SHEET 12 of 30

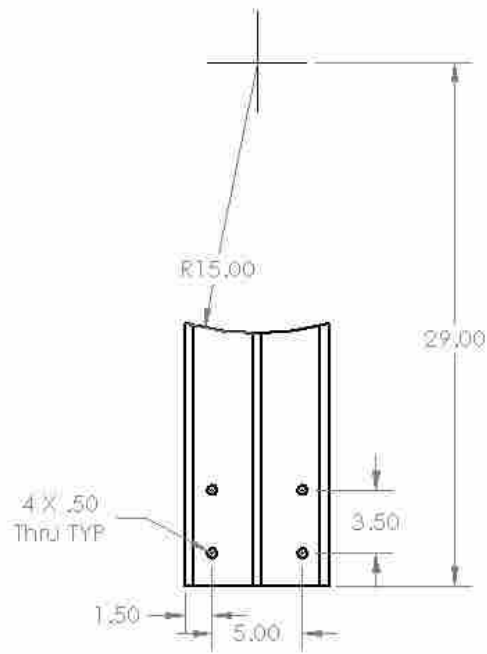
Figure B12: Drawing of 12 to 4 Inch Reducer

ITEM NO.	DRAWING NUMBER	DESCRIPTION	QTY.
3-1	13	30" Carbon Steel X-Heavy Pipe with Holes for Pipes Drilled in it	1

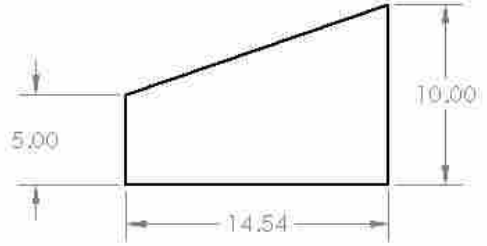
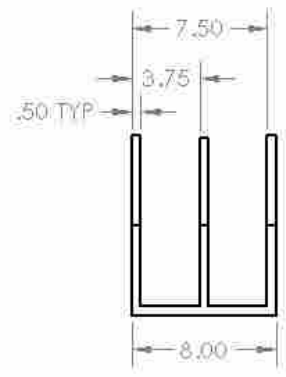
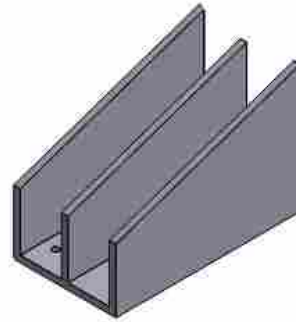


DATE	2/18/2019	MADE BY	Cody Carpenter	CR'D BY	
Dry Feed Oxy-Coal Combustion Reactor					
Main Reactor Shell					
SHEET	DWG NO	13		REV	13
SCALE	1/4" = 1'-0"	CAD FILE		SHEET 13 of 30	

Figure B13: Drawing of Main Reactor Shell



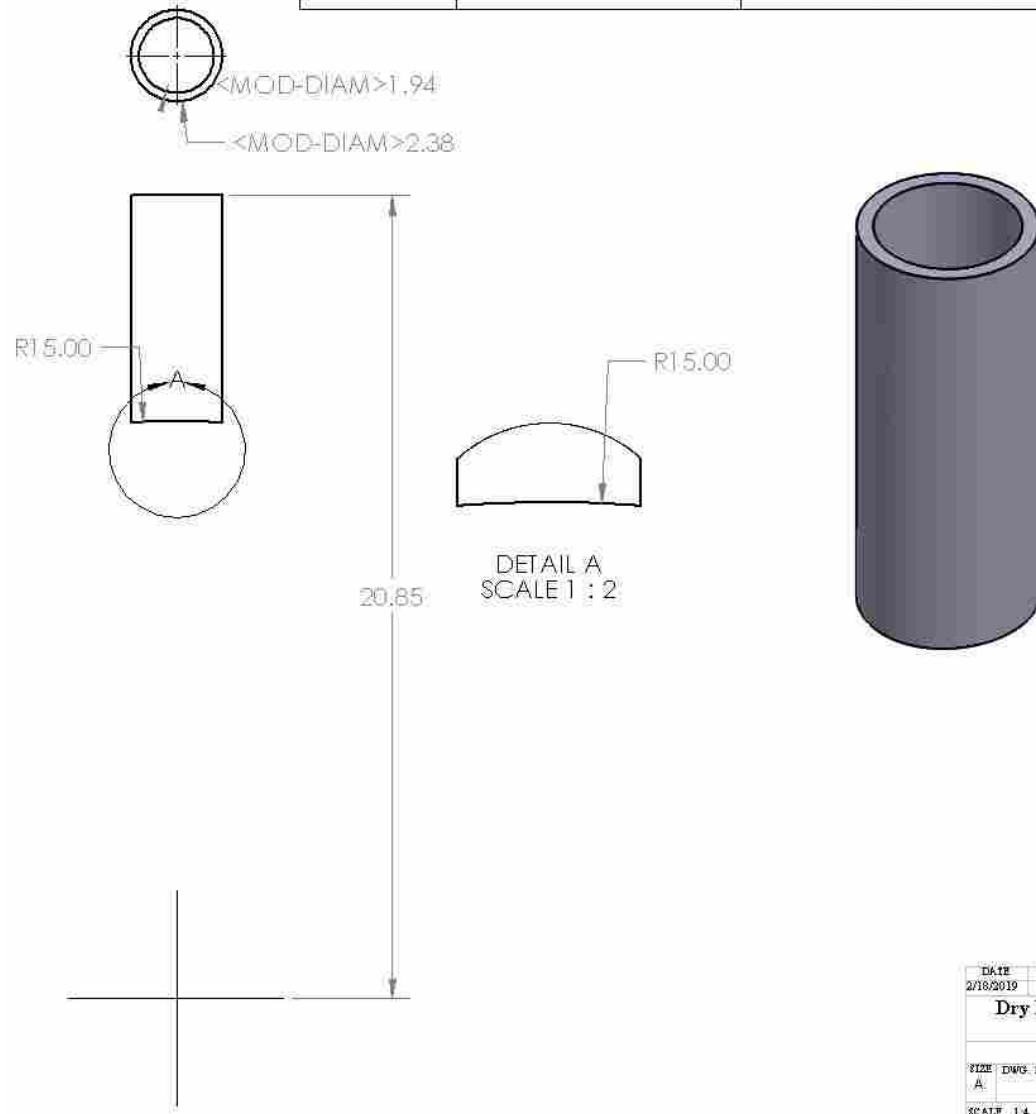
ITEM NO.	DRAWING NUMBER	DESCRIPTION	QTY.
3-7	14	Carbon Steel Support Leg- To be Welded onto Steel Reactor Shell	2



DATE	MADE BY	CRD BY
2/18/2019	Jody Carpenter	
Dry Feed Oxy-Coal Combustion Reactor		
Reactor Support Leg		
SIZE	DWG NO	REV
A	14	3
SCALE	CAD FILE	SHEET 14 of 30

Figure B14: Drawing of Reactor Support Leg

ITEM NO.	DRAWING NUMBER	DESCRIPTION	QTY.
4-4	15	2" X-Heavy Pipe-Carbon Steel	20



DATE	MADE BY	CHECK BY
2/18/2019	Cody Carpenter	
Dry Feed Oxy-Coal Combustion Reactor		
2" X-Heavy Steel Pipe		
SIZE	DWG. NO.	REV.
A	15	3
SCALE: 1:4 CAD FILE:		SHEET 15 of 20

Figure B15: Drawing of 2 Inch X-Heavy Steel Pipe

ITEM NO.	DRAWING NUMBER	DESCRIPTION	QTY.
5-1	16	30" Steel Pipe X-Heavy with 2.5" and 12" hole Cut Through the Shell	1

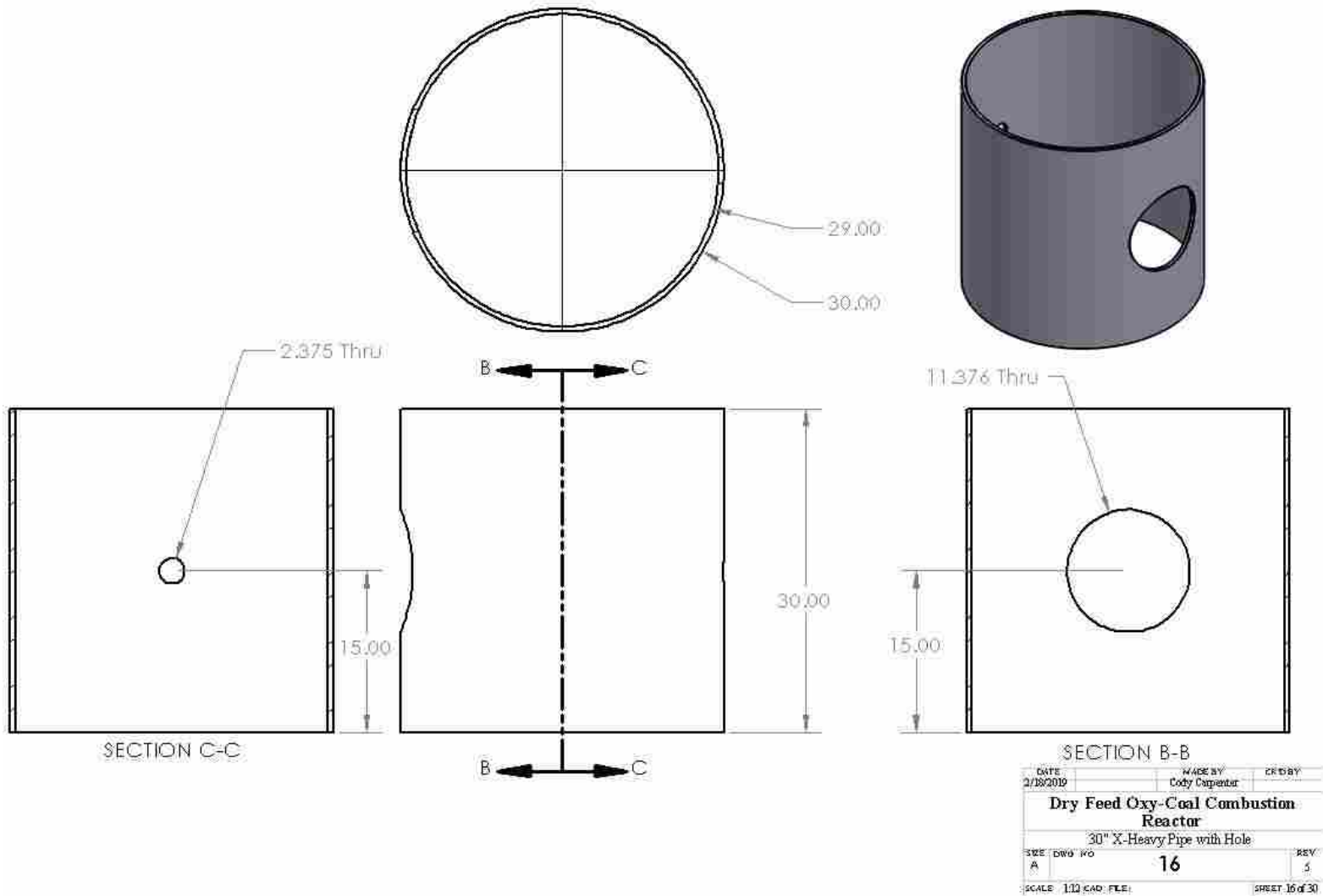
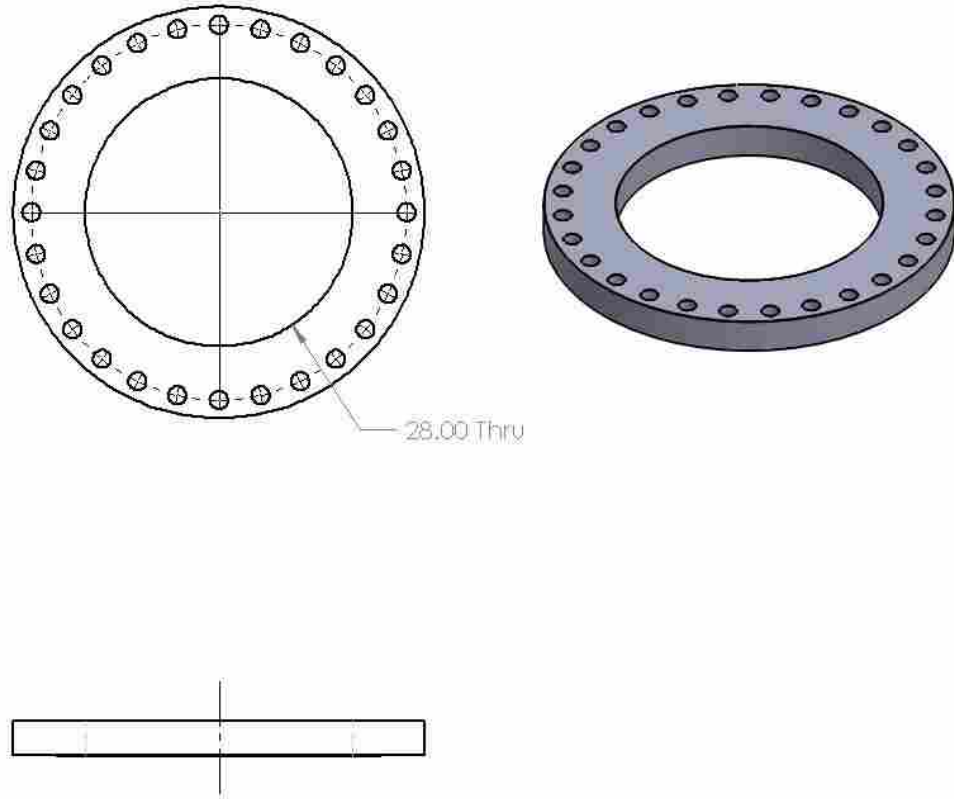


Figure B16: Drawing of 30 Inch X-Heavy Pipe with Hole

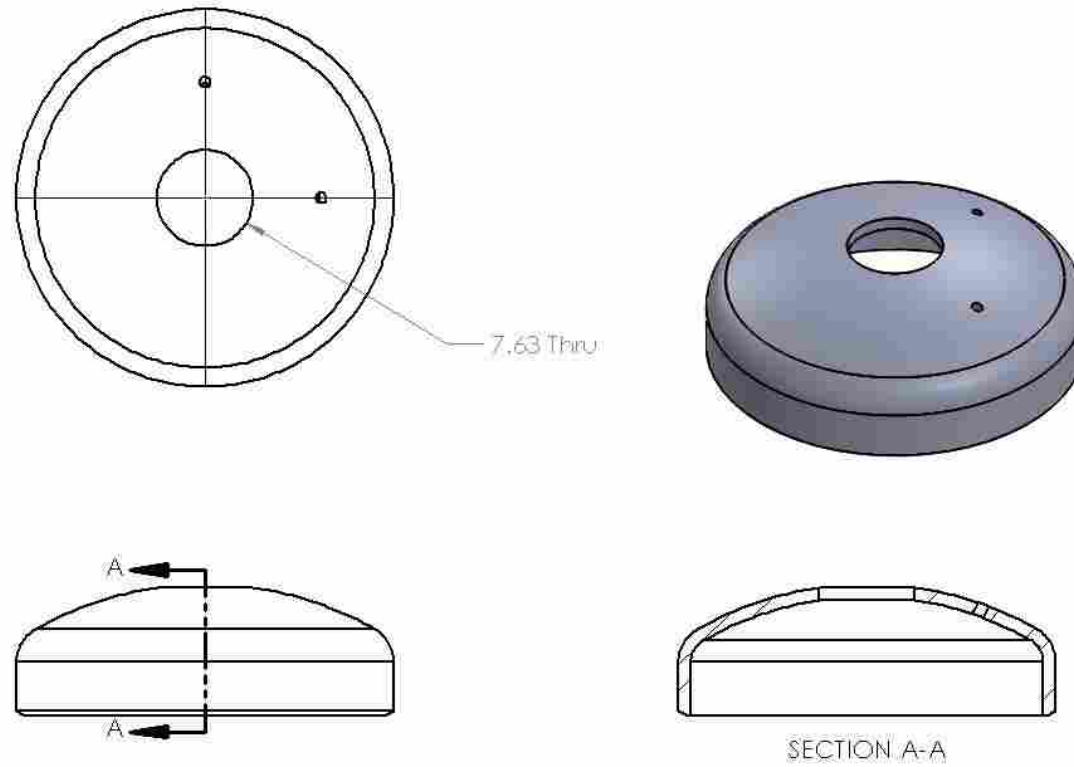
ITEM NO.	DRAWING NUMBER	DESCRIPTION	QTY.
8a-1	17	30" 300# Blind Flange with 28" hole in it for Cap	1



DATE	MADE BY	CRD BY
2/18/2019	Cody Carpenter	
Dry Feed Oxy-Coal Combustion Reactor		
30" 300# Blind Flange with Hole for Cap		
SIZE	DWG. NO.	REV.
A	17	3
SCALE: 1:16 CAD FILE:		SHEET 17 of 20

Figure B17: Drawing of 30 Inch Class 300 Blind Flange with Hole for Cap

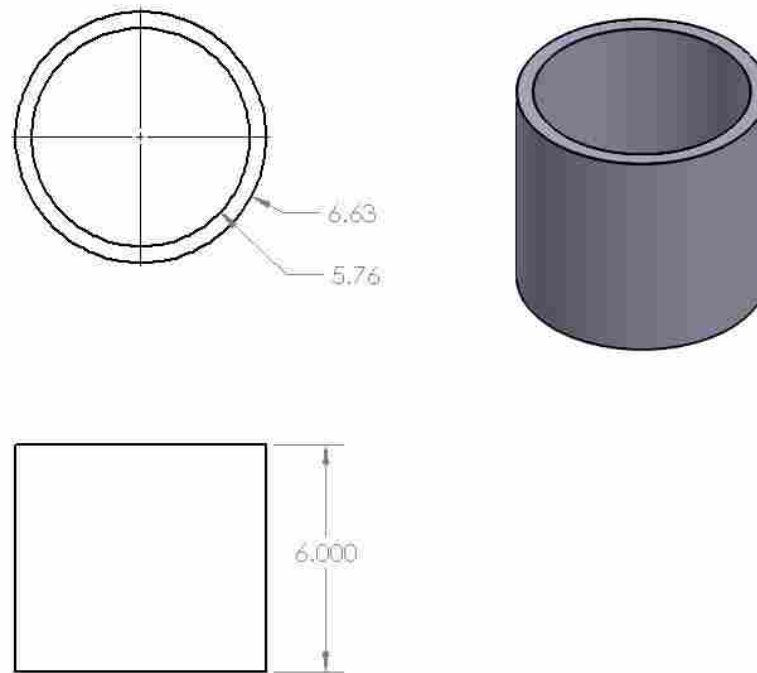
ITEM NO.	DRAWING NUMBER	DESCRIPTION	QTY.
8a-3	18	30" Steel Cap Schedule 20 with Hole in Top for 6" Pipe	1



DATE	2/18/2019	MAD BY	Coby Carpenter	CRD BY	
Dry Feed Oxy-Coal Combustion Reactor					
30" Steel Cap Schedule 20					
FILE	DWG. NO.	18	LEV.	2	
SCALE 1:12 CAD FILE				SHEET 18 of 30	

Figure B18: Drawing of 30 Inch Steel Cap Schedule 20

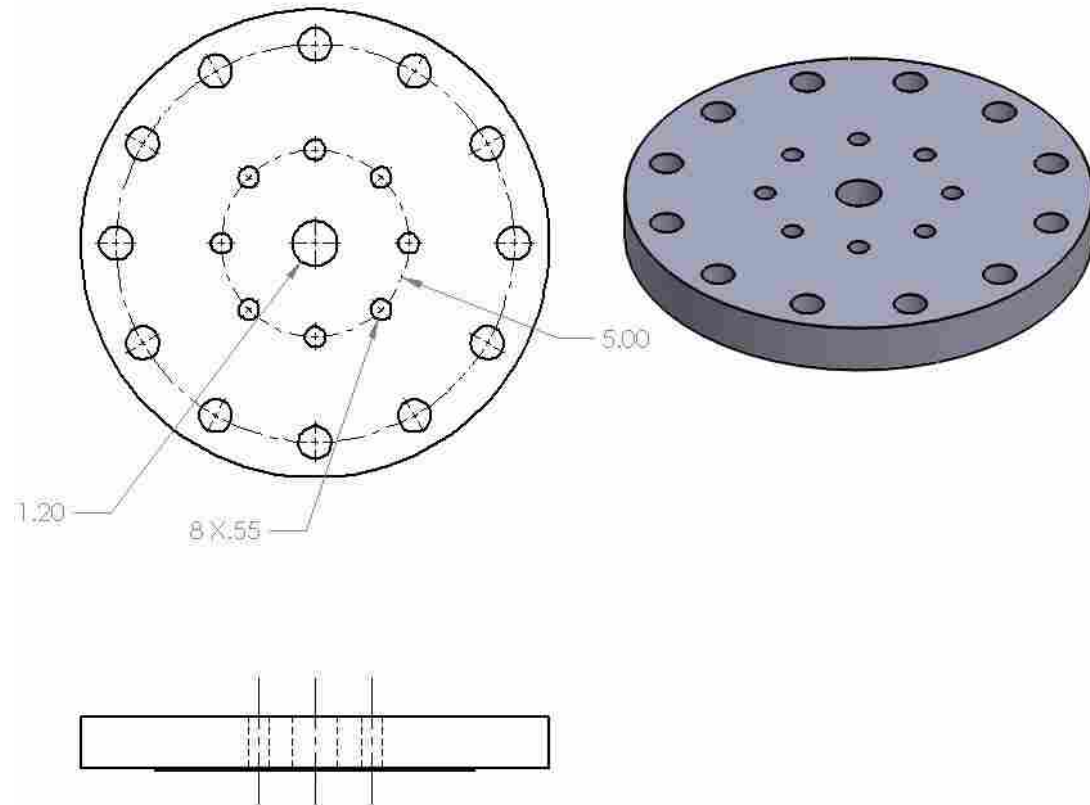
ITEM NO.	DRAWING NUMBER	DESCRIPTION	QTY.
8a-4	19	6" X-Heavy Steel Pipe	1



DATE	MAD BY	CD BY
2/18/2019	Cody Carpenter	
Dry Feed Oxy-Coal Combustion Reactor		
6" X-Heavy Steel Pipe		
SIZE	DWG. NO.	REV.
A	19	2
SCALE: 1:4 CAD FILE:		SHEET 19 of 30

Figure B19: Drawing of 6 Inch X-Heavy Steel Pipe for Top of Cap

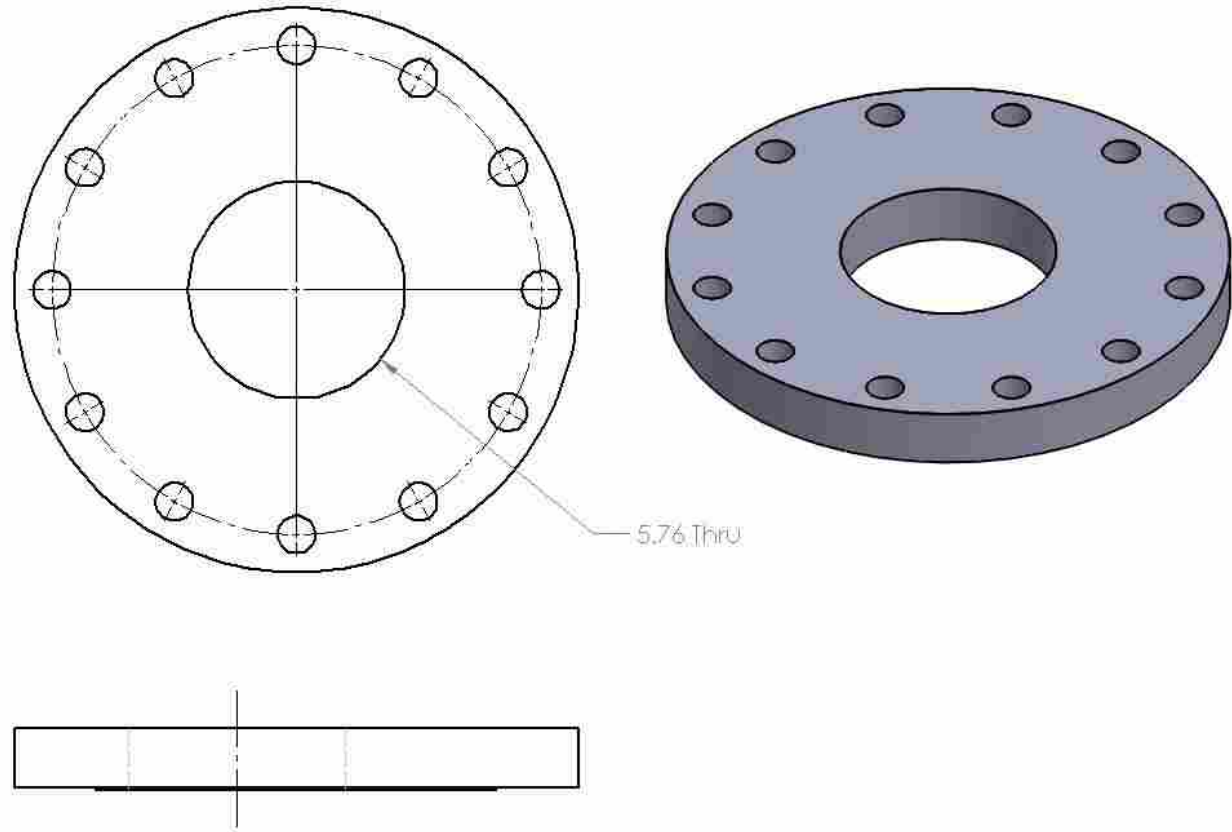
ITEM NO.	DRAWING NUMBER	DESCRIPTION	QTY.
8a-7-1	20	6" 300# Blind Flange with Holes for Tubes	1



DATE	MADE BY	CHKD BY
2/18/2019	Cody Carpenter	
Dry Feed Oxy-Coal Combustion Reactor		
Blind Flange with Holes		
REV	DATE	BY
A	20	2
SCALE 1:4 CAD FILE		SHEET 20 of 30

Figure B20: Drawing of 6 Inch Class 300 Blind Flange with Holes for Tubes

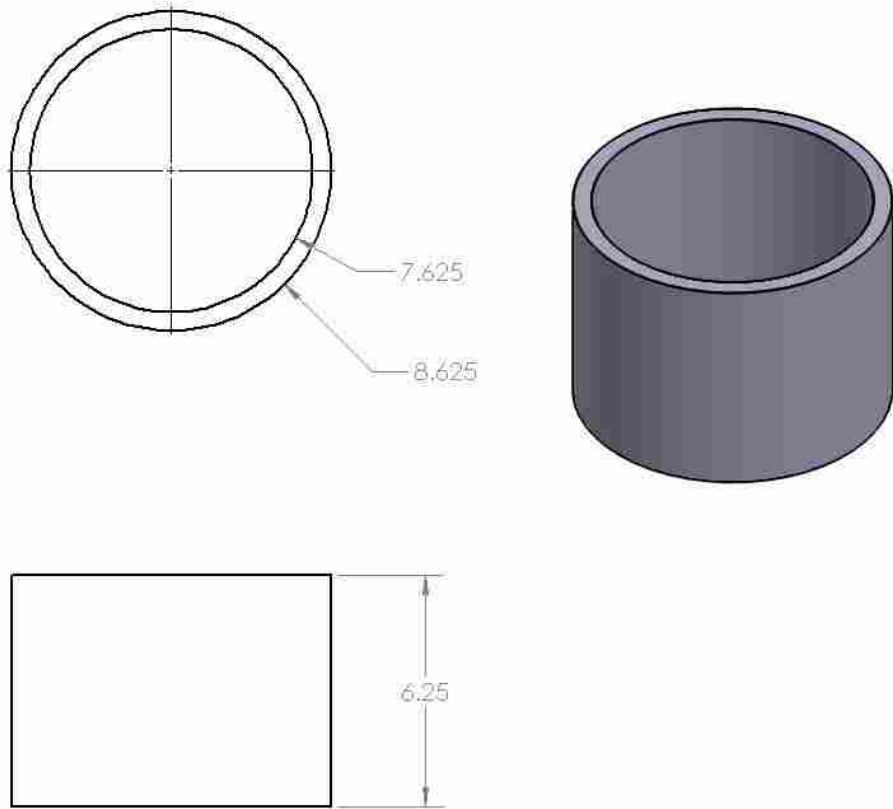
ITEM NO.	DRAWING NUMBER	DESCRIPTION	QTY.
18a-11	21	8" 300# Blind Flange with Hole for 6" Pipe	1



DATE	2/13/2019	MADE BY	Cody Carpenter	CED BY
Dry Feed Oxy-Coal Combustion Reactor				
8" Blind Flange with hole for 6" Pipe				
SIZE	A	DWG. NO.	21	REV.
				3
SCALE	1:4	CAD FILE	SHEET 21 of 30	

Figure B21: Drawing of 8 Inch Class 300 Blind Flange with Hole for 8 Inch Pipe

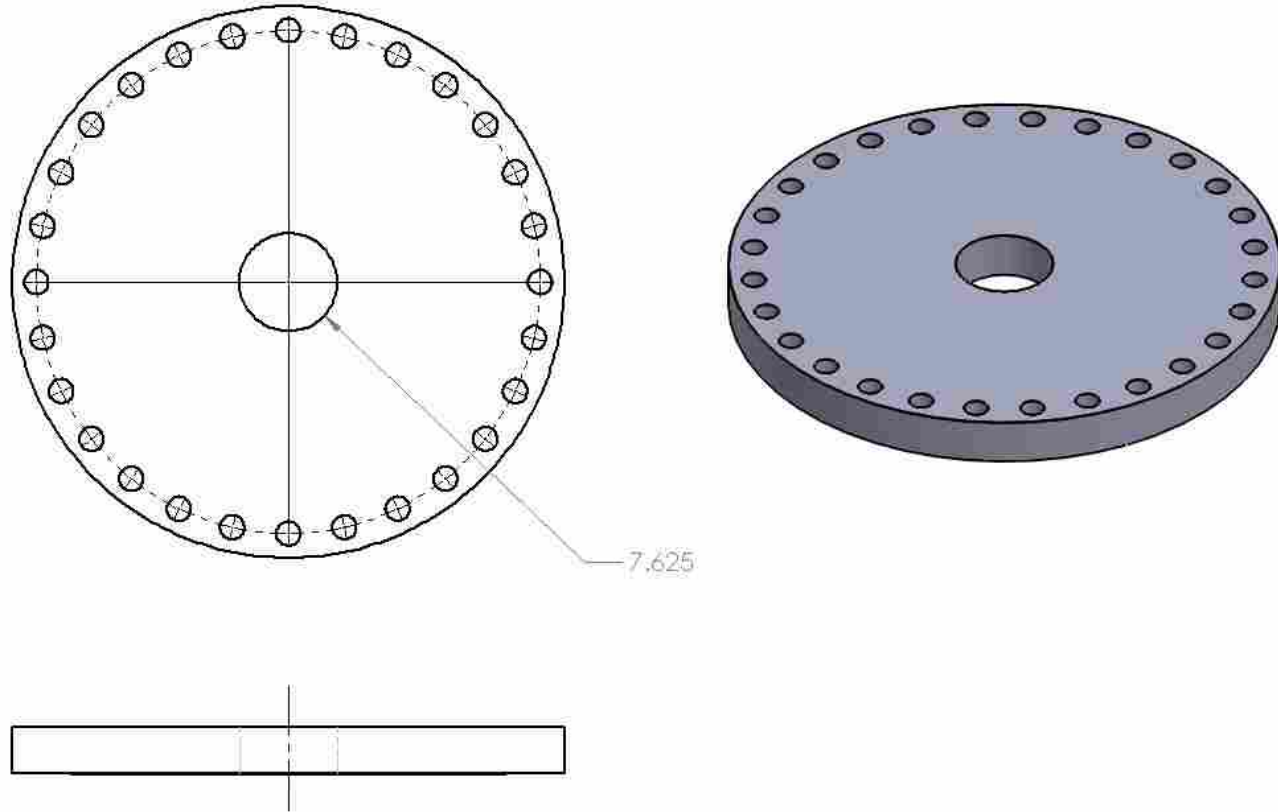
ITEM NO.	DRAWING NUMBER	DESCRIPTION	QTY.
8a-12	22	8" X-Heavy Pipe- Carbon Steel	2



DATE	MADE BY	CRIBBY
2/13/2019	Cody Carpenter	
Dry Feed Oxy-Coal Combustion Reactor		
8" Steel Pipe X-Heavy		
REV	DWG. NO.	LEV.
A	22	2
SCALE: 1:4 CAD FILE:		SHEET 22 of 30

Figure B22: Drawing of 8 Inch X-Heavy Steel Pipe

ITEM NO.	DRAWING NUMBER	DESCRIPTION	QTY.
8b-4	23	30" 300# Blind Flange with Hole for 8" Pipe	1

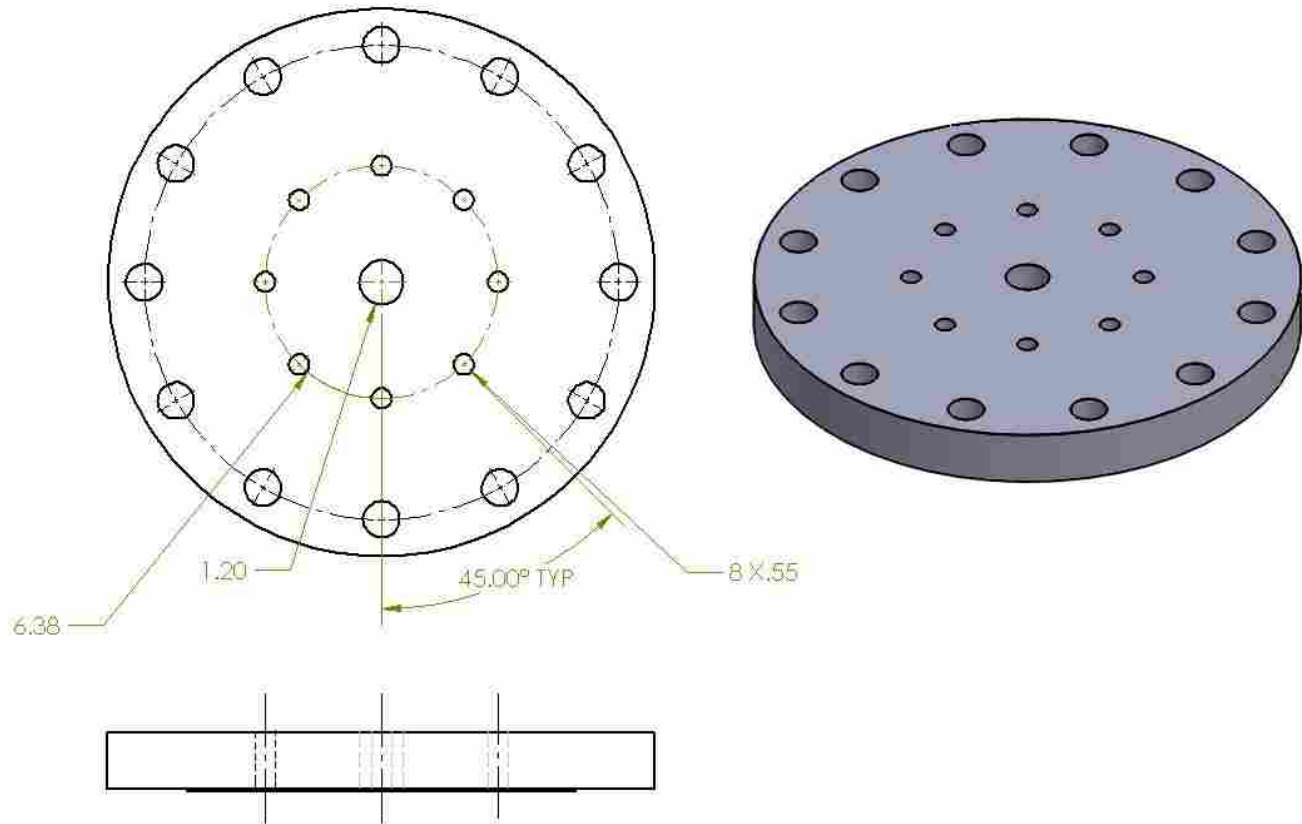


06

DATE	MADE BY	CHK BY:
2/18/2019	Cody Carpenter	
Dry Feed Oxy-Coal Combustion Reactor		
30" #300 Blind Flange with hole for 8" Pipe		
SIZE	DWG. NO.	REV.
A	23	2
SCALE	1:12	FILE
		PAGE 23 of 30

Figure B23: Drawing of 30 Inch Class 300 Blind Flange with Hole for 8 Inch Pipe

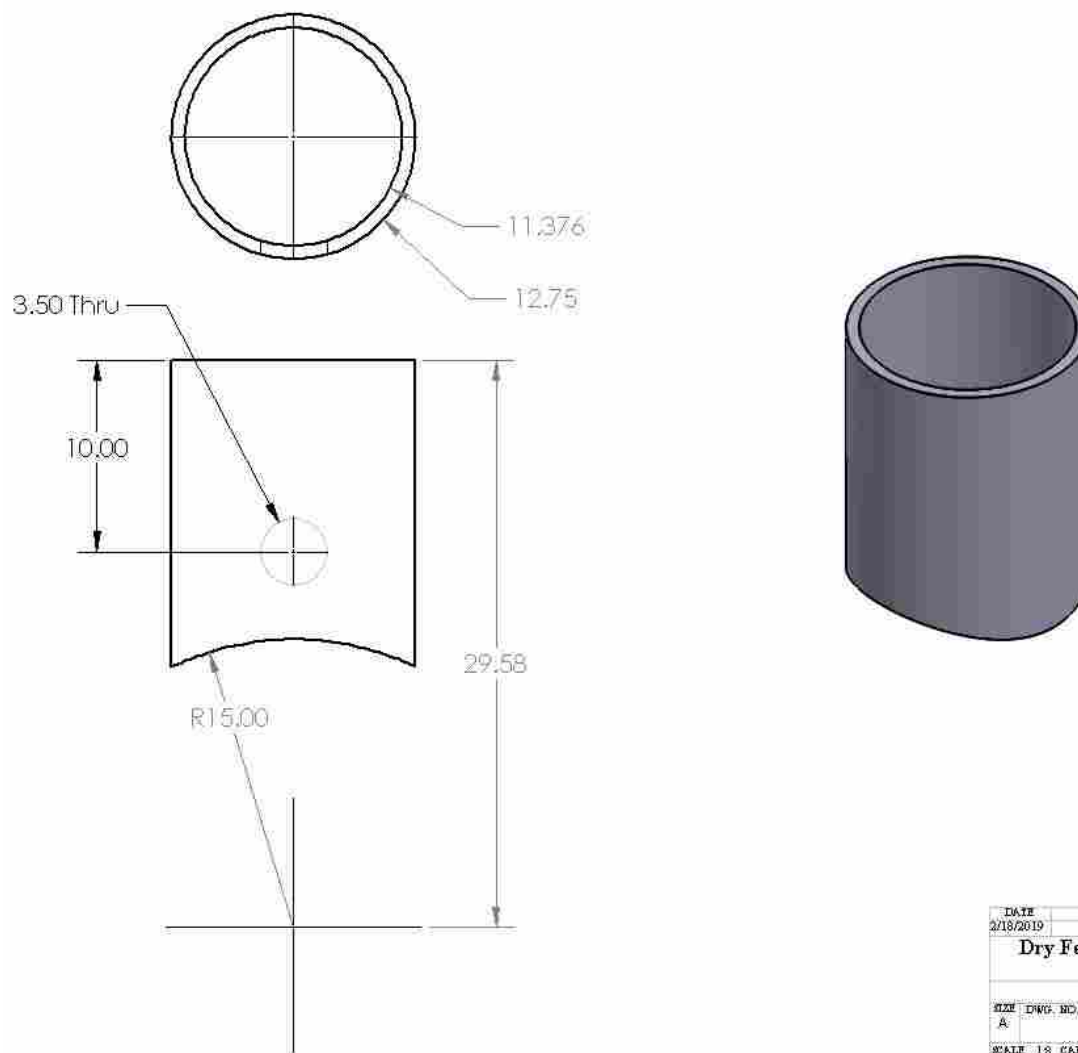
ITEM NO.	DRAWING NUMBER	DESCRIPTION	QTY.
8b-5-1	8 in class 300 Blind Flange with holes for Swageloks	8" 300# Blind Flange with Holes for Swageloks	1



DATE	2/18/2019	MADE BY	Coody Carpenter	CHECK BY	
Dry Feed Oxy-Coal Combustion Reactor					
8" 300# Blind Flange with Holes for Swageloks					
SIZE	DWG. NO.	REV			
A	24	3			
SCALE 1:2 CAD FILE					SHEET 24 of 30

Figure B24: Drawing of 8 Inch Class 300 Blind Flange with Holes for Swageloks

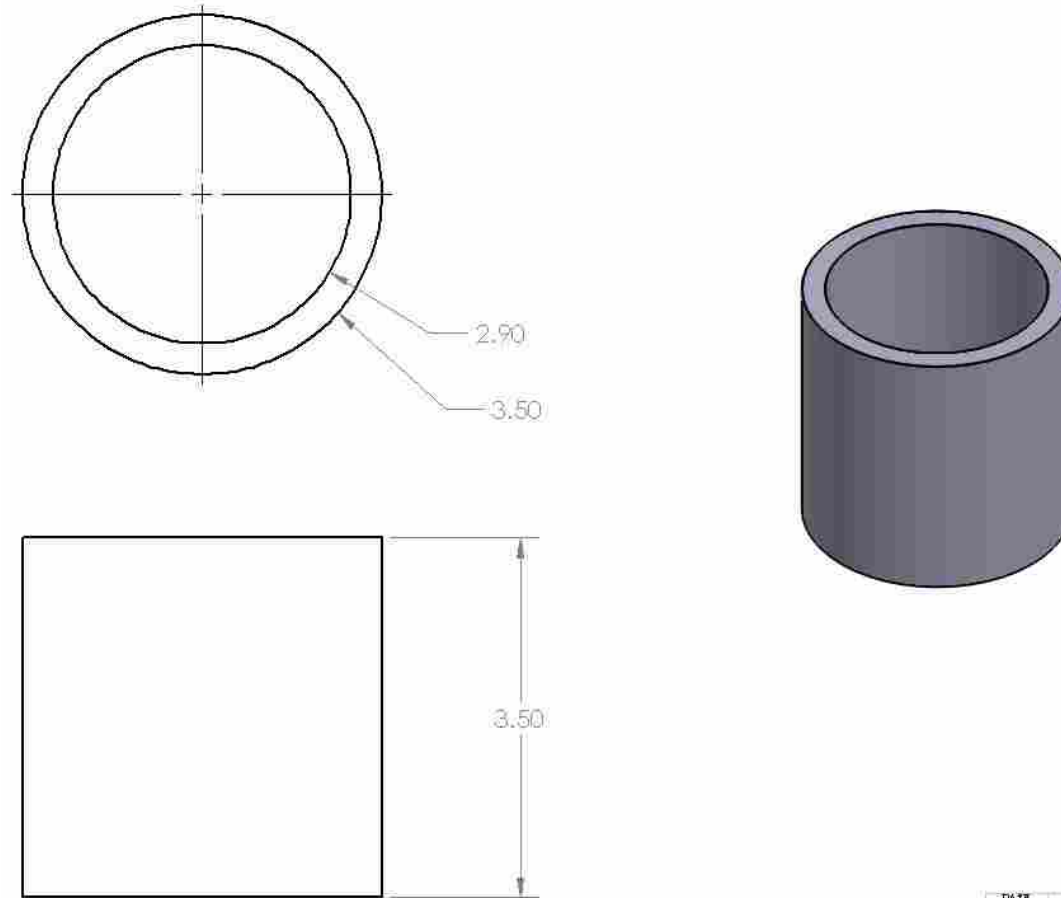
ITEM NO.	DRAWING NUMBER	DESCRIPTION	QTY.
9-2	25	12" Sch. 80 Pipe-Carbon Steel	1



DATE	MADE BY	CHKD BY
2/18/2019	Cody Carpenter	
Dry Feed Oxy-Coal Combustion Reactor		
12" Sch. 80 Steel Pipe		
SIZE	ENG. NO.	REV.
A	25	3
SCALE 1:8 CAD FILE		SHEET 25 of 30

Figure B25: Drawing of 8 Inch Class 300 Blind Flange with Holes for Swageloks

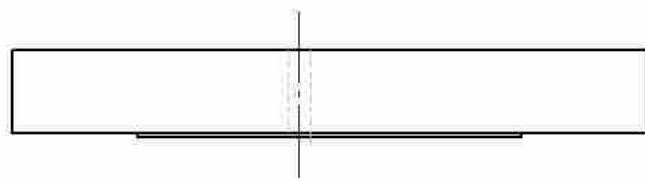
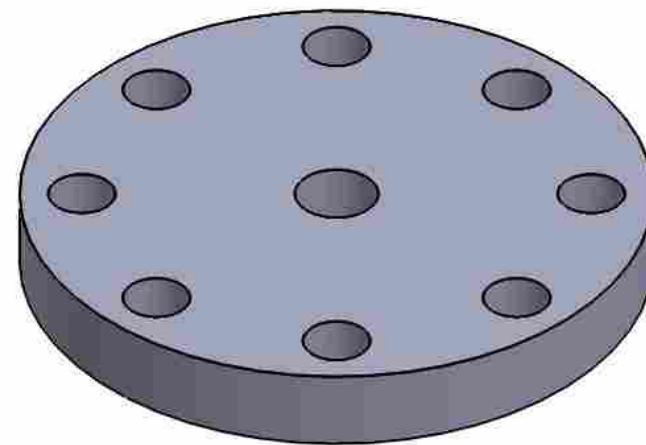
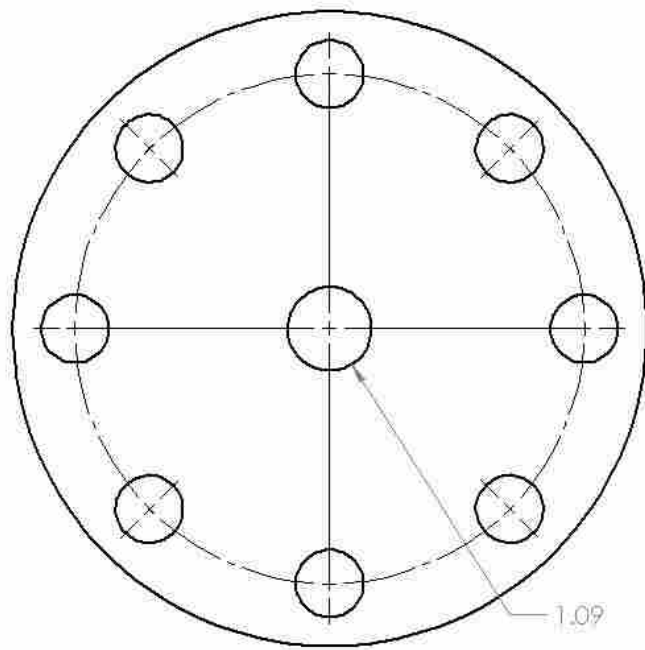
ITEM NO.	DRAWING NUMBER	DESCRIPTION	QTY.
9-6	26	3" Carbon Steel Pipe X-Heavy	1



DATE	MAD BY	CRD BY
2/18/2019	Cody Carpenter	
Dry Feed Oxy-Coal Combustion Reactor		
3" Pipe X-Heavy		
SIZE	DWG. NO.	LEV.
A	26	2
SCALE: 1:3 CAD FILE:		SHEET 26 of 30

Figure B26: Drawing of 3 Inch X-Heavy Pipe

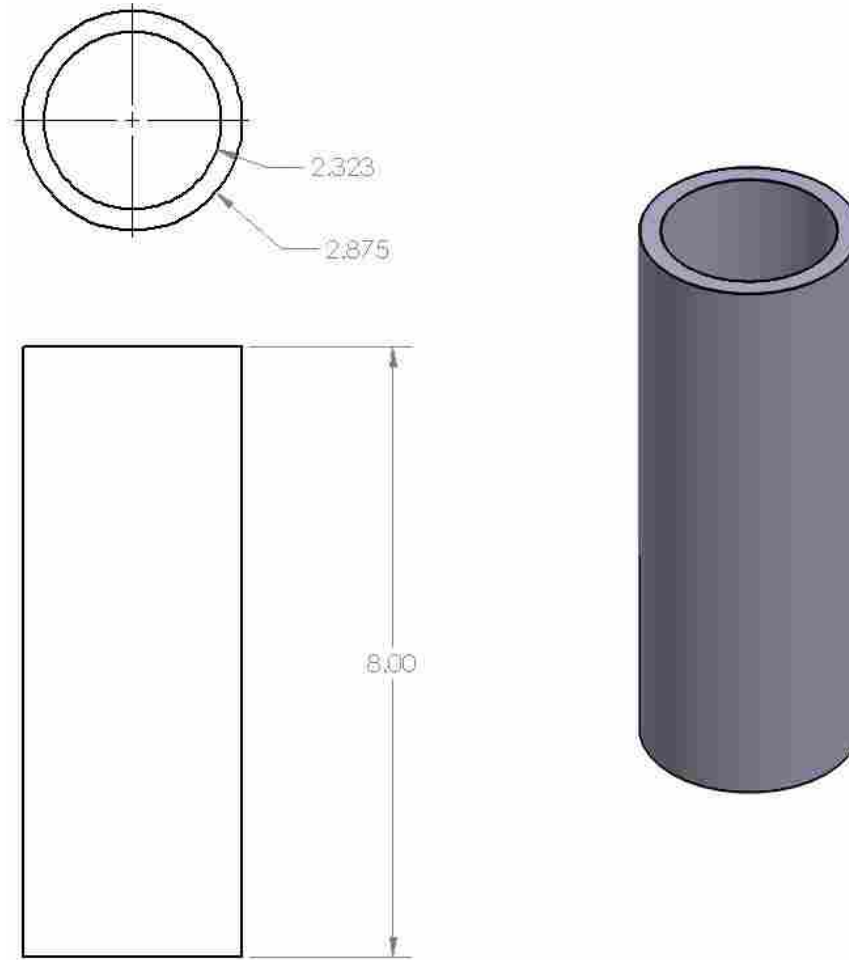
ITEM NO.	DRAWING NUMBER	DESCRIPTION	QTY.
9-9	27	3" 300# Blind Flange with Hole for 3/4" Pipe	1



DATE	3/18/2019	MADE BY	Cody Carpenter	CHECKED BY	
Dry Feed Oxy-Coal Combustion Reactor					
3" 300# Blind Flange with Hole for 3/4" Pipe					
SIZE	A	DWG. NO.	27	REV.	3
SCALE	1:2	CAD FILE:		SHEET 27 of 30	

Figure B27: Drawing of 3 Inch Class 300 Blind Flange with Hole for 3/4 Inch Pipe

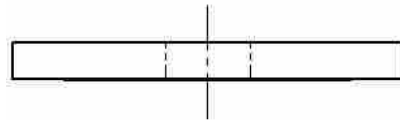
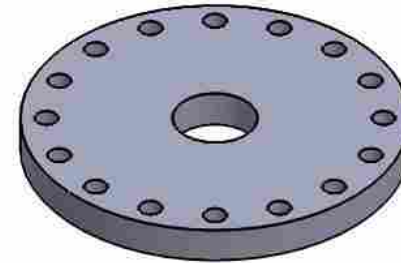
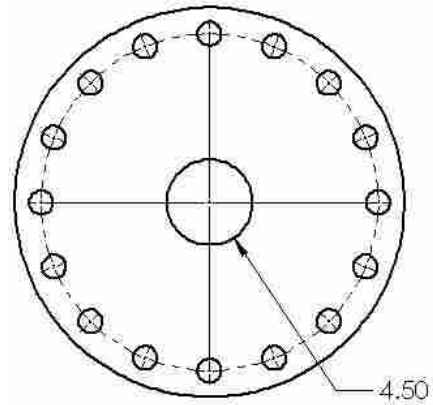
ITEM NO.	DRAWING NUMBER	DESCRIPTION	QTY.
10-2	28	2.5" X-Heavy Pipe- Carbon Steel	1



DATE	MADE BY	CRD BY
2/18/2019	Cody Carpenter	
Dry Feed Oxy-Coal Combustion Reactor		
2.5" X-Heavy Steel Pipe		
SIZE	DWG. NO.	REV.
A	28	2
SCALE	1:2 CAD FILE:	SHEET 28 of 30

Figure B28: Drawing of 2.5 Inch X-Heavy Steel Pipe

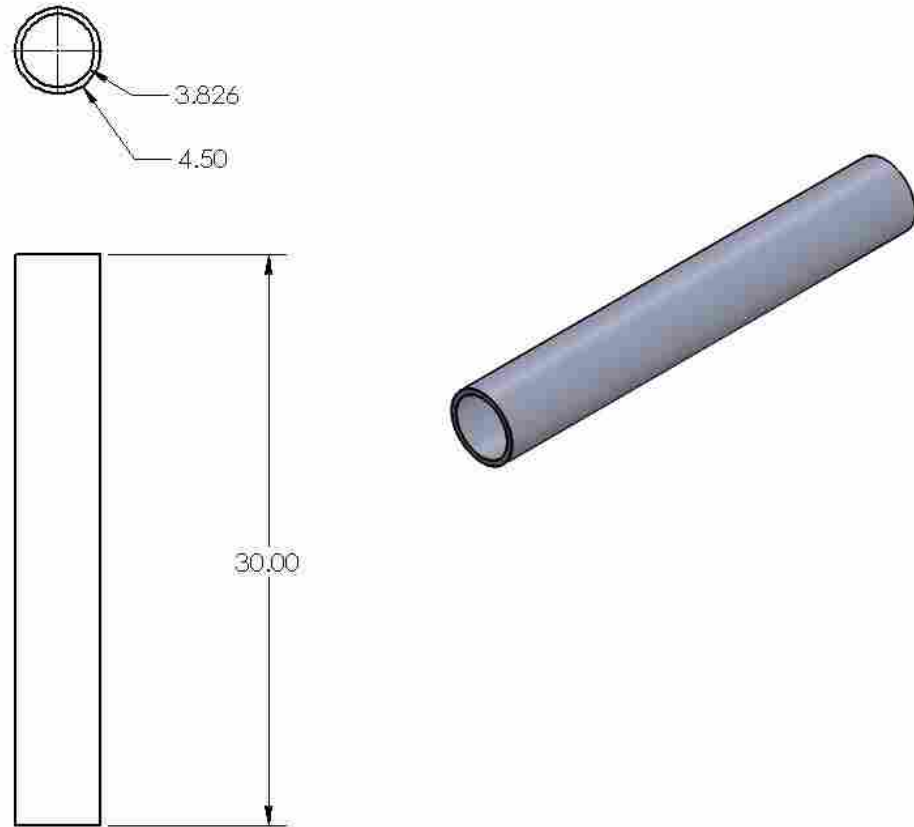
ITEM NO.	DRAWING NUMBER	DESCRIPTION	QTY.
12-1	29	12" 300# 309 Steel Blind Flange with Hole for 4" Pipe	1



DATE	MADE BY	CRD BY
2/18/2019	Cody Carpenter	
Dry Feed Oxy-Coal Combustion Reactor		
12" 300# Blind Flange with Hole for 4" Pipe		
SIZE	DWG. NO.	REV.
A	29	
SCALE 1:8 CAD FILE:		SHEET 29 of 30

Figure B29: Drawing of 12 Inch Class 300 Blind Flange with Hole for 4 Inch Pipe

ITEM NO.	DRAWING NUMBER	DESCRIPTION	QTY.
12-2	30	4" 309 Steel Pipe X-Heavy	1



DATE	2/19/2019	MADE BY	Cody Carpenter	CHKD BY	
Dry Feed Oxy-Coal Combustion Reactor					
4" X-Heavy Steel Pipe					
SIZE	DWG. NO.	30	REV.		
A					
SCALE	1:8	CAD FILE	SHEET 30 of 30		

Figure B30: Drawing of 4 Inch X-Heavy Steel Pipe